University of Stavanger

FACULTY OF SCIENCE AND TECHNOLOGY

MASTER'S THESIS

Study programme/specialization: Petroleum Engineering/ Drilling Technology	Spring/~~Autumn~~ semester, 2018 Open
Author: Maalidefaa Moses Tantuoyir	…….. (Signature of author)
Programme coordinator: Supervisor(s): Mesfin Belayneh.	
Title of master's thesis: **Heat Transfer Modeling and Simulation in Geothermal Wells**	
Credits: 30	
Keywords: Insulators Heat Exchange Conductivity Heat Transfer Coefficient Overall Heat Transfer Heat Loss Geothermal Energy	Number of pages: ……146…… + Supplementary material/other: …5… Place: Stavanger Date/year: 15-06-2018

Abstract

Geothermal energy is among the fastest growing renewable energies. In the field of geothermal, energy conversion refers to the power plant technology that converts the hot geothermal fluids into electric power. The two primary sources of geothermal energy are hydrothermal resources mainly found at shallower depth and hot dry rock resources normally found in a deeper formation.

The higher the energy extraction, the better for the power plant energy conversion. However, in poorly designed wellbore, the up flowing geothermal fluid induces a radial heat flux from the well toward the rock. Because of heat transfer, the surface temperature will be reduced and will not be sufficient for the power plant energy conversion. To maintain/preserve heat transfer, it is therefore important to design a well with appropriate material and identify the right operational parameters.

In this thesis, an inner insulator was included in the production tube/casing to develop a heat transfer analytical model with the objective of significantly reducing heat loss from the reservoir to the surface, reduce the effect of corrosion and erosion of production casing/tubing and predict the effect of high flow rate on heat transfer in hard-rock geothermal wells. Several case scenario have been simulated with analytical model and with commercial Landmark / WELLCAT™ software.

Results showed that high flowrate leads to low heat loss to the formation, placing an inner insulator in the production casing conserves heat produced from the reservoir to the surface as compared to placing on an outer insulator, thermal conductivity of cement is insignificant when the value is above 1 [BTU/hr-ft-ºF] and the thermal conductivity of casings is significant when the well is completed without insulators.

Acknowledgements

This thesis is submitted in fulfilment of the requirements for the degree of Master's in Science at the University of Stavanger. I would like to express my gratitude to my supervisor Mesfin A. Belayneh at the University of Stavanger for all of his time and effort in helping me with this thesis. He was always available whenever I had a question about my research or writing. Mesfin consistently allowed this paper to be my own work but steered me in the right direction whenever necessary.

I would also like to express my very profound gratitude to my family for providing me with continuous support and patience throughout my years of study and through the process of writing this thesis.

Finally, I would like to thank all my colleagues who gave me the necessary help to be able to finish this degree and thesis successfully. This accomplishment would not have been possible without them.

Maalidefaa Moses Tantuoyir,
University of Stavanger, Norway.
June 2017.

Table of Contents

ABSTRACT I

ACKNOWLEDGEMENTS II

LIST OF FIGURES VI

LIST OF TABLES X

NOMENCLATURE XI

ABBREVIATIONS XIV

1 INTRODUCTION 1

1.1 BACKGROUND AND MOTIVATION 1

1.2 PROBLEM FORMULATION 3

1.3 OBJECTIVES AND SCOPES OF STUDY 6

1.4 RESEARCH APPROACH 6

1.5 STRUCTURE OF THE THESIS 7

2 LITERATURE STUDY 8

2.1 INTRODUCTION TO GEOTHERMAL ENERGY 8

2.1.1 Geothermal Well design 11

2.1.2 Geothermal Energy: Challenges 13

2.1.3 Geothermal Energy Advantage and Disadvantages 15

2.2 CHEMISTRY OF GEOTHERMAL FLUIDS AND THEIR CONSEQUENCES 17

2.2.1 Corrosion 18

2.2.2 Scaling 22

2.3 MATERIAL SELECTION 24

2.3.1 Metallic Materials 24

2.3.2 Non-Metallic Materials 26

3 THEORY 27

3.1 TUBULAR STRESS THEORY 27

3.2 CYLINDER TYPES 28

3.2.1 Thin Walled Cylinder Stress 29

3.2.2 Thick Walled Cylinder Stress 31

3.2.3 Failure Criteria – von Mises *33*
3.2.4 Tubular Design Models *34*
3.3 HEAT TRANSFER MECHANISMS **36**
3.3.1 Conduction *37*
3.3.2 Convection *38*
3.3.3 Radiation *38*
3.4 RATE OF HEAT FLOW **39**
3.4.1 Thermal Conductivity *39*
4 MATHEMATICAL MODELING **41**
4.1 WELL SET-UP AND ASSUMPTIONS **41**
4.2 HEAT TRANSFER MODELING **43**
4.2.1 Model 1: At Reservoir Section *45*
4.2.2 Model 2: At Middle Section *47*
4.2.3 Model 3: At Top Section *49*
5 RESULTS **52**
5.1 WELLCAT™ SOFTWARE RATE OF FLUID PRODUCTION **52**
5.1.1 Simulation Arrangement *52*
5.1.2 Fluid Temperatures *55*
5.2 HEAT TRANSFER SIMULATION **57**
5.2.1 Simulation Setup *57*
5.2.2 Simulation Results *60*
6 DISCUSSION **110**
6.1 HEAT TRANSFER MODEL **110**
6.1.1 Effect of Insulators *111*
6.1.2 Effect of Non-insulation *114*
6.1.3 Effect of Cement Thermal Conductivity *115*
6.1.4 Effect of Thickness of Insulators *116*
6.1.5 Effect of Varying the Conductivity of the Insulators *119*
6.2 EFFECT OF FLOWRATE ON FLUID HEAT LOSS **122**
7 SUMMARY AND CONCLUSION **124**
REFERENCES **126**
APPENDIX **131**

APPENDIX A: REVIEWED CHEMISTRY OF GEOTHERMAL FLUIDS 131
APPENDIX B: SIMULATION PARAMETERS 133

List of Figures

Figure 1.1: World energy outlook 2017, (IEA., 2017). 2
Figure 1.2: World primary energy consumption by fuel type in million ton of oil equivalent (IEA, 2015) 3
Figure 1.3: General well configuration involving a variety of elements (Hasan & Kabir, 1994) 5
Figure 2.1: Geothermal well injection and power plant (Field et al., 2012). 10
Figure 2.2: Classification of geothermal resources by temperature (Williams et al., 2011). 11
Figure 2.3: Typical geothermal well (C Teodoriu & Cheuffa, 2011)..... 12
Figure 2.4: Geothermal and oil and gas industry average well costs compared with depth,(Initiative, 2006). 15
Figure 2.5: Electrochemical process (Kristanto, Kusumo, & Abdassah, 2005). 19
Figure 2.6: Uniform corrosion (Catalin Teodoriu, 2015). 20
Figure 2.7: Corroded water injecting carbon steel tubing (Bellarby, 2009). 21
Figure 2.8: Calcite Scaling Inside a Slotted Liner in Krafla KJ-19 (Fridriksson & Thórhallsson). 23
Figure 3.1: Triaxial stress on circular pipe(Belayneh, 2018). 28
Figure 3.2: Illustration of a thin walled cylinder(Belayneh, 2018). 29
Figure 3.3: Free body diagram of closed end thin walled cylinder(Belayneh, 2018). ... 30
Figure 3.4: Stresses in thick walled cylinder(Belayneh, 2018). 31
Figure 3.5: Stress distribution across cylinder's wall(Belayneh, 2018). 33
Figure 3.6: Burst pipe(Belayneh, 2018). 35
Figure 3.7: Collapsed pipe(Belayneh, 2018). 36
Figure 3.8: Temperature boundary conditions for a slab (Nathan Amuri, 2017). 37
Figure 3.9: Heat Convection through two media(Nathan Amuri, 2017). 38
Figure 4.1: Illustration of injection well, reservoir and production well(Nathan Amuri, 2017). 41
Figure 4.2a: Illustration of the horizontal cross-section of the well 42
Figure 4.2b: Illustration of the vertical cross-section of the well 43
Figure 4.3a: Illustration of the horizontal cross-section of the reservoir section of the well 46
Figure 4.3b: Illustration of vertical cross-section of the reservoir section 46
Figure 4.4a: Illustration of the horizontal cross-section of the well 48
Figure 4.4b: Illustration of vertical cross-section of the reservoir section 48
Figure 4.5a: Illustration of the horizontal cross-section of the well 50
Figure 4.5b: Illustration of vertical cross-section of the reservoir section 50
Figure 5.1: Schematic of the well used for flowrate simulation on WellCAT™ 53

Figure 5.2: Displays the well temperature across the working tube..... 56
Figure 5.5: Geothermal well schematic..... 59
Figure 5.6: Thermal resistance versus cement thermal conductivity in the reservoir section..... 61
Figure 5.7: Overall heat transfer coefficient versus cement thermal conductivity-uninsulated reservoir section. 61
Figure 5.8: Heat exchange versus cement thermal conductivity-uninsulated reservoir section..... 63
Figure 5.9: Thermal resistance versus cement thermal conductivity-outer insulated reservoir section..... 64
Figure 5.10: Overall heat transfer coefficient versus cement thermal conductivity-outer insulated reservoir section. 65
Figure 5.11: Heat exchange versus cement thermal conductivity-outer insulated reservoir section..... 66
Figure 5.12: Thermal resistance versus cement thermal conductivity-inner insulated reservoir section..... 67
Figure 5.13: Overall heat transfer coefficient versus cement thermal conductivity-inner insulated reservoir section. 68
Figure 5.14: Heat exchange versus cement thermal conductivity-inner insulated reservoir section..... 69
Figure 5.15: Thermal resistance versus cement thermal conductivity-outer and inner insulated reservoir section. 70
Figure 5.16: Overall heat transfer coefficient versus cement thermal conductivity-outer and inner insulated reservoir section. 71
Figure 5.17: Heat exchange versus cement thermal conductivity-outer and inner insulated reservoir section..... 72
Figure 5.18: Effect of conductivity of insulators at the reservoir section. 73
Figure 5.19: Effect of conductivity of insulators at the reservoir section. 73
Figure 5.20: Effect of conductivity of insulators at the reservoir section. 74
Figure 5.21: Effect of conductivity of insulators at the reservoir section. 75
Figure 5.22: Effect of conductivity of insulators at the reservoir section. 76
Figure 5.23: Effect of conductivity of insulators at the reservoir section. 77
Figure 5.24: Thermal resistance versus cement thermal conductivity-uninsulated middle section..... 78
Figure 5.25: Overall heat transfer coefficient versus cement thermal conductivity-uninsulated middle section. 79
Figure 5.26: Heat exchange versus cement thermal conductivity-uninsulated middle section..... 80
Figure 5.27: Thermal resistance versus cement thermal conductivity-outer insulated middle section..... 81

Figure 5.28: Overall heat transfer coefficient versus cement thermal conductivity-outer insulated middle section. 82
Figure 5.29: Heat exchange versus cement thermal conductivity-outer insulated middle section. 83
Figure 5.30: Thermal resistance versus cement thermal conductivity-inner insulated middle section. 84
Figure 5.31: Overall heat transfer coefficient versus cement thermal conductivity-inner insulated middle section. 84
Figure 5.32: Heat exchange versus cement thermal conductivity-inner insulated middle section. 85
5.33: Thermal resistance versus cement thermal conductivity-inner insulated middle section. 86
5.34: Overall heat transfer coefficient versus cement thermal conductivity-inner insulated middle section. 87
Figure 5.35: Heat exchange versus cement thermal conductivity-inner insulated middle section. 88
Figure 5.36: Effect of conductivity of both insulators-Middle Section. 89
Figure 5.37: Effect of conductivity of both insulators-Middle Section. 89
Figure 5.38: Effect of conductivity of both insulators-Middle Section. 90
Figure 5.39: Effect of conductivity of both insulators-Middle Section. 91
Figure 5.40: Effect of conductivity of both insulators-Middle Section. 91
Figure 5.41: Effect of conductivity of both insulators-Middle Section. 92
Figure 5.42: Thermal resistance versus cement thermal conductivity-uninsulated top section. 94
Figure 5.43: Overall heat transfer versus cement thermal conductivity-uninsulated Top Section. 95
Figure 5.44: Heat exchange versus cement thermal conductivity-uninsulated Top Section. 96
Figure 5.45: Thermal resistance versus cement thermal conductivity-outer Insulated Top Section. 97
Figure 5.46: Overall heat transfer coefficient versus cement thermal conductivity-outer insulated Top Section. 97
Figure 5.47: Heat exchange versus cement thermal conductivity-outer insulated Top Section. 98
Figure 5.48: Thermal resistance versus cement thermal conductivity-inner insulated Top Section. 99
Figure 5.49: Overall heat transfer versus cement thermal conductivity-inner insulated Top Section. 100
Figure 5.50: Heat exchange versus cement thermal conductivity-inner insulated Top Section. 101

Figure 5.51: Thermal resistance versus cement thermal conductivity-inner and outer insulated Top Section. 102
Figure 5.52: Overall heat transfer coefficient versus cement thermal conductivity-inner and outer insulated Top Section. 103
Figure 5.53: Heat exchange versus cement thermal conductivity-inner and outer insulated Top Section. 104
Figure 5.54: Thermal resistance versus cement thermal conductivity-inner and outer insulated Top Section. 105
Figure 5.55: Overall heat transfer versus cement thermal conductivity-inner and outer insulated Top Section. 106
Figure 5.56: Heat exchange versus cement thermal conductivity-inner and outer insulated Top Section. 107
Figure 5.57: Thermal resistance versus cement thermal conductivity-inner and outer insulated Top Section. 108
Figure 5.58: Overall heat transfer coefficient versus cement thermal conductivity-inner and outer insulated Top Section. 108
Figure 5.59: Heat exchange versus cement thermal conductivity-inner and outer insulated Top Section. 109
Figure 6.1: Heat exchange versus cement thermal conductivity of reservoir section. . 112
Figure 6.2: Heat exchange versus cement thermal conductivity of middle section. 113
Figure 6.3: Heat exchange versus cement thermal conductivity of top section. 114
Figure 6.4: Heat exchange versus cement thermal conductivity for uninsulated well. 115
Figure 6.5: Comparison heat exchange versus cement thermal conductivity between outer insulated wells and inner and outer insulated wells. 116
Figure 6.6: Average heat exchange versus thickness of insulators –Reservoir Section117
Figure 6.7: Average heat exchange versus thickness of insulators –Middle Section... 118
Figure 6.8: Average heat exchange versus thickness of insulators –Top Section..... 119
6.9: Average heat exchange versus different conductivity of insulators-Reservoir Section 120
6.10: Average heat exchange versus different conductivity of insulators-Middle Section. 121
6.11: Average heat exchange versus different conductivity of insulators-Top Section. 122
Figure 6.12: Comparison of the percentage heat loss in the wellbore with different flowrates. 123

List of Tables

Table 1: Casing grades used in geothermal wells (Kalvenes, 2017) 13
Table 2. Advantages and challenges of geothermal resources(Gehringer & Loksha, 2012). 16
Table 3. Types and use of geothermal resources (Gehringer & Loksha, 2012). 17
Table 4: Typical composition of geothermal waters (Community, 2016). 18
Table 5: Casing and tubing configuration 54
Table 6: Tubing grading 54
Table 7: A-annulus fluid content 55
Table 8: Well design parameters 57
Table 9: Input parameters for simulation 58
Table 10: Wellbore and fluid temperatures for different well sections 60
Table 11: Computed chemical composition of the deep fluid supplying the CL3 well, Ribeira Grande geothermal field in the Azores(Carvalho, Forjaz, & Almeida, 2006). 131
Table 12: Alteration minerals observed in well cuttings and associated with fossil geothermal systems in Iceland as well as mineral types hosting trace elements in geothermal systems(Kaasalainen, Stefánsson, Giroud, & Arnórsson, 2015). 132
Table 13: Well parameters used for simulation of the reservoir section. 133
Table 14: Well Parameters used for simulating the middle section of the well. 134
Table 15: Well parameters used for simulating the top section of the well. 135

Nomenclature

A = *Area*

a = *Inner radius of cylinder*

b = *Outer radius of cylinder*

E = *Modulus of elasticity*

F_a = *Axial force*

h_c = *Heat conduction*

h_f = *Film heat transfer coefficient*

h_r = *Heat radiation*

k_{csg} = *Conductivity of casing*

$k_{ins}^{o} = Conductivity\ of\ outer\ insulator$

$k_{ins}^{i} = Conductivity\ of\ inner\ insulator$

k_t = *Conductivity of production tubing*

ΔL = *Change in length*

P = *Pressure*

P_i = *Inner pressure*

P_o = *Outer pressure*

Q = *Rate of heat flow*

r = *Radius of cylinder*

r_i = *Inside radius*

r_O = *Outer pressure*

$r_{ins}^{o} = Radius\ of\ outer\ insulator$

$r_t^o = Radius\ of\ production\ tubing$

$r_c^o = Outer\ radius\ of\ casing$

$r_c^i = Inner\ radius\ of\ casing$

$r_t^i = Inner\ radius\ of\ production\ tubing$

r_{wb} = *Radius of wellbore*

SF = *Safety factor*

t = *Thickness*

T = *Temperature*

ΔT = *Change in temperature measured from a uniform reference temperature*

T_a = *Inner radius temperature of cylinder*

T_b = *Outer radius temperature of cylinder*

T_f = *Formation temperature*

T_{wb} = *Wellbore temperature*

T_c^o = *Outer temperature of casing (intermediate)*

$T_{cem}^o = Outer\ temperature\ of\ cement$

$T_t^o = Outer\ temperature\ of\ production\ tubing$

$T_{cond.}^0 = Outer\ temperature\ of\ conductor\ casing$

T_{cs}^o = *Outer temperature of surface casing*

$T_{ins}^o = Outer\ temperature\ of\ outer$ *insulator*

$T_{ins}^{oi} = Outer\ temperature\ of\ inner\ insulator$

$T_c^i = Inner\ temperature\ of\ casing(intermediate)$

$T_{cem.}^i = Inner\ temperature\ of\ cement$

$T_{cond.}^i = Inner\ temperature\ of\ conductor\ casing$

$T_{cs}^i = Inner\ temperature\ of\ surface\ casing$

$T_{ins}^i = Inner\ temperature\ of\ inner\ insulator$

$T_t^i = Inner\ temperature\ of\ production\ tubing$

T_{ins}^{io} = *Outer temperature of inner insulator*

$U_{to} = Overall\ heat\ transfer\ coefficient$

$^1/_{U_{to}} = Heat\ transfer\ resistance$

x, y, z = Dimensionless parameter

Δx = *Length of cylinder*

α = *Coefficient of liners thermal expansion*

$\sigma_h = Hoop\ stress$

$\sigma_y = Yield\ stress$

$\sigma_{max} = Maximum\ stress$

$\sigma_{min} = Minimum\ stress$

$\sigma_{VME} = Von - Misses\ stress$

$\sigma_r = Radial\ stress$

$\sigma_\theta = Tangential\ stress$

$\sigma_z = Vertical/Axial\ stress$

ϑ = *Poisson's ratio*

Abbreviations

AISI = American Iron and Steel Institute

API = American Petroleum Institute

Bbl./d = Barrels per day

BTU = British Thermal Unit

$CaCO_3$ = Calcite (Calcium Carbonate)

CO_2 = Carbon dioxide

Cond. = Conductor casing

CS = Surface casing

CSG = Casing

EGS = Enhanced Geothermal System

FeS = Iron sulphide

GSHPs = Ground Source Heat Pumps

GW, GW_e = Giga Watt (Equivalent)

HCl = Hydrogen Chloride

H_2S = Hydrogen Sulphide

H_2SO_4 = Sulphric Acid

IDDP = Icelandic Deep Drilling Project

MD = Measured Depth

MIT = Massachusetts Institute of Technology

NaCl = Sodium Chloride(Brine)

NORSOK = Norsk Sokkels Konkuranseposisjon
OD = Outer Diameter
pH = Power of Hydrogen
ppm = Parts per Million
RKB = Rotary Kelly Bushing
SiO_2 = Silicon Oxide (Silica)
SSC = Sulphide Stress Cracking
TOC = Top of Cement
TOL = Top of Liner

(Left Blank Intentionally)

1 Introduction

Geothermal energy is among the fastest growing renewable energies, which exploits energy rocks below ground. The higher energy extraction is the better for the power plant energy conversion. However, during production, due to temperature difference between the well and the surrounding rock, the up flowing geothermal fluid induces a radial heat flux from the well toward the rock. Because of heat transfer, the surface temperature will be reduced and will not be sufficient for the power plant energy conversion. This heat transfer process and temperature distribution of the up flowing fluid can be determined by analytic methods.

In this thesis work, an attempt is made to develop a heat transfer model extending the work initially developed by (G Paul Willhite, 1967). The extension method was by introducing inner insulation in the production tube of the well and analyzing the effect of different parameters of the insulators on the overall heat exchange between the wellbore and the formation. Moreover, the study evaluated the effect of flow rate on the overall heat transfer in a wellbore that was built in Landmark/WellCAT™ Software.

1.1 Background and motivation

Due to population growth, energy demand also increases gradually and there is therefore a demand for more reliable energy sources which are more environmentally friendly. Renewables capture two-thirds off global investments in power plants to 2040 as they become for most countries, the least cost source of energy (IEA., 2017), as illustrated in Figure 1.1.

Geothermal energy amongst others represents part of these renewables. Making use of heat energy from the inner parts of the Earth to produce other useful sources of energy (like electricity) involves extracting high temperature fluids like water, gas or a mixture

of both. The average geothermal gradient is approximately 25°C/km (Finger & Blankenship, 2010). Utilizing higher thermal energy involves drilling at deeper depths to about 3,5 km (Elders, Friðleifsson, & Albertsson, 2014).

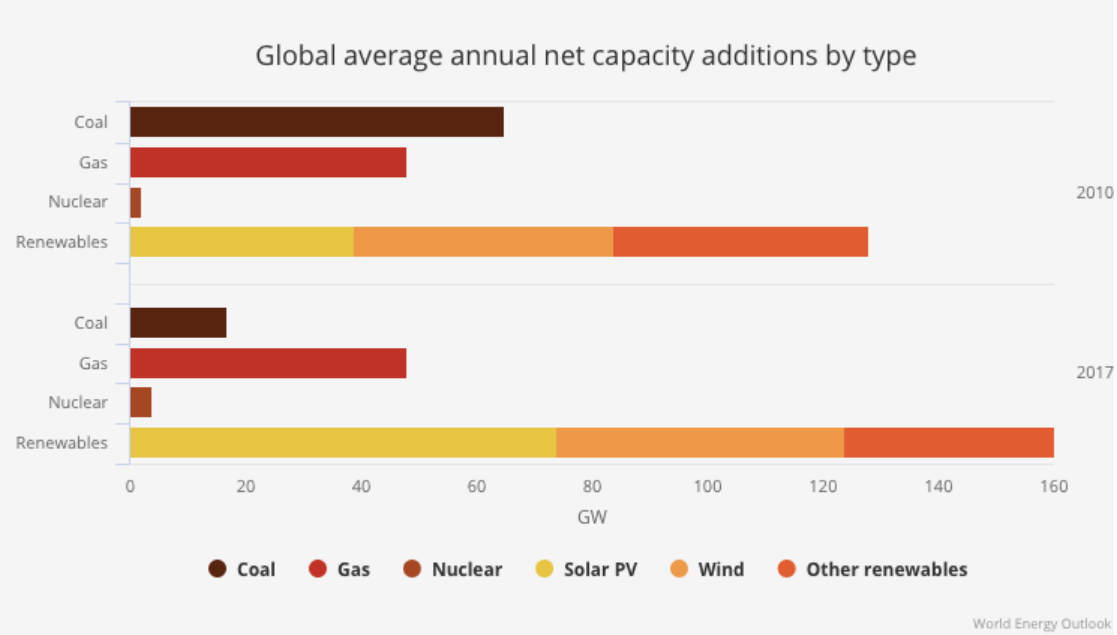

Figure 1.1: World energy outlook 2017, (IEA., 2017).

Utilization of geothermal energy relies strongly on solving the problems encountered during production and well construction. Some of these common problems have been related to the chemistry of the geothermal fluids which sometimes contain quite considerable concentrations of minerals and gases which can cause scaling and corrosion in wells and surface installations (Gunnlaugsson, Ármannsson, Þórhallsson, & Steingrímsson, 2014). This can lead to a reduction in the amount of heat transferred from the bottom of the reservoir to the surface. Casings are generally subjected to thermal cycling during production which may lead to large stress resulting in casing or connections exceeding their yield limit(Maruyama, Tsuru, Ogasawara, Inoue, & Peters, 1990).

Several global agencies like the IEA and energy companies like Equinor ASA have indicated the growing interest of bioenergy projects to be the as dominant energy source

((Bioenergy, 2015);(Statoil, 2017)). Figure 1.2 shows the predicted energy consumption until the year 2030. Geo-heat is a clean form of renewable energy and geothermal wells are drilled for sustainable energy development. Standard geothermal wells have temperatures of about 250°C(482ºF) and they typically produce approximately 5 megawatts of power. To maximize all this heat produced for energy conversion efficiency, there is the need for proper well design which will reduce heat loss, corrosion, erosion, scaling and other geothermal well problems.

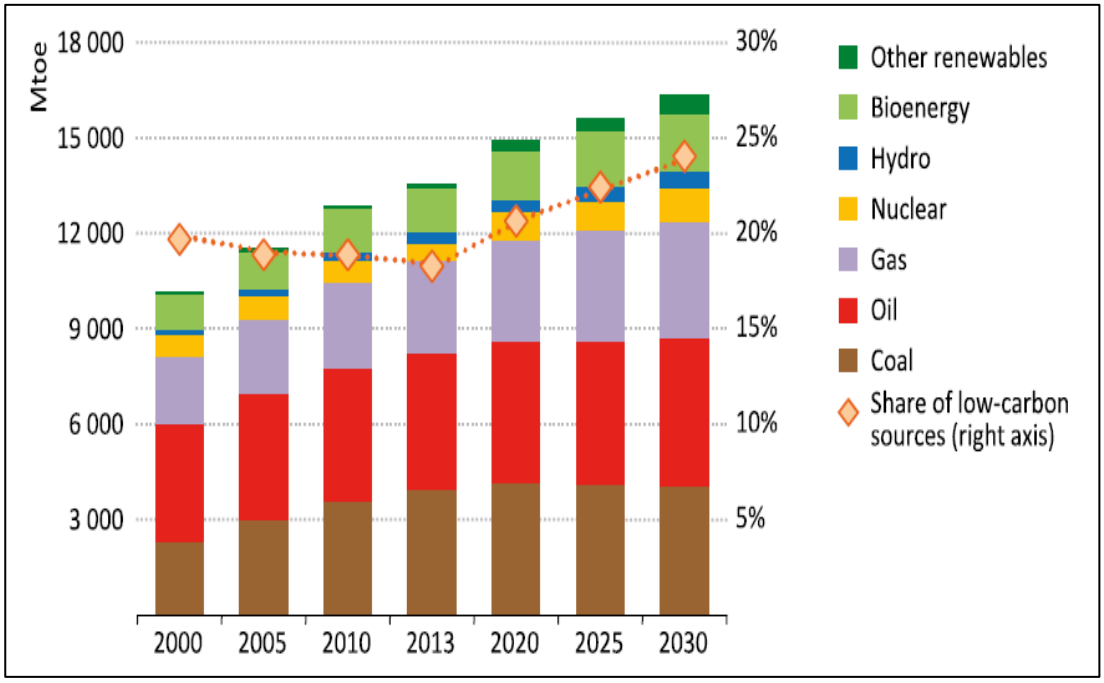

Figure 1.2: World primary energy consumption by fuel type in million ton of oil equivalent (IEA, 2015)

1.2 Problem Formulation

Several investigators have developed the heat flow from the tubing to the formation with a model using the overall heat transfer coefficient which included thermal resistances for conduction and convection in the tubing, conduction through the tubing, insulation, casing and cement material((G. Paul Willhite, 1967); (Hasan & Kabir, 1994)). Figure 1.3

illustrates the model used by (Hasan & Kabir, 1994). With this current practice, there is still about 45-50% heat loss from the reservoir to the surface of geothermal wells.

Despite a promising potential of geothermal energy as one of green energy source, heat loss from produced fluid, scaling, thermal flux, erosion and corrosion of casing reduce the maximization of the heat produced with the current industrial practice of placing insulators behind casings.

Published papers related to heat transfer modeling in geothermal wells include a variety of heat loss prevention methods through the influence of cement thermal properties (Ichim, Teodoriu, & Falcone, 2016), heat loss prevention through the placement of an insulator between the production casing/tubing and annulus (Hasan & Kabir, 1994), effect of varying heat flux on heat transfer (Hashmi, 2014).

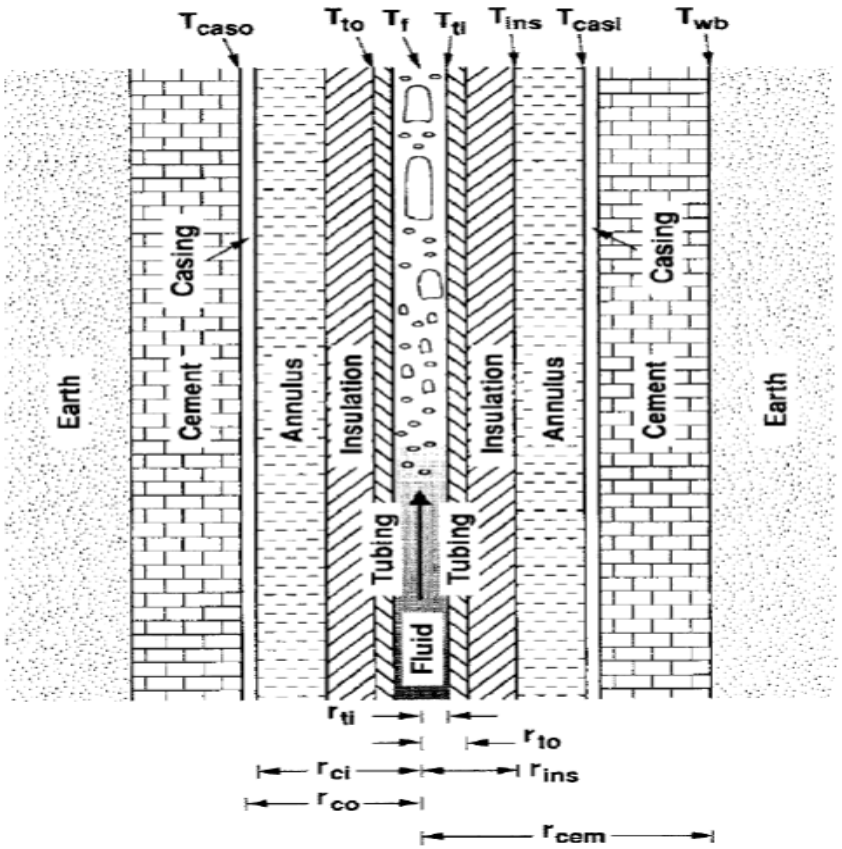

Figure 1.3: General well configuration involving a variety of elements (Hasan & Kabir, 1994)

In geothermal wells, there is less consideration of placing insulators inside production casing to reduce heat loss and common problems such as erosion from dissolved solids, scaling and corrosion. This is due to issues related to cost, well intervention and hole size. In this thesis, it is therefore possible to hypothesize that the overall heat loss when an inside insulator is placed in the production casing is less than when an insulator is placed outside the production casing.

This thesis therefore addresses issues such as:

- Mechanisms for controlling heat loss and extract maximum energy
- Methods for controlling long term well integrity

1.3 Objectives and Scopes of Study

The objectives and scopes proposed for this study include:

- Develop a model to investigate if placing an insulator inside the production casing in geothermal wells will result in less heat loss in the wellbore during production as compared to placing the insulator outside the production casing.
- Investigate the effect of high production rates on the overall heat transfer of fluids.
- Investigate the combined effect of placing insulators inside and outside the production casing.
- Using commercial software to simulate the temperature profile and investigate the main operational controlling parameters which suite for maximum heat extraction.

1.4 Research Approach

This thesis approached by improving upon the overall heat transfer model used by (Ichim et al., 2016) and testing the new model with geothermal well production data to predict the overall heat transfer from the reservoir to the surface of the well. The new model will form the foundation for studying; the effect of placing insulators inside and outside the production casing, the effect of varying the thickness of the insulators and also the effect of different thermal conductivities of the insulators on the overall heat transfer.

Commercial WellCAT™ will also be used to study the effect different production rates on the overall heat exchange between the wellbore and the formation.

This work aims to establish a model which will aid in geothermal well design process, aiming to propose improved well completion method for deep geothermal wells. The overall objective of this thesis is to ensure increased production well lifetime and economic viability of deep geothermal wells.

1.5 Structure of the Thesis

The structure of the thesis and the objectives of every step is presented below:

- **Chapter 2** – This chapter contains generic literature about geothermal energy to create an understanding of the subject in order to develop a model for the heat transfer problem. Geothermal energy concepts, chemistry of geothermal fluids, material selection and typical problems associated with the geothermal field will be presented. Geothermal well design is considered to allow the transfer of well design concepts from the petroleum industry.
- **Chapter 3** – This chapter will address the theory behind the commercial WellCAT™ software which we will use for simulating the effect of flowrate on heat transfer in the well. Different types of heat transfer will also be discussed.
- **Chapter 4** – This chapter presents the model developed and used in this thesis.
- **Chapter 5** – Results obtained from simulations in commercial WellCAT™ and Excel will be presented in this section.
- **Chapter 6** – This chapter presents further discussion of the results from chapter 5. Comparison will be made between the current practice in the industry and the newly proposed model.
- **Chapter 7** – In this chapter, a conclusion is made from the discussion in chapter 6 and areas of further work is suggested.

2 Literature study

This chapter contains generic literature about geothermal energy to create an understanding of the subject in order to develop a model for the heat transfer problem. Geothermal energy concepts, heat transfer mechanisms and typical problems associated with the geothermal field will be presented. Geothermal well design is considered to allow the transfer of well design concepts from the petroleum industry.

2.1 Introduction to Geothermal Energy

The extraction of natural thermal energy from within the earth is termed as geothermal energy. This form of energy exploitation is renewable and environmentally friendly and one of the main advantages of it is reliability(Panwar, Kaushik, & Kothari, 2011). Geothermal resources have been identified in over 80 countries across the world (Fridleifsson, 2001). A total of 13.1 GWe of conventional geothermal energy has been installed worldwide as at 2016(Matek, 2016). According to Finger and Blankenship (2010), the average temperature gradient increases at 25°C/km approximately with depth. Heat sources which provide temperatures below 100°C (212ºF) at an economic depth are classified as low temperature systems. Areas with magmatic intrusions (example: Reykjanes, Iceland) could reach in excess of over 400°C(752ºF) (Dickson & Fanelli, 2001).

A geothermal system can be described according to (Hochstein, 1990) as “convective water in the upper crust of the Earth, which, in a confined space, transfers heat from a heat source to a heat sink, usually the free surface”. (Dickson & Fanelli, 2001) classified a geothermal system into 3 main elements which include: a heat source, a reservoir and a fluid (which transfers the heat). The fluid normally originates from the reservoir but in cases where the reservoir has low permeability, cooler fluid (like sea water) could be injected in to the reservoir and produced later (Finger & Blankenship, 2010). An example of a typical geothermal system is shown in the Figure 2.1.

The heat energy from geothermal wells can be used to produce electricity. According to (Fridleifsson, 2001), geothermal reservoirs suitable for the production of electricity usually have temperatures above 150°C(302ºF). The Icelandic Deep Drilling Project(IDDP) of 4,5 [km] deep well (Friðleifsson et al., 2017) has successfully reached a supercritical target of 426°C (Friðleifsson et al., 2017).

Usually, the fluid in a geothermal system is water, but depending on the effects of temperature and pressure, it can be in liquid, vapor or a mixture of both phases (Finger & Blankenship, 2010). Geothermal fluids are commonly highly corrosive with the presence of H_2S and CO_2 gases (Finger & Blankenship, 2010). The highly corrosive and scaling characteristics of these fluids make geothermal well operations very difficult. Depending on the whether it is a high-water content or a dry steam content, a system can contain large amounts of silica which cause scaling or hydrogen chloride (HCl) and H_2S attacks. Both scenarios could also occur at the same time (Ocampo-Diaz, Valdez-Salaz, Shorr, Sauceda, & Rosas-González, 2005).

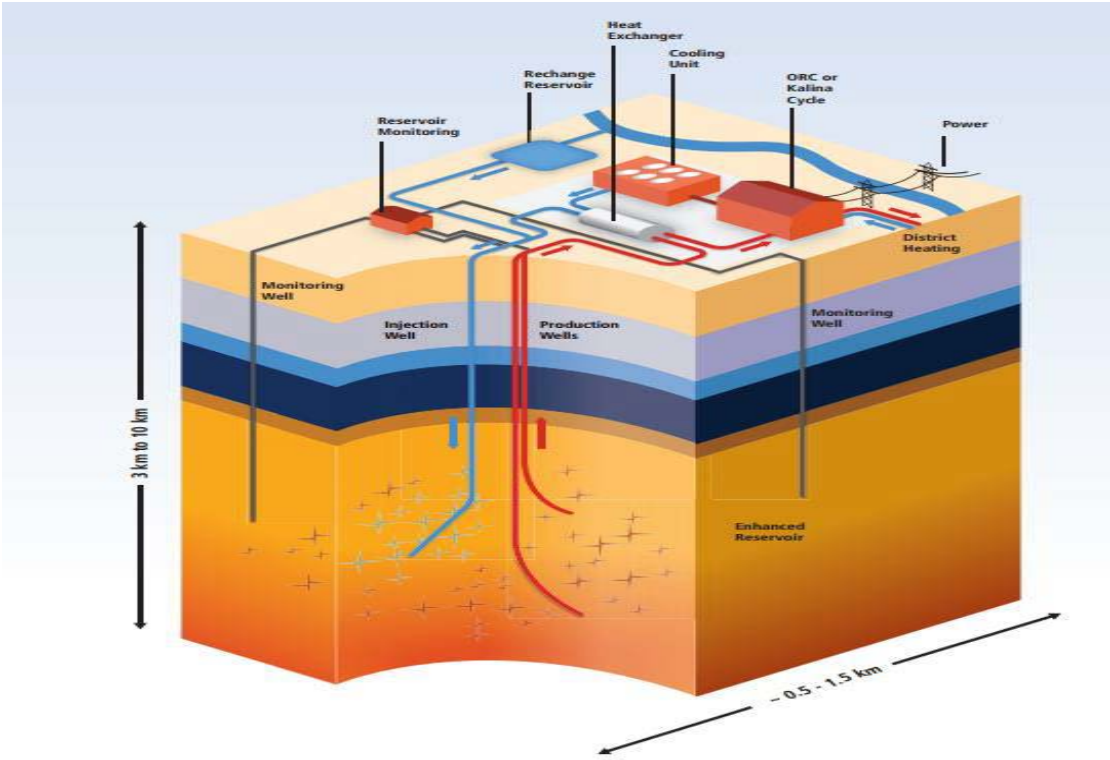

Figure 2.1: Geothermal well injection and power plant (Field et al., 2012).

Enthalpy is a measurement of the energy used to the heat content of fluids which is transported from the geothermal reservoir to the surface. Several authors have classified the resources by dividing them into low, intermediate and high enthalpy resources (Dickson & Fanelli, 2001). Figure 2.2 (Williams, Reed, & Anderson, 2011) shows an overview of these categories.

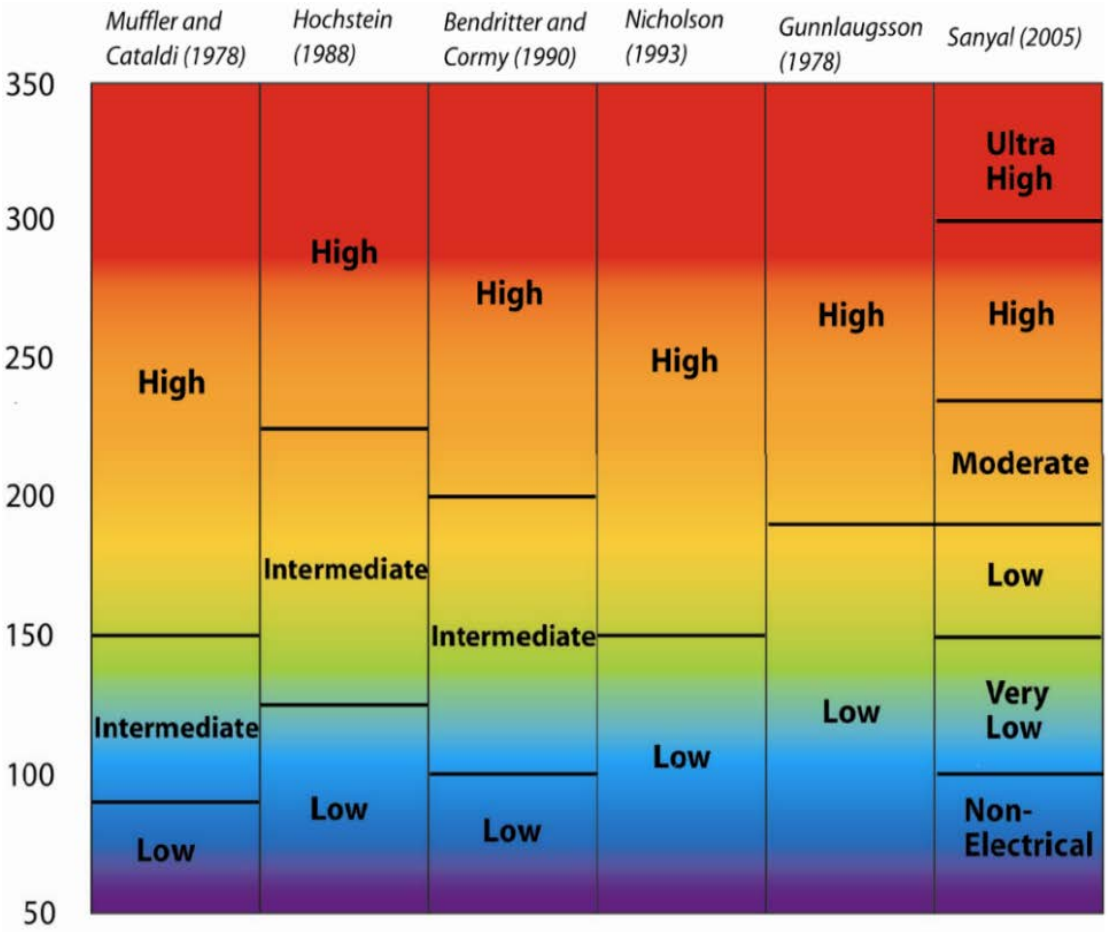

Figure 2.2: Classification of geothermal resources by temperature (Williams et al., 2011).

2.1.1 Geothermal Well design

Geothermal wells are a modification of the wells that already exist in the petroleum industry for higher temperatures and larger well diameters(Finger & Blankenship, 2010). Geothermal well design depends on the purpose of the well as production wells will require a well detailed planning of the strength and diameter of the material than exploration wells. Casing fatigue and cement integrity are the key issues for geothermal wells since they have a higher life expectancy than oil and gas wells (Catalin Teodoriu & Falcone, 2009). Figure 2.3 (C Teodoriu & Cheuffa, 2011) shows an example of a geothermal well.

Geothermal production wells require high production rates, often above 100 000 [kg/hr] (20 975 bbl./d) as compared to oil and gas wells (Finger & Blankenship, 2010). This is to minimize the heat loss from the reservoir to the surface of the well. Therefore, larger diameter casings are used (Þórhallsson, Matthíasson, Gíslason, Ingason, & Palsson, 2003). A two-phase flow that is vapor dominated in a large casing will reduce the pressure drop and improve productivity(Finger & Blankenship, 2010).

The presence of CO_2, H_2S and other elements in geothermal wells, make them highly corrosive and therefore require non-standard casing (Lukawski et al., 2014).
Commonly, API buttress casing connections are used ((Ingason et al., 2015);(Catalin Teodoriu & Falcone, 2009)). Examples of common casing grades are presented in table 1. These are commonly used by different authors and has been collected by (Catalin Teodoriu & Falcone, 2009).

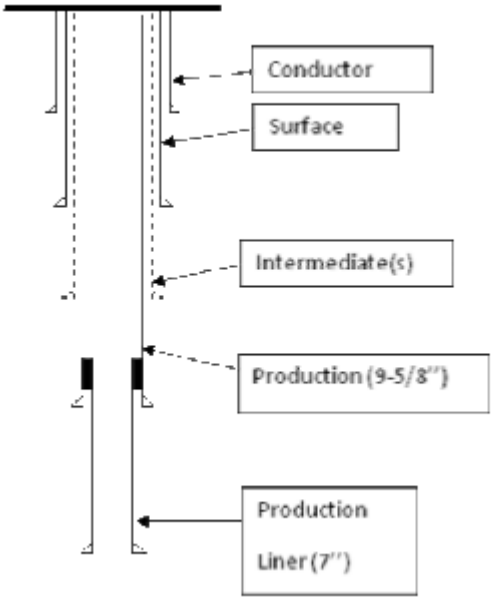

Figure 2.3: Typical geothermal well (C Teodoriu & Cheuffa, 2011)

Table 1: Casing grades used in geothermal wells (Kalvenes, 2017)

Casing grade	Comment	Author
J-55		(Brunetti & Mezzetti, 1970; Carden, Nicholson, Pettitt, & Rowley, 1983; Chiotis & Vrellis, 1995)
K-55	Usually replaces J-55 for deep wells	(Teodoriu & Falcone, 2009)
N-80		(Brunetti & Mezzetti, 1970; Carden et al., 1983; Chiotis & Vrellis, 1995; Ragnars & Benediktsson, 1981; Witcher, 2001)
L-80	Usually replaces N-80 in the presence of H_2S	(Lazzarotto & Sabatelli, 2005)
T-95	Has replaced C-95	(Teodoriu & Falcone, 2009)
S-95	In the absence of H_2S	(Carden et al., 1983)
P-110	In the absence of H_2S	(Teodoriu & Falcone, 2009)
9 Chrome L-80	For extreme environments	(Teodoriu & Falcone, 2009)
13 Chrome L-80	For extreme environments	(Teodoriu & Falcone, 2009)
Beta-C Titanium	For severe conditions	(Pye, Holligan, Cron, & Love, 1989)

2.1.2 Geothermal Energy: Challenges

The positive aspect of geothermal energy can be described by properties such as reliability, sustainability, and flexibility. However, worldwide, the advancement of the development of geothermal systems for deep geothermal is rather slow. It is reported that for worldwide deep geothermal for electricity production annual growth rate between 2010 and 2014 is only 3% (10.9 to 12.6 GWe). On the other hand for GSHPs around 8.5% (33.1 to 49.9 GWth) (Lund & Boyd, 2016). Comparing with other renewable resources, such as wind and solar photovoltaic the geothermal annual growth is lower (Ren, 2015).

The main barriers for both deep and shallow geothermal systems are (Initiative, 2006):

- High investment costs.
- Lack of public understanding along with the inherent resistance to change.
- Deep geothermal systems related risks and uncertainty related the resource quality and reservoir productivity.

Even though geothermal is considered as a viable, and environmentally friendly energy source, there are several challenges associated with it and its challenges are not easily met. Among others, the main challenges are:

- The reservoirs are extreme high temperatures and requires special temperature resistant material.
- The drilling formation is characterized by hard and corrosive rock.
- The formation is highly fractured and lost circulation is significant.
- The possible CO_2 intrusion/attack on casing and surface on well site Environmental concern.
- Structural integrity of cement and casing is also an issue.
- The presence of toxic gasses.
- Ballooning and reverse ballooning (well expansion/contraction) resulted from water injection and/or steam production.
- Heat loss to formation.
- Thermal cycling.
- Thermal expansion in annulus.

All of these challenges along with geothermal reservoirs and drilling needs to be solved through a higher technology in order to exploit an optimal production thermal fluid through reservoir rock and well flow.

In addition, identifying and characterizing of deep geothermal energy is also another challenge. The assessment of the local geothermal potential cost a lot since it depends on factors. Among others, the geothermal gradient, the permeability and connectivity of rock and also the presence of hot water.

According to MIT study on EGS dataset covering 34(Initiative, 2006), the experts indicated that drilling cost is also a challenging. As shown on Figure 2.4, the geothermal wells are more expensive to drill as compared with the oil and gas wells of the same depth. The figure prediction shows as the depth increase the cost increase exponentially.

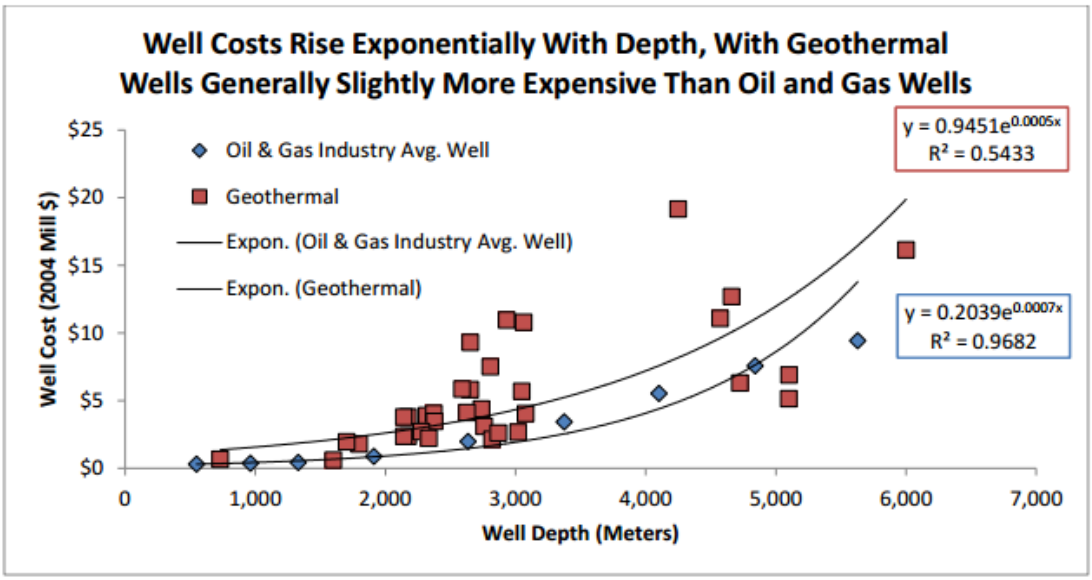

Figure 2.4: Geothermal and oil and gas industry average well costs compared with depth,(Initiative, 2006).

2.1.3 Geothermal Energy Advantage and Disadvantages

Like any other energy resources in the world, geothermal energy has its own set of advantages and disadvantages, some of these merits / challenges are listed in Table 2. As shown on the Table 3, as temperature higher than 200°C (392ºF), the more useful it is for power generation and other uses.

Table 2. Advantages and challenges of geothermal resources(Gehringer & Loksha, 2012).

The Pros and Cons of Geothermal Power

ADVANTAGE	DOWNSIDE/CHALLENGE
Globally inexhaustible (renewable)	Resource depletion can happen at individual reservoir level
Low/negligible emission of CO_2 and local air pollutants	Hydrogen sulfide (H_2S) and even CO_2 content is high in some reservoirs
Low requirement for land	Land or right-of-way issues may arise for access roads and transmission lines
No exposure to fuel price volatility or need to import fuel	Geothermal "fuel" is non-tradable and location-constrained
Stable base-load energy (no intermittency)	Limited ability of geothermal plant to follow load/respond to demand
Relatively low cost per kWh	High resource risk, high investment cost, and long project development cycle
Proven/mature technology	Geothermal steam fields require sophisticated maintenance
Scalable to utility size without taking up much land/space	Extensive drillings are required for a large geothermal plant

Table 3. Types and use of geothermal resources (Gehringer & Loksha, 2012).

Types and Uses of Geothermal Resources

RESOURCE TYPE BASED ON TEMPERATURE	GEOGRAPHICAL AND GEOLOGICAL LOCATION	USE / TECHNOLOGY
High: >200°C	Globally around boundaries of tectonic plates, on hot spots and volcanic areas	Power generation with conventional steam, flash, double flash, or dry steam technology
Medium: 150-200°C	Globally mainly in sedimentary geology or adjacent to high temperature resources	Power generation with binary power plants, e.g., ORC or Kalina technology
Low: <150°C	Exist in most countries (average temperature gradient of 30°C/km means that resources of about 150°C can be found at depths of about 5 km)	Direct uses (space and process heating, etc.) and, depending on location and power tariff offered, power generation with binary power plant

2.2 Chemistry of Geothermal Fluids and Their Consequences

Geothermal fluids contain different concentration of dissolved elements. The most important characteristics of geothermal fluids are: salinity(amount of dissolved solids) and pH (Povarov, Tomarov, & Semenov, 2000). The amount of and nature of these dissolved chemicals normally depend on the temperature and geology of the reservoir. Lower temperature reservoirs normally have less amount of dissolved chemicals as compared to reservoirs with higher temperatures even though there might be exceptions. Corrosion-aggressive gases are generally found in the following composition (Povarov et al., 2000): Carbon dioxide (60-95%) and hydrogen sulphide (2-15%). Table 4 shows a typical composition of geothermal waters according to Geothermal Community (Geothermal Systems and Technologies, 2014).

Table 4: Typical composition of geothermal waters (Community, 2016).

Species	Wairakei[2] wells ~ 1.5km	Rotorua[3] springs	Waitoa[4] springs	for comparison	
				Seawater[5]	River water
Cl-	2156	560	57	19350	5.7
Na+	1200	485	220	10760	4.8
SiO_2	660	490	175	0.005-0.01	13
K+	200	58.5	43	399	2
HBO_2^-	115	21.6	1.2	0.004	-
HCO_3^-	32	167	3177	142	23
SO_4^{2-}	25	88	<1	2710	6.7
Ca^{2+}	17.5	1.2	37	411	15
Li+	13.2	4.7	0.6	0.18	-
F-	8.1	6.4	0.3	0.0013	-
NH_3	0.15	0.2	-	-	-

[1] figures given in ppm, where ppm = mg/kg; [2] "neutral chloride" waters; [3] "acid sulfate" waters; [4] "alkali carbonate waters; [5] seawater has a pH range of 8.1-8.3 and river water has a pH range of 5-6.5

The presence of these elements leads to long-term well integrity problems like corrosion, erosion and scaling of the casings used for well completion.

2.2.1 Corrosion

Corrosion can be defined as the wear off of a material, usually metal, because of a reaction with its environment. This happen in the presence of an anode, cathode, electrolyte and an electrical current. The process of corrosion is illustrated in Figure 2.5 below.

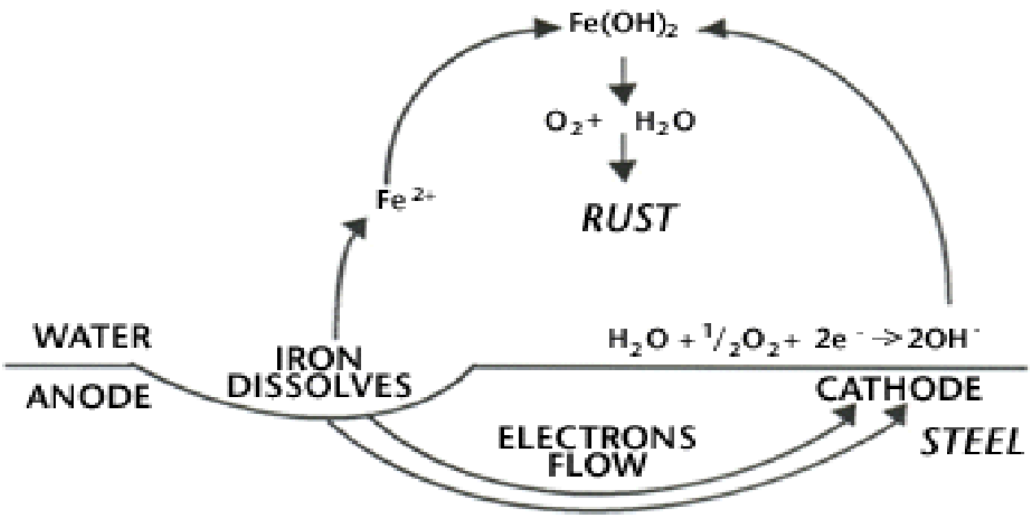

Figure 2.5: Electrochemical process (Kristanto, Kusumo, & Abdassah, 2005).

Increases in temperature may significantly influence corrosion (Schweitzer, 1996). Metallic and non-metallic materials in the well such as the wellhead, casing and cement are exposed to these fluids and therefore require extra precautions (Shadravan & Shine, 2015). Corrosion can both occur both internal and external parts of the casing, and the later primarily occurs when cement deteriorates which leaves the casing unprotected (Skimin, Snyder, & Dickie, 1979). Corrosion problems occur frequently in the well due to the highly corrosive geothermal steam and brine. (Ocampo-Diaz et al., 2005) listed the factors that contribute to corrosion attack:

- Carbon dioxide, CO_2
- Hydrogen Sulfide, H_2S
- Hydrogen Chloride, HCl
- Iron Sulfide, FeS
- Sulfuric acid, H_2SO_4
- Oxygen
- Temperature
- Suspended Solids
- Flow hydrodynamics

Common types of corrosion that occur in geothermal wells include: uniform corrosion, carbon dioxide corrosion, erosion corrosion, hydrogen sulphide corrosion, pitting, oxygen corrosion etc.

2.2.1.1 Uniform Corrosion

Uniform corrosion is the regular, uniform removal of metal from the surface and consequently it leads to a relatively uniform thickness reduction (Schweitzer, 1996). It is the basis for most corrosion prediction equations. The principle of uniform corrosion is shown on Figure 2.6.

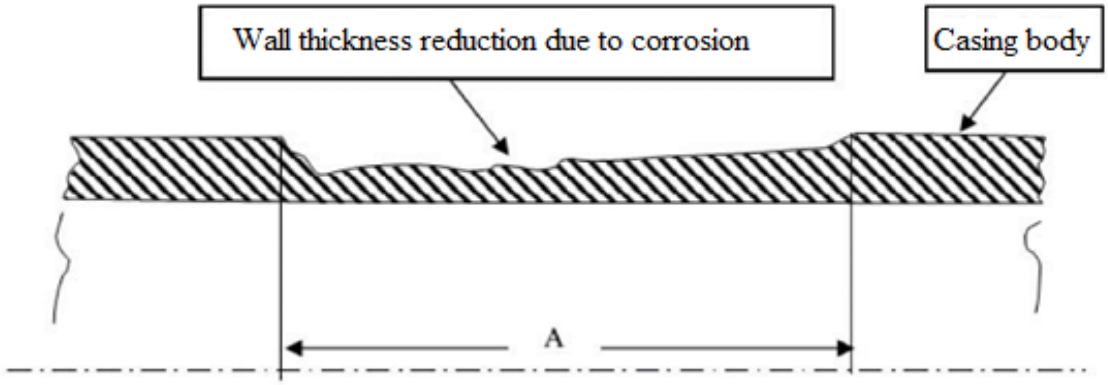

Figure 2.6: Uniform corrosion (Catalin Teodoriu, 2015).

2.2.1.2 Carbon dioxide Corrosion

The acidic nature of dissolved CO_2 dissolved helps in the deteriorating of metals which is known as carbon dioxide or sweet corrosion. The level of acidity of the solution depends on the partial pressure of the gas. Sweet corrosion rates are very high in fresh water environments at very high flow rates(Bellarby, 2009). The aggressiveness of CO_2 corrosion depends on the temperature, material characteristics and partial pressure among other factors(Takabe & Ueda, 2001). CO_2 corrosion can be the cause of both uniform and localize corrosion(Lopez, Perez, & Simison, 2003). A common CO_2 product is $FeCO_3$ as given in the by (Shadravan & Shine, 2015).

$$CO_2 + H_20 + Fe \rightarrow FeCO_3 + H_2$$

2.2.1.3 Oxygen Corrosion

Oxygen can cause problems in widespread water injection wells. Oxygen reacts quickly with carbon steel and most casings use API carbon steel tubing (Bellarby, 2009). According to (Byars & Gallop, 1972), oxygen corrosion have a potential to fill the reservoir completion and create plugging in addition to causing failures of tubing/casing.

Figure 2.7: Corroded water injecting carbon steel tubing (Bellarby, 2009).

2.2.1.4 Stress Corrosion Cracking

The presence of H_2S and CO_2 in produced fluids lead to the reaction with steal to form semi protective film of rust. The rust can easily be washed away on the surface by the flow of fluid. This leads to the exposure of more material for chemical attack in the presence of high temperature and pH. In much lower concentrations of sulphide, sulphide stress cracking (SSC) can occur (Bellarby, 2009). There are three contributing causes of stress cracking; environment, stress and material (Hodson-Clarke, Rudolf, Bour, &

Russell, 2016). In order to prevent stress corrosion cracking, any of the three cause has to be eliminated.

2.2.1.5 Erosion Corrosion

This kind corrosion takes place in flowing systems where turbulence occurs, typically in pipe bends (elbows), tube constrictions and other structures that alter flow direction or velocity. The mechanism for this type of corrosion is the continual flow of water, which removes any protective film or metal oxide from the metal surface. The exposed surface corrodes, and the resulting oxide is washed away. Erosion corrosion usually leads to rapid failure.

2.2.2 Scaling

The precipitation of salts from geothermal fluid during production is called scaling. Scaling occurs due to change in pressure, temperature or pH. Scaling is a challenge in most geothermal wells and can cause plugging of the well, require repair or replacement of equipment, and reduce well flow and power production((Karlsdottir, Ragnarsdottir, Moller, Thorbjornsson, & Einarsson, 2014);(Ocampo-Diaz et al., 2005); (Ólafsson, Hauksdóttir, Thórhallsson, & Snorrason, 2005)). Several types of scales occur in geothermal wells and installations. Among these include carbonate minerals (Calcite and aragonite), amorphous silicates, and metal oxides and sulphides. According to (Gunnlaugsson et al., 2014) the most common geothermal scales are silica (SiO_2) and calcite ($CaCO_3$). Scales in wells are removed by reaming. The number of times these scales happen depend on how regular they occur and the production levels. The temperature ranges of scaling depositions are (Ármannsson et al., 2014):

- Calcite scaling 180-240℃
- Slica scaling 240-290℃
- Slica and sulphide scaling >290℃

(Mundhenk et al., 2013), conducted an experimental research for understanding corrosion and scaling in a geothermal plant. The in-situ and laboratory experiments showed a substantial connection between corrosion and scaling. Mild steels such as API N80 and P110 were exposed to temperatures from 20℃ to 80℃ and from 1 week to 5 months. Corrosion scale occurred in both experiments and acted as a protector, reducing the corrosion aggression. Figure 2.8 shows a picture of calcite scaling inside a slotted liner in Krafla KJ-19. Most severe calcite scaling was at 280 [m] depth in 210℃ well (Fridriksson & Thórhallsson).

Figure 2.8: Calcite Scaling Inside a Slotted Liner in Krafla KJ-19 (Fridriksson & Thórhallsson).

2.3 Material Selection

Material selection for geothermal well construction is one of the factors of importance in the basic design of geothermal utilization schemes which are expected for long term service. There are localized problems of corrosions in geothermal installations, but most of them are manageable with proper material selection, operation and maintenance.

2.3.1 Metallic Materials

According to NORSOK standard M-001, metallic materials are divided into carbon and low alloyed steels, stainless steels, nickel-based alloys, copper-based alloys and titanium and titanium-based alloys.

2.3.1.1 Carbon and Low Alloyed Metals

Low carbon steels are less expensive and convenient to use in geothermal wells but on the other hand, their usage is limited especially in thin walled systems because of the risk of crack, pit corrosion and uniform corrosion. Sulphur stressed breaking can be seen in steel materials which are subjected to hydrogen sulphide under stressed conditions water environments ((Conover, 1982);(Ellis, 1985)). It increases with the increase in temperature, decrease in strength, decrease in stress, and decrease in the concentration of Sulphur and increase in pH.

2.3.1.2 Stainless Steel

The probability of uniform corrosion decreases in stainless steels in geothermal environments. However, pit corrosion, cracking corrosion, H_2S corrosion may occur depending on which type of stainless steel is used. Increase in Chromium and Molybdenum content in stainless steel, increases the resistance of stainless steel to pit and cracking corrosion. The addition of Molybdenum and silica increases the resistance to stressed corrosion (Conover, 1982). According to (Kaya & Hoshan, 2005), AISI 430(Ferrite) is preferred when geothermal fluids contain high concentration of chlorine

ions, Sulphur and oxygen. AISI 300 series stainless steels show well performance in geothermal condensates at low temperatures and geothermal fluids not containing oxygen (Lichti, 1989). The types of stainless steels according to NORSOK standard M-001 include: Martensitic, Ferrite, Austenitic and Duplex stainless steel.

2.3.1.3 Titanium and Titanium Alloys

Corrosion rates of titanium materials in geothermal environments are usually lower(Kaya & Hoshan, 2005). Titanium is fairly resistant to corrosion as compared to the other metallic materials. Pit and cracking corrosions are still observed at high temperatures and for high chlorine ion concentrations ((Conover, 1982);(Ellis, 1985)).

Titanium alloys are much more resistant to local corrosion than pure titanium. Titanium alloys are much more resistant to local corrosion than pure titanium. Ti-code-7 (Ti-0.15 Pd), Ti code-12 (Ti-0.3 Mo-0.8 Ni), and Ti-code-29 (Ti-6 Al-4 V-0.1 Ru) show well resistance (Kaya & Hoshan, 2005). Titanium alloy scan be used in when the concentration of chlorine ion is greater than 5000 ppm and the temperature above 100 ℃ (Sanada et al., 2000). On the basis of cost, using titanium and its alloys is more expensive than using other metallic alloys.

2.3.1.4 Nickel Based Alloys

Nickel based alloys withstand corrosion much better than the other materials. The combination of nickel with other metals helps in their resistance to different kind of corrosions depending on the kind of combination. For example, for high temperature geothermal wells, it is suitable to use Ni-Co-Mo alloys as material (Sanada et al., 2000). On the other hand, Inconel-625 and Hastelloy C-625 are very strong for the corrosion ((Conover, 1982);(Ellis, 1985);(Lichti, 1989)).

2.3.1.5 Copper Based Alloys

Copper based alloys have been known to show cracks in the presence of high amount of Sulphur in geothermal wells. In cases when the amount of ammoniac and ammonium are low, the cracks on the metal surfaces are limited((Conover, 1982);(Ellis, 1985);(Lichti,

1989)). Experiments done on copper-zinc and copper-tin alloys shows that they are not suitable for corrosion. Similarly, copper alloys are not very suitable for excessive heat (Kaya & Hoshan, 2005).

2.3.2 Non-Metallic Materials

Metals are generally used in geothermal well completions. Non-metallic materials are being used in some special cases such as the use of elastomers. The initial investment is lower in non-metallic materials than in metallic materials (Kaya & Hoshan, 2005). Non-metallic materials are general strong against corrosive environments as compared to metals and alloys. Some specific non-metallic materials which are used in the geothermal field are listed below((Conover, 1982);(Ellis, 1985);(Lichti, 1989);(Sanada et al., 2000);(Lund, Lienau, & Culver, 1990)):

- Elastomers
- Cements
- Concrete and polymer composition
- Fiber reinforced materials

3 Theory

This part of the thesis presents the theory of tubing stress analysis, which is the basis of tubing/casing/drill string design. It also presents the basic theory behind the commercial WellCAT™ simulation used later in this work.

3.1 Tubular Stress Theory

This section presents the theory of thermal and pressure induced stresses in circular cylinder, which describes the state of stress in drill string/tubing/casing. From the theory, we will compute limiting curves, string (tube/drill pipe/casing) collapse and burst design equations, a permissible tensile load will be compute.

Three pressure limit models to that exist are:

1. Triaxial
2. Biaxial
3. API

However, for the purpose of this thesis, we will evaluate on the triaxial pressure limit model. Figure 3.1 is a circular pipe with wall thickness, *t*, and inner radius, *r*. The pipe is pressurized internally and externally with P_i and P_o, respectively. It is also loaded axially with load F_a and also be loaded with torque. The figure shows an element of material subjected to stress σ_h, σ_θ, and σ_z in three perpendicular directions(Belayneh, 2018).

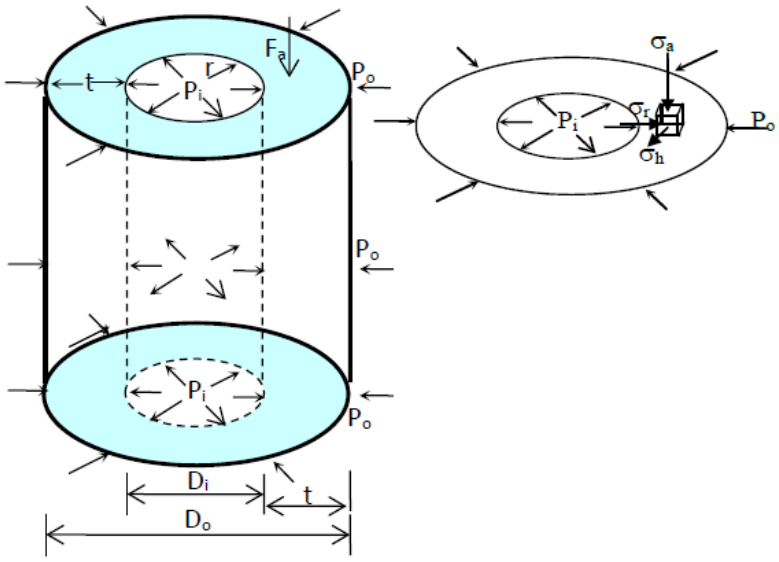

Figure 3.1: Triaxial stress on circular pipe(Belayneh, 2018).

3.2 Cylinder Types

There are two categories of circular cylinder which are using on the stress and failure analysis theory. Following are the categories of the circular cylinder,

1. Thick walled cylinder. This type of cylinder is defined when,

$$t > \frac{1}{10} r_i \tag{3.1}$$

2. Thin walled cylinder. This type of cylinder is defined when,

$$t < \frac{1}{10} r_i \tag{3.2}$$

Where, t is defined as the thickness of the cylinder and r is defined as the inner cylinder radius.

3.2.1 Thin Walled Cylinder Stress

Thin walled cylinder is defined previously on the equation (3.2). For the analysis of thin walled cylinder, assume a thin-walled cylinder subjected with internal pressure, P_i as illustrated on the Figure 3.2.

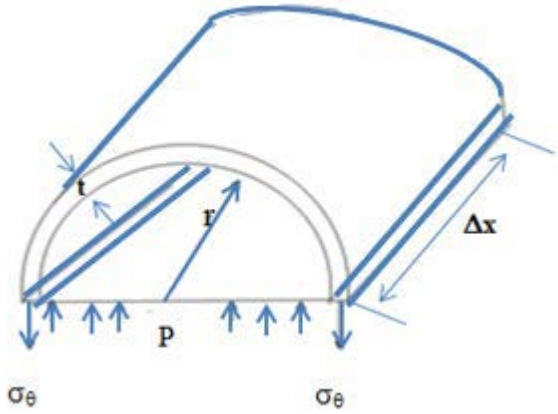

Figure 3.2: Illustration of a thin walled cylinder(Belayneh, 2018).

Where, *Δx* is defined as the length of the cylinder, *t* is defined as the thickness of the cylinder and *P* is defined as the pressure at cylinder wall.

The analysis of thin walled cylinder is categorized into two cases. First case is open thin walled cylinder and closed end thin walled cylinder.

3.2.1.1 Open Thin Walled Cylinder

3.2.1.1.1 Hoop Stress

Only hoop stress exists.

$$2\sigma_\theta . t\Delta X = 2 . r . \Delta X . P \tag{3.3}$$

Hence, the solution for the hoop stress is

$$\sigma_\theta = \frac{P . r}{t} \tag{3.4}$$

3.2.1.1.2 Axial Stress

The axial stress does not exist on the open end thin walled cylinder case.

3.2.1.2 Closed-End Thin Walled Cylinder

In this situation, the hoop and axial stress exist on the thin walled cylinder.

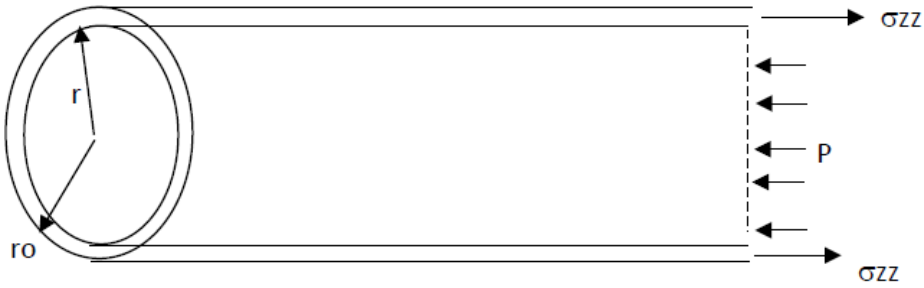

Figure 3.3: Free body diagram of closed end thin walled cylinder(Belayneh, 2018).

3.2.1.2.1 Hoop Stress

The solution for hoop stress on the closed end thin walled cylinder case is the same with the open end thin walled cylinder case.

$$\sigma_\theta = \frac{P.r}{t} \tag{3.5}$$

3.2.1.2.2 Axial Stress

From the balance of force concept, the axial force is given as,

$$\sigma_z.\pi(r_o^2 - r^2) = \pi.r^2.P \tag{3.6}$$

Or the equation (3.6) can be written as,

$$\sigma_z.\pi(2.r.t + r^2) = \pi.r^2.P \tag{3.7}$$

By assuming t^2 is very small, the $2.r.t + r^2$ is approximated into $2.r.t$ form. The equation (3.6) can be written as,

$$\sigma_z.2.\pi.r.t = \pi.r^2.P \tag{3.8}$$

The axial stress on the closed end thin wall cylinder is obtained by,

$$\sigma_z = \frac{P.r}{2.t} \tag{3.9}$$

3.2.2 Thick Walled Cylinder Stress

Thick walled cylinder is defined previously on the equation (3.1). For the analysis of this particular cylinder, assume uniform pressure is imposed to the cylinder. Stresses are produced across the thickness of cylinder in the radial, axial and circumferential direction as described in Figure 3.4 below. The stresses which appear on the cylinder are called as the radial, axial, and tangential stresses respectively. The derivation stress field on the thick-walled cylinder is needed to obtain design safety operational limits of the pipe (Belayneh, 2018).

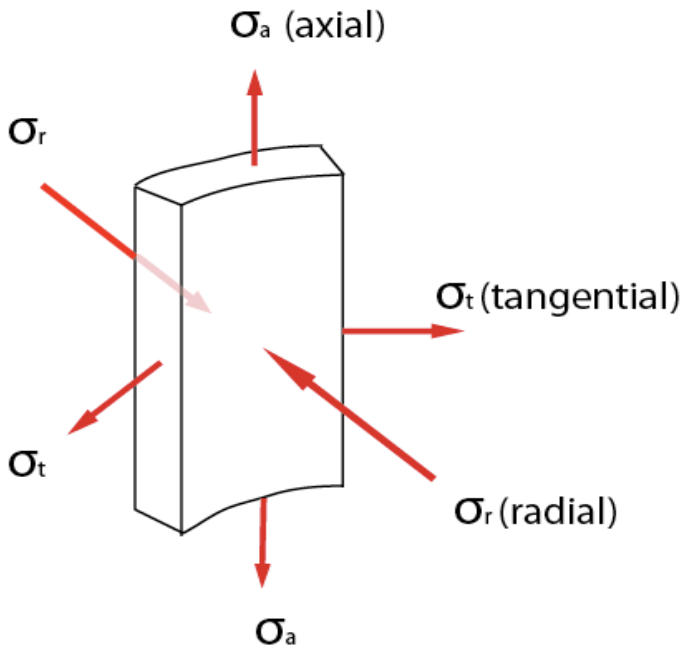

Figure 3.4: Stresses in thick walled cylinder(Belayneh, 2018).

3.2.2.1 Stress Fields in Thick Walled Cylinder

Using combination of equilibrium equation, compatibility and constitutive relations, and suitable boundary conditions. The derivation stress field across wall thickness of cylinder can be obtained. Following are the derivation result of the stress field across the wall thickness of cylinder(Belayneh, 2018).

3.2.2.1.1 Radial Stress

$$\sigma_r = \frac{p_a a^2 - p_b b^2}{b^2 - a^2} - \frac{a^2 b^2}{(b^2 - a^2) r^2}(p_a - p_b) + \sigma_r(\Delta T) \qquad (3.10)$$

3.2.2.1.2 Hoop Stress

$$\sigma_\theta = \frac{p_a a^2 - p_b b^2}{b^2 - a^2} - \frac{a^2 b^2}{(b^2 - a^2) r^2}(p_a - p_b) + \sigma_\theta(\Delta T) \qquad (3.11)$$

3.2.2.1.3 Axial Stress

Prior to solving the axial stress, the "real force", F_a and "effective force", F_e must be defined. The actual axial force in the pipe wall is called real force and effective force is the axial force by neglecting effects of pressure on the pipe.

$$\sigma_a = \frac{F_a}{A} + \frac{P_a a^2 - P_b b^2}{(b^2 - a^2)} + \sigma_a(\Delta T) \qquad (3.12)$$

Equation (3.10) to (3.12) are the solution for thick walled cylinder. Moreover, the relationship between real and effective force can be written as:

$$F_a = F_a + P_a A_a - P_b A_b \qquad (3.13)$$

The equation (3.13) on the above is applied for thin walled cylinder case. Hence the equation (3.13) is used for the drilling pipe case since most of drilling pipe are thin walled cylinder. Figure 3.5 below is the illustration of the stress distribution across the wall of cylinder for thick walled cylinder case.

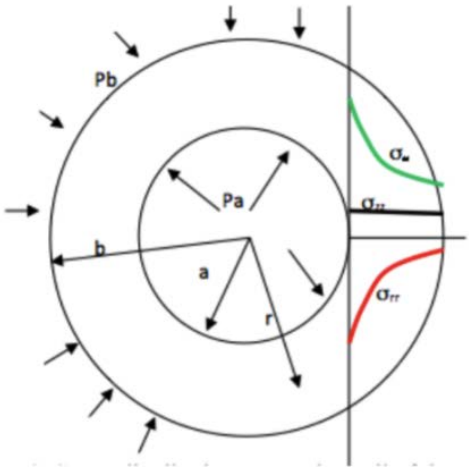

Figure 3.5: Stress distribution across cylinder's wall(Belayneh, 2018).

Temperature induced stresses for steady-state temperature distribution in a thick-walled cylinder can be given as in equations (3.14)-(3.16). The stresses will be added with pressure induced stresses given in equation (3.10)-(3.12). These stresses are (BORES & SCHMIDT, 2003):

$$\sigma_r(\Delta T) = \frac{\alpha E \Delta T}{2(1-\vartheta)ln\left(\frac{b}{a}\right)}\left[-ln\left(\frac{b}{r}\right) + \frac{a^2(b^2-r^2)}{r^2(b^2-a^2)}ln\left(\frac{b}{a}\right)\right] \quad (3.14)$$

$$\sigma_\theta(\Delta T) = \frac{\alpha E \Delta T}{2(1-\vartheta)ln\left(\frac{b}{a}\right)}\left[1 - ln\left(\frac{b}{r}\right) - \frac{a^2(b^2-r^2)}{r^2(b^2-a^2)}ln\left(\frac{b}{a}\right)\right] \quad (3.15)$$

$$\sigma_z(\Delta T) = \frac{\alpha E \Delta T}{2(1-\vartheta)ln\left(\frac{b}{a}\right)}\left[1 - 2ln\left(\frac{b}{r}\right) - \frac{2a^2}{(b^2-a^2)}ln\left(\frac{b}{a}\right)\right] \quad (3.16)$$

3.2.3 Failure Criteria – von Mises

The von Mises yield condition is commonly used to describe the yielding of steel under combined states of stress. Unlike others, this theory takes the intermediate stress in to considerations. For instance, for a cylindrical structure, the initial yield limit is based on the combination of the three principle stresses (axial stress, radial stress, and hoop stress)

and the shear stress caused by torque. Yielding as a function of the combined three stresses is given by:

$$\sigma_{VME} = \sqrt{\frac{1}{2}\{(\sigma_\theta - \sigma_r)^2 + (\sigma_r - \sigma_a)^2 + (\sigma_a - \sigma_\theta)^2\} + 3\boldsymbol{\tau}^2} \quad (3.17)$$

Note that if there is no torque, the shear stress term drops out of the equation. The yield limits for tubing are calculated by setting the von Mises stress, σ_{VME} to the yield stress, σ_y for the material.

3.2.4 Tubular Design Models

Pipe yields when the Von-Mises stress reaches yielding. The tri-axial stress intensity design factor is given by:

$$SF = \frac{\sigma_y}{\sigma_{VME}} \quad (3.18)$$

σ_y is minimum yield strength.

3.2.4.1 Tri-axial Burst

The burst pressure may be calculated by solving for P_i and given as:

$$P_i = \frac{\beta\sigma_a - 2\sigma_a + 2\beta^2 P_o - \beta P_O \pm \sqrt{-3\beta^2\sigma_a^2 - 6\beta^2\sigma_a P_o - 3\beta^2 P_O^2 + 4(\beta^2 - \beta + 1)\sigma_y^2}}{2(\beta^2 - \beta + 1)} \quad (3.19)$$

There are two solutions for P_i from the equation above (positive and negative square roots). Practically, only positive real number(s) represent the burst pressure. In the equation, if σ_y is replaced with σ_{S-SF} and σ_a is replaced with σ_{amax}, the outcome of the equation is then results the burst design pressure for triaxial method. Where the allowable maximum stress is given by:

$$\sigma_{S-SF} = \sigma_y / SF \quad (3.20)$$

And the maximum axial stress is given by:

$$\sigma_{amax}=\sigma_a + \sigma_{DL} \tag{3.21}$$

σ_{DL} = Dogleg Yield Stress

The Figure 3.6 below shows an example of a burst pipe.

Figure 3.6: Burst pipe(Belayneh, 2018).

3.2.4.2 Tri-axial Collapse

The equation for solving the triaxial collapse pressure is given by:

$$P_o = \frac{-\sigma_a+2\beta P_i-P_i\pm\sqrt{-3\sigma_a^2-6\sigma_a P_i-3P_i^2+4\sigma_y^2}}{2\beta} \tag{3.22}$$

For collapse pressure design, there can be one or two solution(s). When bending stress is considered, Equation 3.22 is replaced with equation 3.21. This results in the solution for collapse pressure design with maximum bending stress effects. Figure 3.7 shows an example of a collapsed pipe.

Figure 3.7: Collapsed pipe(Belayneh, 2018).

3.1.4.3 API Burst

The API burst rating (Filippov et al., 1999) is based on Barlow's formula for thin walled pipe. This has been given as:

$$P_b = Tolerance * \frac{2\sigma_y t}{D} \tag{3.23}$$

Where σ_y is the minimum yield strength (bar), *t* is the nominal tubing thickness (m), D is the tubing outer diameter (m), Tolerance =1/SF is the wall thickness tolerance correction (fraction). According to API the safety factor is 8/7. The tolerance is therefore = 87,5%. This factor assumes that 12.5% of the thickness could have been removed by corrosion or wear effects. For casing the most common issue is wear, and for tubing it is corrosion.

3.3 Heat Transfer Mechanisms

Heat transfer is the transfer of thermal energy due to change in temperature. The movement of heat is from hot to cold surfaces. Heat transfer mechanism is divided into e

main methods; conduction, convection and radiation. These mechanisms are independent of each other but they all result into the overall heat transfer in a system.

3.3.1 Conduction

Heat conduction is the transfer of energy (internal energy) from higher internal energy to the neighboring lesser less energetic. Figure 3.8 illustrates the Heat transfer through a plane slab. The temperature at one side is higher than the other side ($T_1 > T_2$). For one dimensional, the heat transfer flux is proportional to the change in temperature and inversely proportional to the distance between the as showed in equation 3.24.

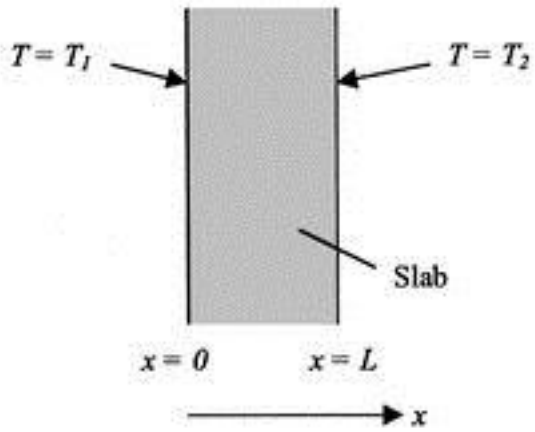

Figure 3.8: Temperature boundary conditions for a slab (Nathan Amuri, 2017).

In order to emphasize the heat flux proportionality with temperature, the equation can be expanded and written in the following form:

$$\dot{Q_{cd}} = -k\frac{dT}{dx} = -k\frac{T_2 - T_1}{L} \tag{3.24}$$

Where $\dot{Q_{cd}}$ is conductive heat flux, T is temperature and *k* is thermal conductivity.

3.3.2 Convection

Convection is the mode of heat transfer through a liquid or gas medium in motion. This can be from a solid surface to liquid or gas. When the motion of a medium is caused by an external source such as pump or the wind (Figure 3.9), then the convection is called force convection. In contrast, buoyancy forces cause the so-called natural convection, which is also caused by density differences within the fluid, owing to temperature variation within the fluid.

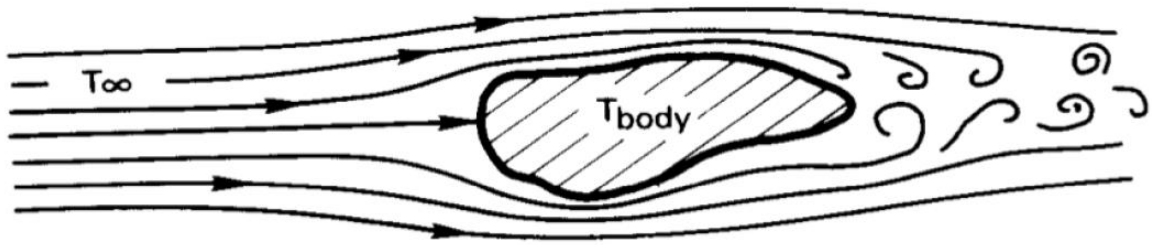

Figure 3.9: Heat Convection through two media(Nathan Amuri, 2017).

Newton's law of cooling as shown below represents the convection heat flux:

$$\dot{Q_{cv}} = -kA_s(T_S - T_\infty) \tag{3.25}$$

Where T_s is the temperature of the heat source and T_∞ is the temperature of the surrounding fluid, $\dot{Q_{cv}}$ convectional heat flux, k is thermal conductivity.

3.3.3 Radiation

Radiation is the energy released by an object in the form of electromagnetic waves owing to changes in the electronic distribution of the atoms. The heat emitted by radiation an object depends on many factors, such has hot is an object, object's ability to absorb heat and the color of an object. Stefan–Boltzmann law represents radiation that is achieved at a room temperature:

$$\dot{Q_{rd}} = \sigma A_s T_s^4 \tag{3.26}$$

Where $\dot{Q_{rd}}$ the radiation heat flux, σ Stefan-Boltzmann constant, A_S area of radiated surface and T is the absolute temperature.

3.4 Rate of Heat Flow

The rate of heat flow is the defined as the heat flow per unit length of the wellbore. It is also known as overall heat transfer or heat exchange. The following equation represents the rate of heat flow, Q (Ichim et al., 2016).

$$Q = -2\pi \cdot r_{to} \cdot U_{to}\left(T_f - T_{wb}\right) \tag{3.27}$$

Where U_{to} the overall heat transfer coefficient in [BTU/hr-ft^2-°F], $(T_f - T_{wb})$ is the temperature difference between the wellbore interface and wellbore fluid and $2\pi \cdot r_{to}$ is the tubing outside area. A positive heat exchange implies that heat flows from the wellbore to the formation and a negative heat exchange implies the opposite.

3.4.1 Thermal Conductivity

Thermal conductivity is the ability of a material to conduct heat. It is an important property of materials in geothermal wells. It is "the quantity of heat(Q) transmitted through a unit thickness(L) in one direction normal to a surface of unit area(A) due to a unit change in temperature gradient(ΔT) under steady conditions and when the heat transfer is dependent only on the temperature gradient" (Ichim et al., 2016). It is represented by equation 3.28 (Ichim et al., 2016).

$$k = \frac{Q \cdot L}{A \cdot \Delta T} \tag{3.28}$$

It is expressed in [W/mK] or [BTU/hr-ft-°F].

In this work, the thermal conductivity of cement will be varied from 0,14 to 7 [W/mK] as conventional thermal conductivity of cement ranges from 0.2 to 3.63 [W/mK] ((Wenger et al., 2011); (Baghban, Hovde, & Jacobsen, 2013)). The thermal conductivity of insulators and casings will also be varied to determine their effect on the overall heat transfer of fluid in geothermal wells.

4 Mathematical Modeling

This chapter presents the modeling for overall heat transfer coefficient and heat-loss calculations across the production tubing to well formation. The analysis is based on the classical paper published by (G. Paul Willhite, 1967). The idea of this analysis is as the fluid well flowing to surface, we will try to analyze the heat loss in the presence of inner and outer insulator and in the absence of insulator for various cement heat conductivity.

4.1 Well Set-up and Assumptions

As shown in Figure 4.1, steam flows from reservoir to surface or injected downward to the reservoir, there exist heat transfer mechanisms, which were described in section 3.2, and hence the fluid flow losses heat energy to the surrounding formation. This heat loss may result in the change of thermodynamic states and hence phase change with subsequent reduction in steam quality and enthalpy may occur.

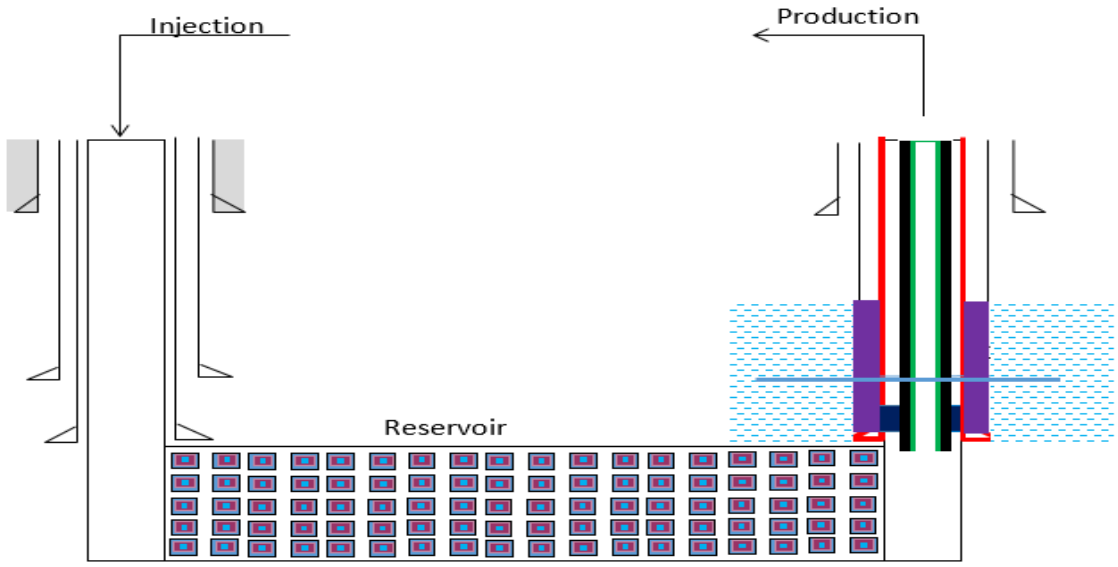

Figure 4.1: Illustration of injection well, reservoir and production well(Nathan Amuri, 2017).

As indicated by (G. Paul Willhite, 1967), heat loss attains a quasi-steady state at which the rate of heat loss is a monotonically decrease with as time increases. However, for simplicity, in this thesis the assumptions for the modeling are:

1. Heat transfer is assumed to be a steady state heat transfer around the wellbore.
2. The thermal property of the wellbore and formation such as heat diffusivity and the conductivity are assumed to be constant throughout the well structure.
3. Water is a working fluid.
4. Seawater is used as completion fluid, which is completely isolated from production fluid.

Consider a typical well construction, which contains tubing, annular completion fluid, casing, cement and formation. Figure 4.1.2a and 4.1.2b illustrate the horizontal and the vertical cross-sections of the overburden part of production well. As fluid flows along the tubing, as mentioned earlier, the heat transfer occurs through the three mechanisms from well to the undisturbed formation temperature.

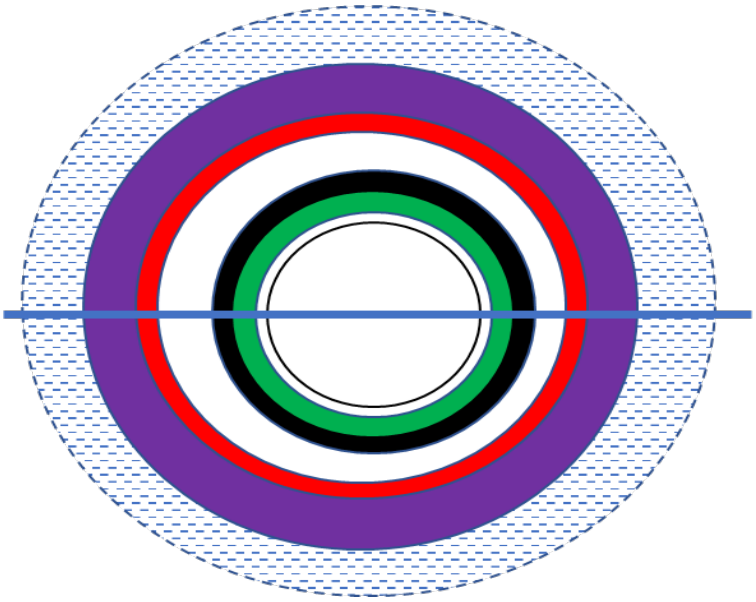

Figure 4.2a: Illustration of the horizontal cross-section of the well

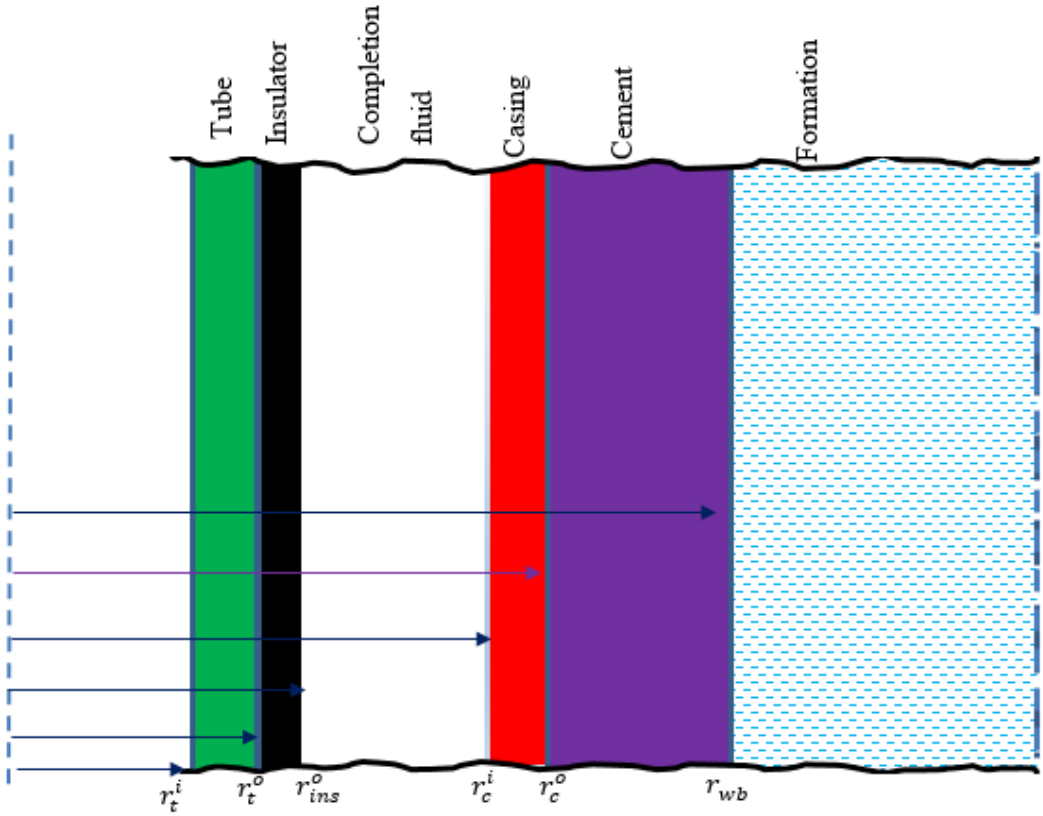

Figure 4.2b: Illustration of the vertical cross-section of the well

4.2 Heat Transfer Modeling

Due to temperature difference between the flowing fluid and the formation, heat influx radially across the wellbore structure. As shown in Equation 4.9, the higher the temperature difference and the cross-sectional area is the higher rate of heat flow. This shows the direct proportional and the proportionality constant term is known as the over-all heat transfer coefficient. The physical meaning of the overall heat transfer coefficient is that it analogues like a net resistance for flowing fluid, tubing, insulating material, casing completion fluid, casing wall and cement sheath to the flow of heat.

There are three heat transfer mechanisms, conduction, convection and radiation. Heat transfer rate in the annulus is due to the combined effect of natural convection and

conduction (h_c) and radiation, (h_r) (G. Paul Willhite, 1967). The heat transfer Q, is therefore given as (G. Paul Willhite, 1967):

$$Q = 2\pi r_{ins}^{o}(h_c + h_r)(T_{ins}^{o} - T_c^{i})\Delta L \quad 4.1$$

The heat transfer rate between the flowing fluid in the tube and the inside wall the tubing is given as:

$$Q = 2\pi r_t^{i} h_f (T_f - T_t^{i})\Delta L \quad 4.2$$

Where, h_f is the film heat transfer coefficient on the inside surface of the tube. The temperature difference $(T_f - T_t^{i})$ is the temperature between fluid flowing and the temperature at the inner wall.

Heat transfer through conduction in each components is given as (G. Paul Willhite, 1967):

Tubing $$Q = \frac{2\pi k_t (T_t^{i} - T_t^{o})\Delta L}{\ln(\frac{r_t^{o}}{r_t^{i}})} \quad 4.3$$

Outer Insulator $$Q = \frac{2\pi k_{ins}^{o} (T_t^{o} - T_{ins}^{o})\Delta L}{\ln(\frac{r_{ins}^{o}}{r_t^{o}})} \quad 4.4$$

Casing $$Q = \frac{2\pi k_{csg} (T_c^{i} - T_c^{o})\Delta L}{\ln(\frac{r_c^{o}}{r_c^{i}})} \quad 4.5$$

Cement $$Q = \frac{2\pi k_{cem} (T_c^{o} - T_{wb})\Delta L}{\ln(\frac{r_{wb}}{r_c^{o}})} \quad 4.6$$

The temperature difference between the well and the formation can be written as the sum of the temperature difference across each components of Figure 4.2 given as Equation 4.7:

$$T_f - T_{wb} = (T_f - T_t^i) + (T_t^i - T_t^o) + (T_t^o - T_{ins}^o) + (T_{ins}^o - T_c^i) + (T_c^i - T_c^o) + (T_c^o - T_{wb}) \quad 4.7$$

Inserting the temperature differences obtained from Eq. 4.1- 4.6 into Eq. 4.7, we get:

$$T_f - T_{wb} = \frac{Q}{2\pi\Delta L}\left[\frac{r_t^o}{r_t^i h_f} + \frac{r_t^o \ln(\frac{r_t^o}{r_t^i})}{k_t} + \frac{r_t^o \ln(\frac{r_{ins}^o}{r_t^o})}{k_{ins}} + \frac{r_t^o}{r_{ins}^o(h_c+h_r)} + \frac{r_t^o \ln(\frac{r_c^o}{r_c^i})}{k_{csg}} + \frac{r_t^o \ln(\frac{r_{wb}}{r_c^o})}{k_{cem}}\right] \quad 4.8$$

Assuming that a hot reservoir fluid is flowing through the production tube. Using the temperature difference between the flowing fluid (T_f) and the formation, (T_{wb}) at the formation/cement interface and the outer surface area of the tubing, the steady state heat transfer rate can be given by equation 4.7 as (G. Paul Willhite, 1967):

$$Q = 2\pi r_t^o U_{to}(T_f - T_{wb})\Delta L \quad 4.9$$

Using 4.8 and Eq. 4.9, the overall heat transfer coefficient, which accounts for the net-resistance to the heat flow through the components of the well structure shown on Figure 5.1.2 is given as:

$$\frac{1}{U_{to}} = \frac{r_t^o}{r_t^i h_f} + \frac{r_t^o \ln(\frac{r_t^o}{r_t^i})}{k_t} + \frac{r_t^o \ln(\frac{r_{ins}^o}{r_t^o})}{k_{ins}} + \frac{r_t^o}{r_{ins}^o(h_c+h_r)} + \frac{r_t^o \ln(\frac{r_c^o}{r_c^i})}{k_{csg}} + \frac{r_t^o \ln(\frac{r_{wb}}{r_c^o})}{k_{cem}} \quad 4.10$$

4.2.1 Model 1: At Reservoir Section

The reservoir section of the well consist of the inner and outer insulators, production casing/tubing and the cement behind the production casing. It is assumed that, the production casing is cemented and perforated in this zone. Figures 4.3a and 4.3b show illustrations of the horizontal and vertical cross-sections of the reservoir section of the well respectively.

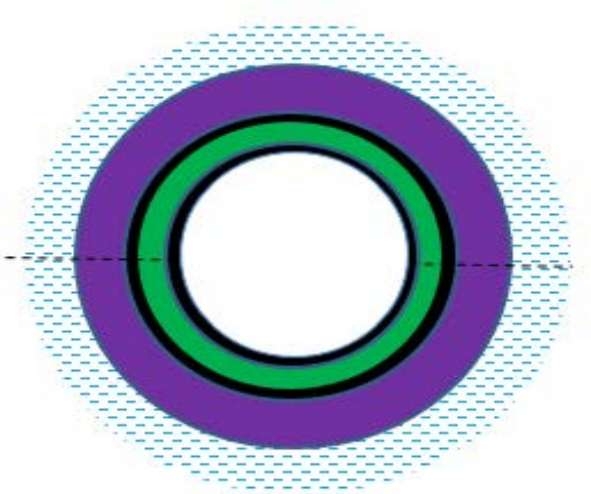

Figure 4.3a: Illustration of the horizontal cross-section of the reservoir section of the well

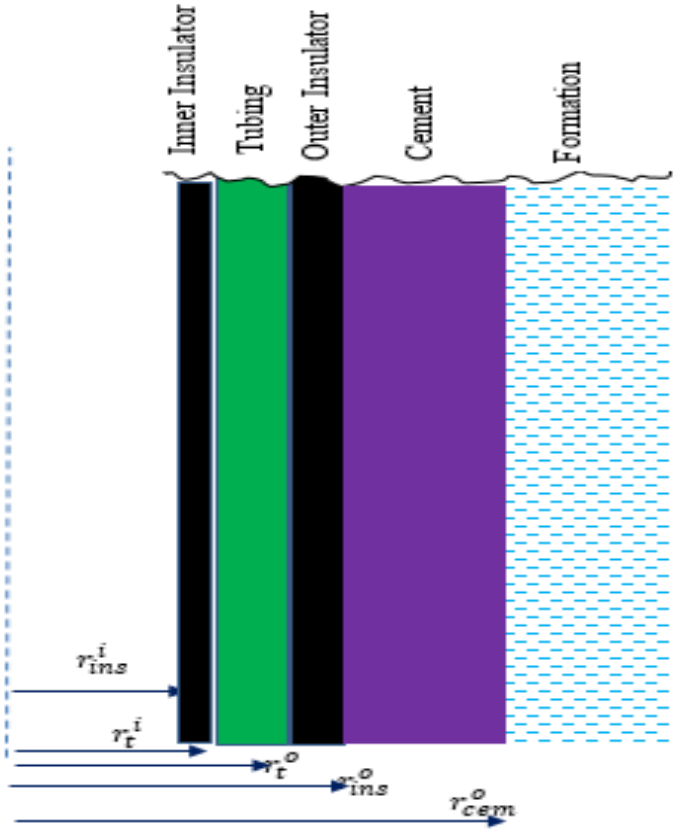

Figure 4.3b: Illustration of vertical cross-section of the reservoir section

Heat transfer through conduction in the inner insulator is given by:

Inner Insulator

$$Q = \frac{2\pi k_{ins}^{i}(T_t^o - T_{ins}^i)\Delta L}{\ln(\frac{r_{ins}^i}{r_t^o})} \quad 4.11$$

The temperature difference between the well and the reservoir can be written as the sum of temperature difference across each component of figure 4.3b given in Equation 4.12.

$$T_f - T_{wb} = (T_f - T_{ins}^i) + (T_{ins}^i - T_{ins}^{io}) + (T_{ins}^{io} - T_t^i) + (T_t^i - T_t^o) + (T_t^o - T_{ins}^{oi}) + (T_{ins}^{oi} - T_{ins}^o) + (T_{ins}^o - T_{cem}^i) + (T_{cem}^i - T_{cem}^o) + (T_{cem}^o - T_{wb}) \quad 4.12$$

Inserting equations 4.1-4.6 and 4.11 into equation 4.12, we get:

$$T_f - T_{wb} = \frac{Q}{2\pi\Delta L}\left[\frac{r_t^o}{r_{ins}^i h_f} + \frac{r_t^o \ln(\frac{r_t^o}{r_t^i})}{k_t} + \frac{r_t^o \ln(\frac{r_{ins}^i}{r_t^o})}{k_{ins}^i} + \frac{r_t^o \ln(\frac{r_{ins}^o}{r_t^o})}{k_{ins}^o} + \frac{r_t^o}{r_{ins}^i(h_c+h_r)} + \frac{r_t^o \ln(\frac{r_{wb}}{r_c^o})}{k_{cem}}\right] \quad 4.13$$

Assuming that hot reservoir fluid is flowing through the inner insulation, production casing, outer insulation, and cement and to the reservoir, the steady state rate of heat transfer can be calculated by using equation 4.7.

The overall heat transfer coefficient for the reservoir section can be calculated by the following equation 4.14

$$\frac{1}{U_{to}} = \frac{r_t^o}{r_{ins}^i h_f} + \frac{r_t^o \ln(\frac{r_t^o}{r_t^i})}{k_t} + \frac{r_t^o \ln(\frac{r_{ins}^i}{r_t^o})}{k_{ins}^i} + \frac{r_t^o \ln(\frac{r_{ins}^o}{r_t^o})}{k_{ins}^o} + \frac{r_t^o}{r_{ins}^i(h_c+h_r)} + \frac{r_t^o \ln(\frac{r_{wb}}{r_c^o})}{k_{cem}} \quad 4.14$$

4.2.2 Model 2: At Middle Section

The middle section consists of the zone above the reservoir section. It is made-up of an intermediate casing which is cemented to the surface of the wellbore, an annulus filled

with sea water as completion fluid, production casing and an outer and inner insulation. Figures 4.4a and 4.4b show illustrations of the horizontal and vertical cross-sections of the middle section of the well respectively.

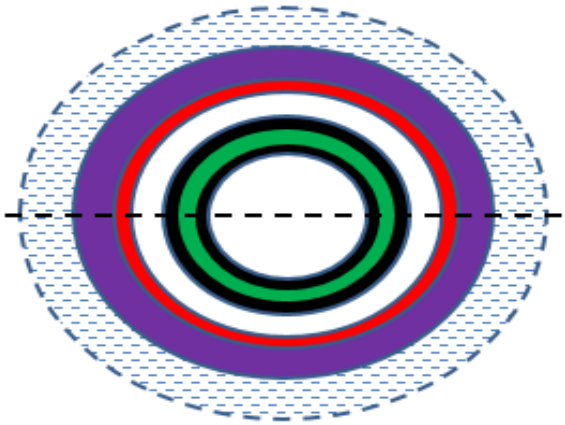

Figure 4.4a: Illustration of the horizontal cross-section of the well

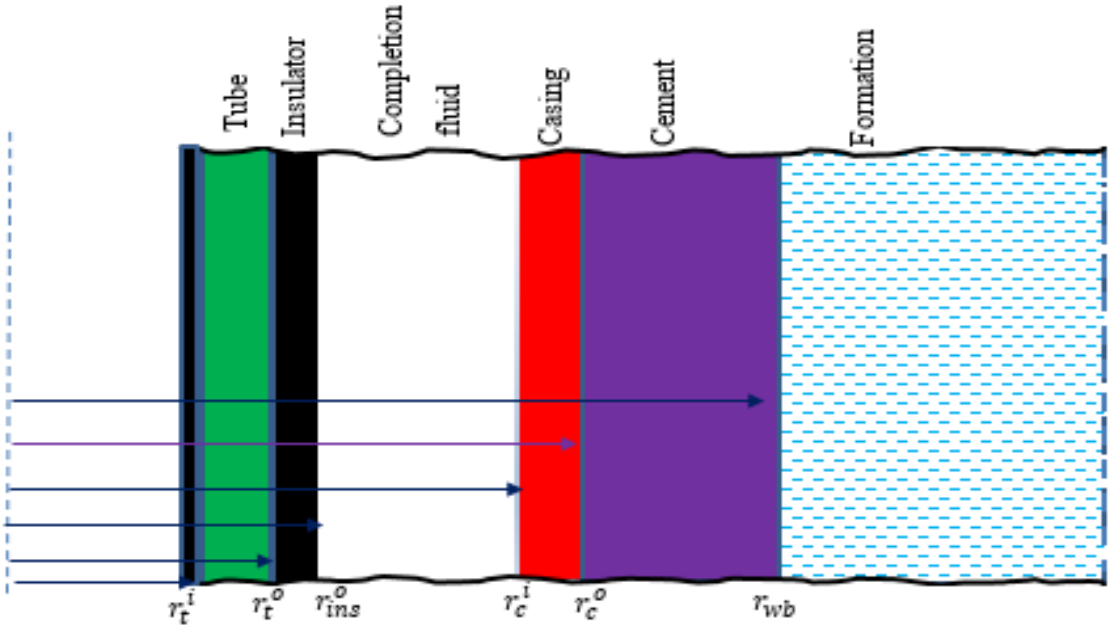

Figure 4.4b: Illustration of vertical cross-section of the reservoir section

The temperature difference between the well and the formation of the middle section can be written as the sum of temperature difference across each component of figure 4.4b given in Equation 4.15.

$$T_f - T_{wb} = (T_f - T_{ins}^i) + (T_{ins}^i - T_{ins}^{io}) + (T_{ins}^{io} - T_t^i) + (T_t^i - T_t^o) + (T_t^o - T_{ins}^{oi}) + (T_{ins}^{oi} - T_{ins}^o) + (T_{ins}^o - T_c^i) + (T_c^i - T_c^o) + (T_c^o - T_{cem}^i) + (T_{cem}^o - T_{wb}) \quad 4.15$$

Inserting equations 4.1-4.6 and 4.15 into equation 4.12, we get:

$$T_f - T_{wb} = \frac{Q}{2\pi\Delta L}\left[\frac{r_t^o}{r_{ins}^i h_f} + \frac{r_t^o \ln(\frac{r_t^o}{r_t^i})}{k_t} + \frac{r_t^o \ln(\frac{r_{ins}^i}{r_t^o})}{k_{ins}^i} + \frac{r_t^o \ln(\frac{r_{ins}^o}{r_t^o})}{k_{ins}^o} + \frac{r_t^o}{r_{ins}^i(h_c+h_r)} + \frac{r_t^o \ln(\frac{r_c^o}{r_c^i})}{k_{csg}} + \frac{r_t^o \ln(\frac{r_{wb}}{r_c^o})}{k_{cem}}\right] \quad 4.16$$

Assuming that hot reservoir fluid is flowing through the inner insulation, production casing, outer insulation, intermediate casing, and cement and to the reservoir, the steady state rate of heat transfer can be calculated by using equation 4.7.

The overall heat transfer coefficient for the middle section can be calculated by the following equation 4.17.

$$\frac{1}{U_{to}} = \frac{r_t^o}{r_{ins}^i h_f} + \frac{r_t^o \ln(\frac{r_t^o}{r_t^i})}{k_t} + \frac{r_t^o \ln(\frac{r_{ins}^i}{r_t^o})}{k_{ins}^i} + \frac{r_t^o \ln(\frac{r_{ins}^o}{r_t^o})}{k_{ins}^o} + \frac{r_t^o}{r_{ins}^i(h_c+h_r)} + \frac{r_t^o \ln(\frac{r_c^o}{r_c^i})}{k_{csg}} + \frac{r_t^o \ln(\frac{r_{wb}}{r_c^o})}{k_{cem}} \quad 4.17$$

4.2.3 Model 3: At Top Section

A conductor and surface casing are added to the other casings and insulations used in as already seen in the middle and reservoir sections of the well. Figures 4.5a and 4.5b show illustrations of the horizontal and vertical cross-sections of the top section of the well respectively.

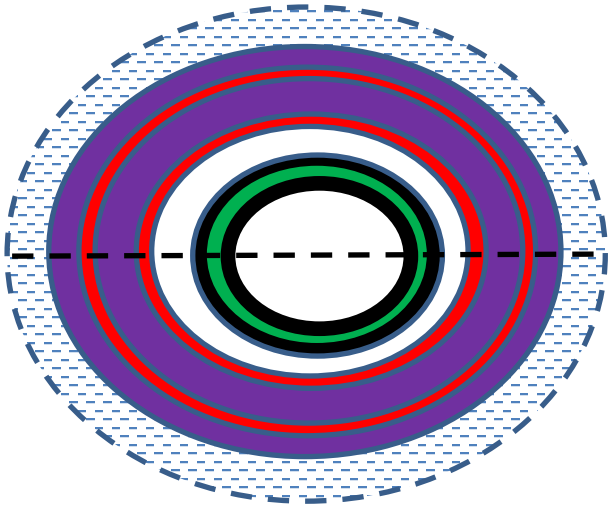

Figure 4.5a: Illustration of the horizontal cross-section of the well

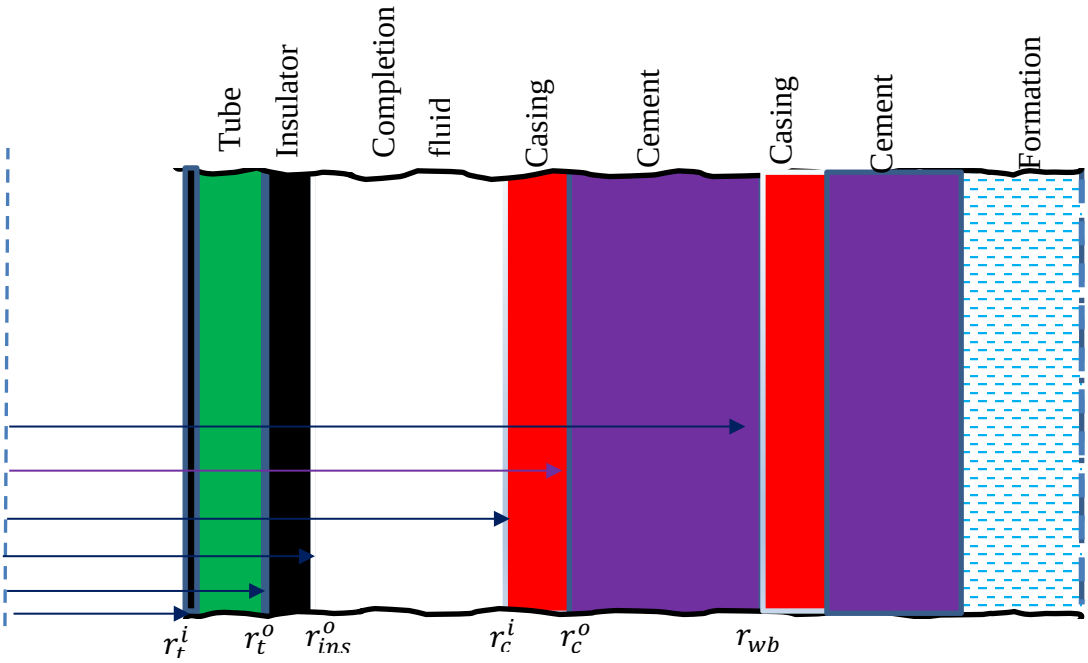

Figure 4.5b: Illustration of vertical cross-section of the reservoir section

The temperature difference between the well and the formation of the middle section can be written as the sum of temperature difference across each component of figure 4.5b given in Equation 4.18.

$$T_f - T_{wb} = (T_f - T_{ins}^i) + (T_{ins}^i - T_{ins}^{io}) + (T_{ins}^{io} - T_t^i) + (T_t^i - T_t^o) + (T_t^o - T_{ins}^{oi}) + (T_{ins}^{oi} - T_{ins}^o) + (T_{ins}^o - T_c^i) + (T_c^i - T_c^o) + (T_c^o - T_{cem}^i) + (T_{cem}^o - T_{cs}^i) + (T_{cs}^o -$$

$$T_{cem}^{i}) + (T_{cem}^{o} - T_{cond.}^{i}) + (T_{cond.}^{i} - T_{cond.}^{o}) + (T_{cond.}^{o} - T_{cem}^{i}) + (T_{cem}^{i} - T_{cem}^{o}) + (T_{cem}^{o} - T_{wb}) \quad 4.18$$

Inserting equations 4.1-4.6 and 4.18 into equation 4.12, we get:

$$T_f - T_{wb} = \frac{Q}{2\pi\Delta L}\left[\frac{r_t^o}{r_{ins}^i h_f} + \frac{r_t^o \ln(\frac{r_t^o}{r_t^i})}{k_t} + \frac{r_t^o \ln(\frac{r_{ins}^i}{r_t^o})}{k_{ins}^i} + \frac{r_t^o \ln(\frac{r_{ins}^o}{r_t^o})}{k_{ins}^o} + \frac{r_t^o}{r_{ins}^i(h_c+h_r)} + \frac{r_t^o \ln(\frac{r_{wb}}{r_c^o})_{int}}{k_{cem}} + \frac{r_t^o \ln(\frac{r_c^o}{r_c^i})_{int}}{k_{csg}} + \frac{r_t^o \ln(\frac{r_{wb}}{r_c^o})_{sc}}{k_{cem}} + \frac{r_t^o \ln(\frac{r_c^o}{r_c^i})_{sc}}{k_{csg}} + \frac{r_t^o \ln(\frac{r_{wb}}{r_c^o})_{cond}}{k_{cem}} + \frac{r_t^o \ln(\frac{r_c^o}{r_c^i})_{cond}}{k_{csg}}\right] \quad 4.19$$

Assuming that hot reservoir fluid is flowing through the insulators, casings, cement and to the reservoir, the steady state rate of heat transfer can be calculated by using equation 4.7.

The overall heat transfer coefficient for the top section can be calculated by the following equation 4.20.

$$\frac{1}{U_{to}} = \frac{r_t^o}{r_{ins}^i h_f} + \frac{r_t^o \ln(\frac{r_t^o}{r_t^i})}{k_t} + \frac{r_t^o \ln(\frac{r_{ins}^i}{r_t^o})}{k_{ins}^i} + \frac{r_t^o \ln(\frac{r_{ins}^o}{r_t^o})}{k_{ins}^o} + \frac{r_t^o}{r_{ins}^i(h_c+h_r)} + \frac{r_t^o \ln(\frac{r_{wb}}{r_c^o})_{int}}{k_{cem}} + \frac{r_t^o \ln(\frac{r_c^o}{r_c^i})_{int}}{k_{csg}} + \frac{r_t^o \ln(\frac{r_{wb}}{r_c^o})_{sc}}{k_{cem}} + \frac{r_t^o \ln(\frac{r_c^o}{r_c^i})_{sc}}{k_{csg}} + \frac{r_t^o \ln(\frac{r_{wb}}{r_c^o})_{cond}}{k_{cem}} + \frac{r_t^o \ln(\frac{r_c^o}{r_c^i})_{cond}}{k_{csg}} \quad 4.20$$

5 Results

5.1 WellCAT™ Software Rate of Fluid Production

Commercial WellCAT™ software (from Landmark) will be used to perform casing calculations. The aim is to determine the integrity of geothermal wells with higher flow rates with and without insulators. Since geothermal wells generally have higher production, usually above 100 000 [kg/hr] (Finger & Blankenship, 2010), a lot of these wells face integrity problems like collapse of well casing in IDDP-1(Friðleifsson et al., 2017). The Prod mode and Tube mode of this software has been used.

5.1.1 Simulation Arrangement

As fluid flows from the reservoir to the surface, the heat transfer through fluid is governed by convention heat flow. However, conductive heat flow governs the heat flow between the wellbore and the surrounding. WellCAT™'s production design module simulates fluid and heat transfer during completion, production, stimulation, testing, and well-servicing operations. The software also analysis of transient and steady-state for single-phase and multiphase flow along the tubing/working string, casing, cementing.
The software simulates the pressure and temperature profiles from downhole to the surface. It is very popular design and analysis tool in the oil industries, which is designed for high-pressure, high-temperature (HP/HT) drilling and production environments.

In this part of the thesis, an inclined and 5000 [m] measured depth well has been considered. The well is drilled horizontally in the reservoir section. Figure 5.1 shows the well structure. The production tubing is 4209 [m] and production liner extended to the reservoir.

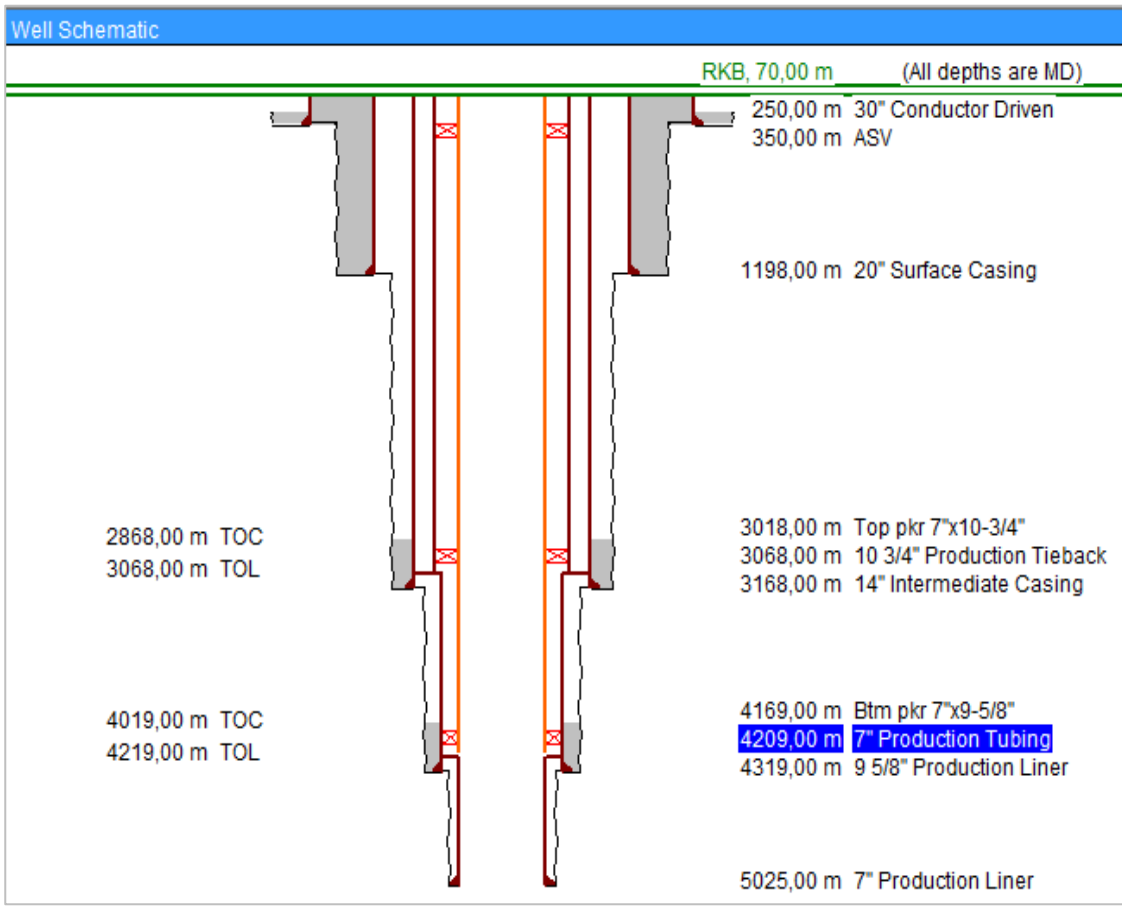

Figure 5.1: Schematic of the well used for flowrate simulation on WellCAT™

Table 5 shows the casing and tubing used for well construction (Figure 5.1). In the table, the type of casing, the position of strings from hanger and the bottom. In addition, the top and bottom position of the cement. As shown, the surface casing is cemented all the way to the surface.

Table 5: Casing and tubing configuration

Casing and Tubing Configuration

	Name	Type	OD (in)	MD (m)			Hole S (in)
				Hanger	TOC	Base	
1	Conductor	Driven	30,000	70,00		250,00	
2	Surface	Casing	20,000	70,00	70,00	1198,00	2
3	Intermediate	Casing	14,000	70,00	2868,00	3168,00	
4	Production	Liner	9 5/8	3068,00	4019,00	4319,00	
5	Production	Tieback	10 3/4	70,00	3068,00	3068,00	
6	Production	Liner	7,000	4219,00	5025,00	5025,00	
7	Production	Tubing	7,000	70,00		4209,00	

Production Tubing

A typical production 13CrL80 production tube was used, which extended up to 4209 [m]. The 13% Cr control corrosion problem, however during the life of the production period it is wise to treat the tubing with corrosion control inhibitors. The main reason is that the surface of the tubing might be damaged due to mechanical friction between coli tubing and also due to CO_2/H_2S/brine and sand production.

Table 6: Tubing grading

String Sections - 7" Production Tubing

	MD (m)		Pipe				Connection		
	Top	Base	Type	OD (in)	Weight (ppf)	Grade	Pipe	Name	Grade
1	70,00	4209,00		7,000	32,000	13CR80 (ACTI		Vam TOP	13CR80

A-annulus content

The A-annulus is filled with 1.0sg NaCl treated brine fluid. In the real operation, this fluid should be treated with corrosive control inhibitors. The fluid in the annulus provided a pressure in order to main in well tubing collapse. The well information is obtained from an oil company via e-post and however due to confidentiality, the authors restrict to report the detail information.

Table 7: A-annulus fluid content

Annulus Contents - 7" Production Tubing			
	MD(m)		Annulus Contents
	Top	Base	
1	70,00	4209,00	1.05 sg Na

Lithology: All the drilling formation are assumed to be impermeable and however, the properties are not identified in this thesis.

5.1.2 Fluid Temperatures

As the fluid flow from the reservoir to the surface, the heat transfer mechanism is due to conduction and convection. Due to the thermal conductivity, and geometry of the well structure (casing/tubing/cement/formation) and completion fluid along with the thermodynamics states of the well flowing fluid properties, the among of heat transfer would be quantified in terms of the temperature profile and the among of enthalpy heat loss during the life of the production, which are simulated and analyzed in this thesis work.

Fluid temperatures

Figure 5.2 displays the fluid temperature profile simulated for different production rates. The geothermal gradient for a typical well is displayed in this graph (shown as undisturbed in the graph). Higher production rates produce fluids with higher temperatures on the surface as shown in the simulation for different flowrates.

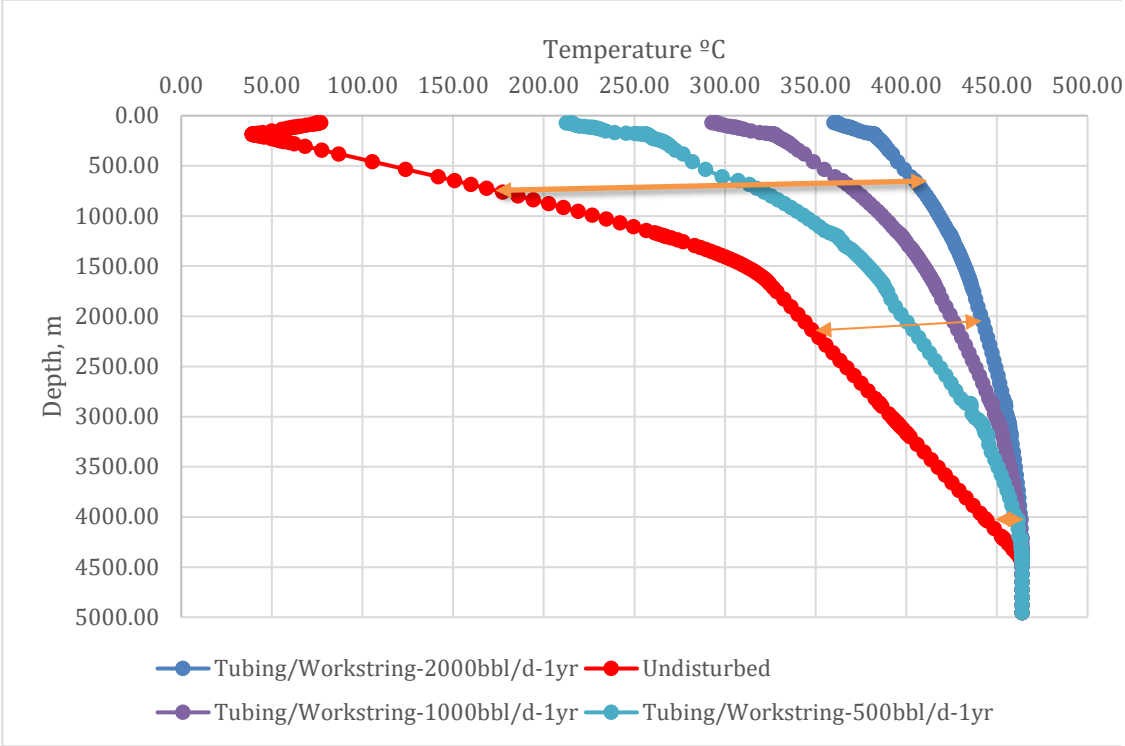

Figure 5.2: Displays the well temperature across the working tube

The fluid temperature profile inside the tubing/working string for the initial production and produces 1-year production operation. As shown on the figure, the long-term production produces 1 year generates a flowing wellhead temperature of 100 ºC hotter than then two-day production initial production. Both the long duration and the production rate cause this higher temperature.

It can also be deducted from the graph that, the higher the production rate of fluid, the lesser the amount of heat loss to the wellbore and the higher the temperature of the fluid produced at the surface. The need for surface pumps in case of a low production rate, is therefore necessary.

We are going to use tubing flowrate of 2000 [bbl/d] after 1 day of production as our fluid temperature (T_f) for further simulation. The geothermal gradient shown in the graph will be used as wellbore temperature (T_w) too.

5.2 Heat Transfer Simulation

5.2.1 Simulation Setup

The geothermal production well we considered in our simulation is an idealized 5000 [m] deep well with the following parameters shown in Table 8. This is an example of a typical well design for geothermal wells with all casings cemented to the surface (Kaldal, Jonsson, Palsson, & Karlsdottir, 2015). The initial reservoir temperature is set at 460 ^{o}C (860^{o}F). Steam is assumed to be produced at a constant rate from the reservoir to the surface. The conductivity of cement was varied from 0.14 to 7 [W/mK] ((Wenger et al., 2011);(Baghban et al., 2013)). Liquid convective heat transfer coefficient, conductivity of tubing material, convective heat transfer coefficient, conductivity of casing material, radiative heat transfer coefficient is kept constant throughout the simulation and as shown in Table 9. The well is divided into 3 sections: reservoir section, middle section and top section as shown in Figure 5.3.

Table 8: Well design parameters

Type of Casing	**Outer Diameter of Casing in Inches**	**Hole Size in Inches**
Conductor	30	36
Surface	20	26
Intermediate	$13^{3/8}$	$17^{1/2}$
Production	8	$10^{3/8}$

Table 9: Input parameters for simulation

Input parameters	**Value**
Temperature	460 [^{o}C]
Well Depth	5000 [m] (16 404 ft)
h_L-Liquid convective heat transfer coefficient	500 [W/m^{2}K]
k_t-Conductivity of tubing material	25 [W/mK]
h_c-Convective heat transfer coefficient	100 [W/m^{2}K]
k_c-Conductivity of Casing material	25 [W/mK]
h_r-Radiative heat transfer coefficient	2 [W/m^{2}K]

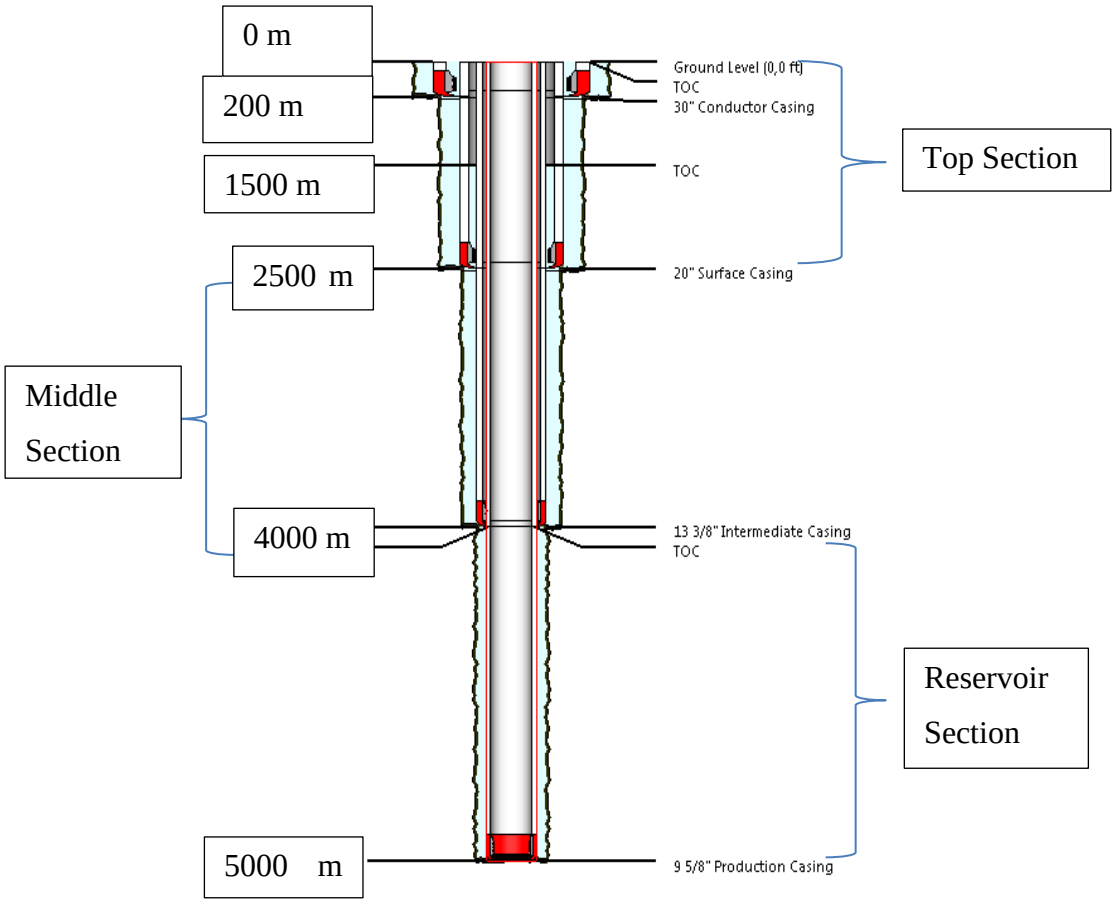

Figure 5.5: Geothermal well schematic

In order to perform sensitivity analysis of the impact of inner insulation for geothermal wells, we assumed a constant wellbore temperature and fluid temperature for each section of the well (top, middle and reservoir section). Table 10 below shows the assumed wellbore temperatures and fluid temperatures of the different sections of the well. These values are used in our further work.

Table 10: Wellbore and fluid temperatures for different well sections

Temp. / Section	Reservoir Section	Middle Section	Top Section
Fluid Temperature	450[ºC]	440[ºC]	410[ºC]
Wellbore Temperature	440[ºC]	340[ºC]	170[ºC]

5.2.2 Simulation Results

On this part, we present the results obtained from variation of different parameters in the reservoir, middle and top section. This is to help us study the effect of an inner insulation to the overall heat transfer of the produced fluid and compare it with the current practice in the industry.

5.2.2.1 Reservoir Section

The reservoir section in this thesis is considered to be the zone just below intermediate casing shoe. It is cemented from the base of the well to the surface with the production casing.

5.2.2.1.1 Heat Transfer of Fluid without Insulators

In this simulation, the well is completed with no inner or outer insulators. That is their thicknesses are zero. Since this is for the reservoir section, the wellbore temperature is assumed to be 440 ºC while the fluid temperature is 450 ºC as shown in Table 4.6 above. The graphs of the overall thermal resistance and the overall heat transfer coefficient plotted against cement thermal conductivity are shown in Figures 5.6 and 5.7 below.

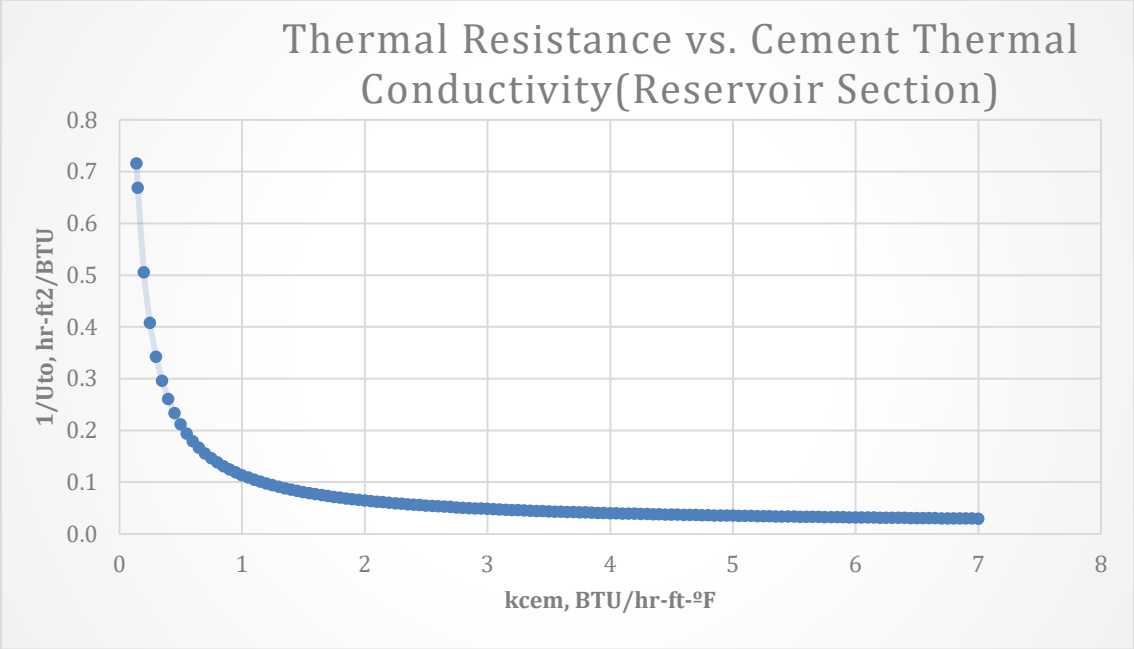

Figure 5.6: Thermal resistance versus cement thermal conductivity in the reservoir section.

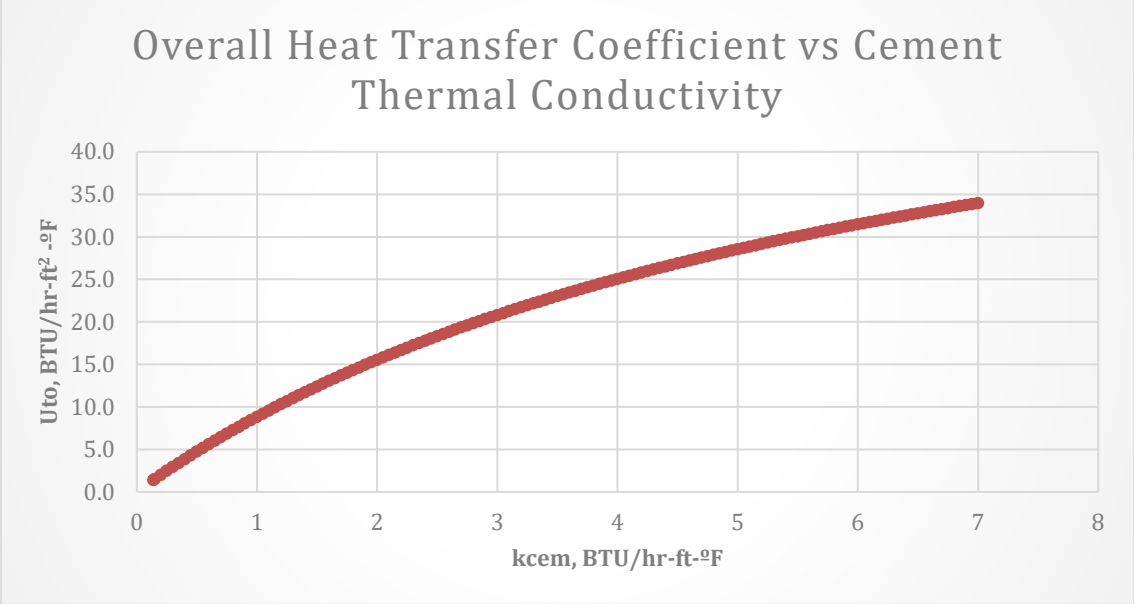

Figure 5.7: Overall heat transfer coefficient versus cement thermal conductivity-uninsulated reservoir section.

From Figure 5.6 above, the thermal conductivity of cement and the overall thermal resistance of the wellbore are inversely proportional, and the decrease in resistance shows an exponential decline behavior initially, followed by a slow decline which begins at approximately 0,2 [BTU/hr-ft-ºF].

The reverse is achieved when plotting the same cement thermal conductivities against overall heat transfer coefficient. There is an exponential increase in the overall heat transfer coefficient as the conductivity of cement increases. This is due to the fact that high cement thermal conductivities lead to higher heat loss in the reservoir.

Figure 5.8 shows a plot of heat exchange versus cement thermal conductivity when there are no insulators. The graph shows an exponential loss of heat to the wellbore from 0 to -1500 [BTU/hr-ft] as cement thermal conductivity increases from 0,14 to 7 [BTU/hr-ft-ºF]. This is to confirm that high cement thermal conductivity leads to a higher rate of heat loss to the wellbore.

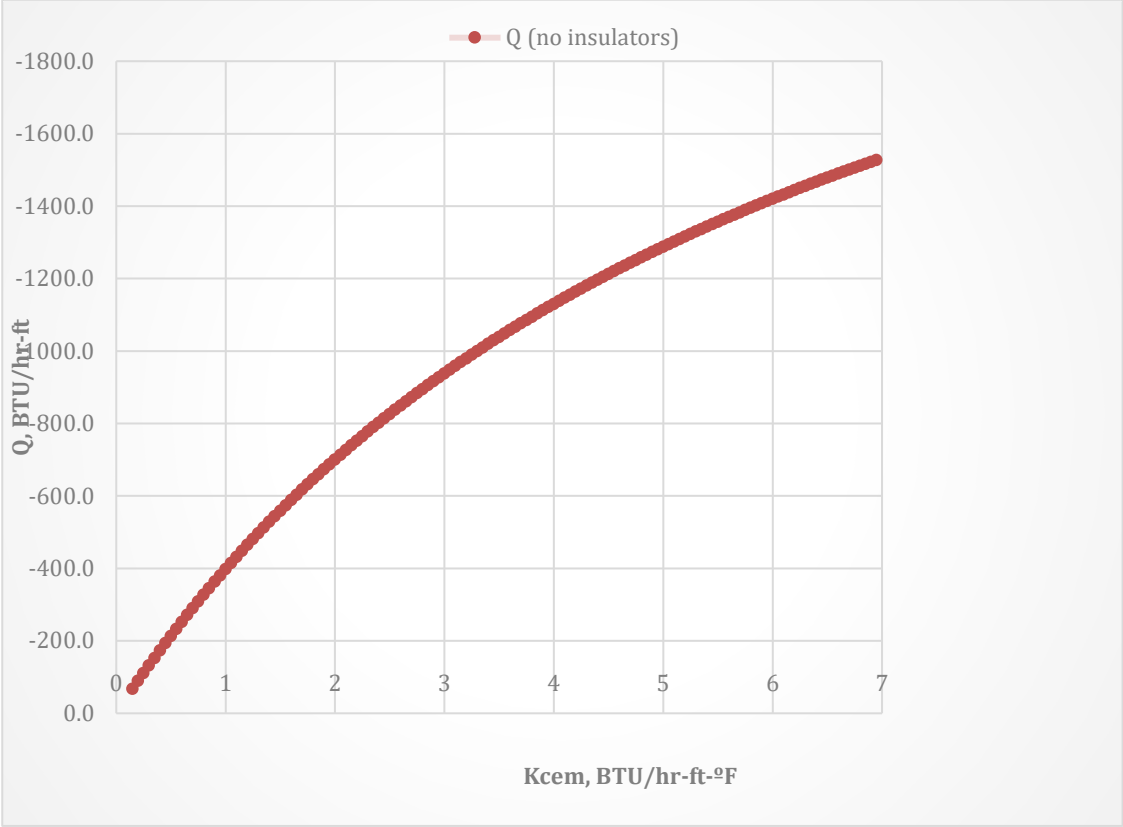

Figure 5.8: Heat exchange versus cement thermal conductivity-uninsulated reservoir section.

5.2.2.1.2 Effect of Thickness of Outer Insulator

This was studied by (Hasan & Kabir, 1994) and it is the current practice in the industry for some parts of the world like in Australia. The effect of the thickness of the outer insulation in this thesis was simulated by increasing the thickness of the outer insulator from 0 to 0,3 [ft]. Thermal conductivity of both insulators remained constant at 0,02 [W/mK].

At a value of 0,175 [ft], graphs of the cement thermal conductivity against the overall thermal resistance and the overall heat transfer coefficient are shown in Figures 5.9 and 5.10 below. The thermal conductivity of cement and the overall thermal resistance of the wellbore are inversely proportional, and the decrease in resistance shows an exponential decline behavior initially, followed by a slow decline which begins at approximately 7,5 [BTU/hr-ft-^{o}F].

The opposite is achieved when plotting the same cement thermal conductivities against overall heat transfer coefficient. Unlike in Figure 5.9, the overall heat transfer coefficient increases exponentially at lower values for cement thermal conductivity (from 0,14 to 0,85 BTU/hr-ft-ºF) and at a much slower rate from 0,85 to 2 [BTU/hr-ft-ºF].

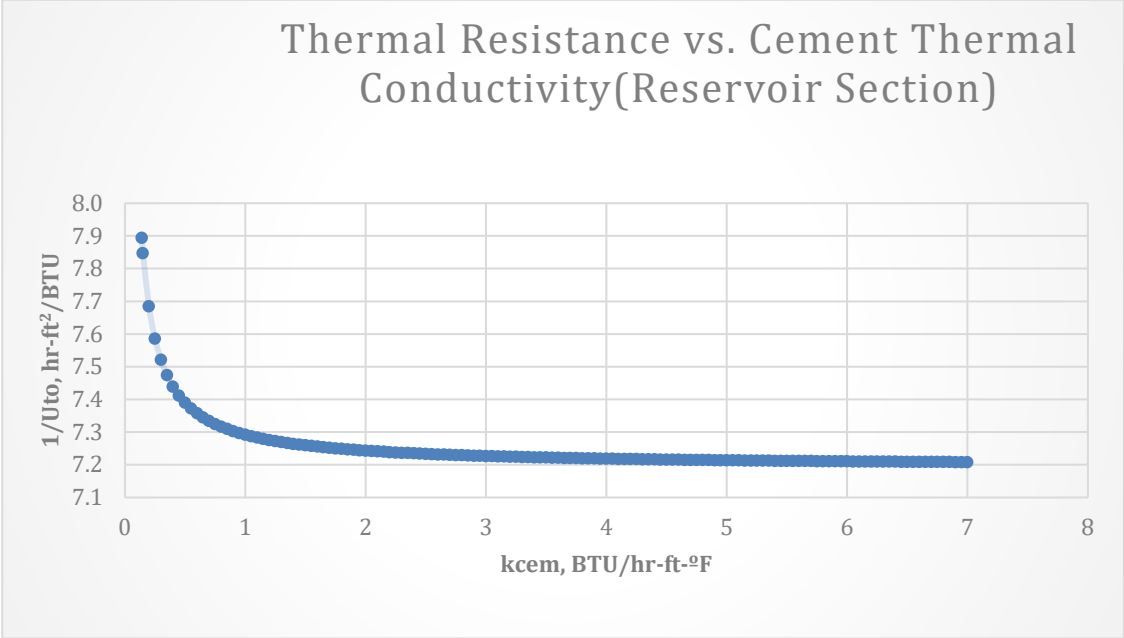

Figure 5.9: Thermal resistance versus cement thermal conductivity-outer insulated reservoir section.

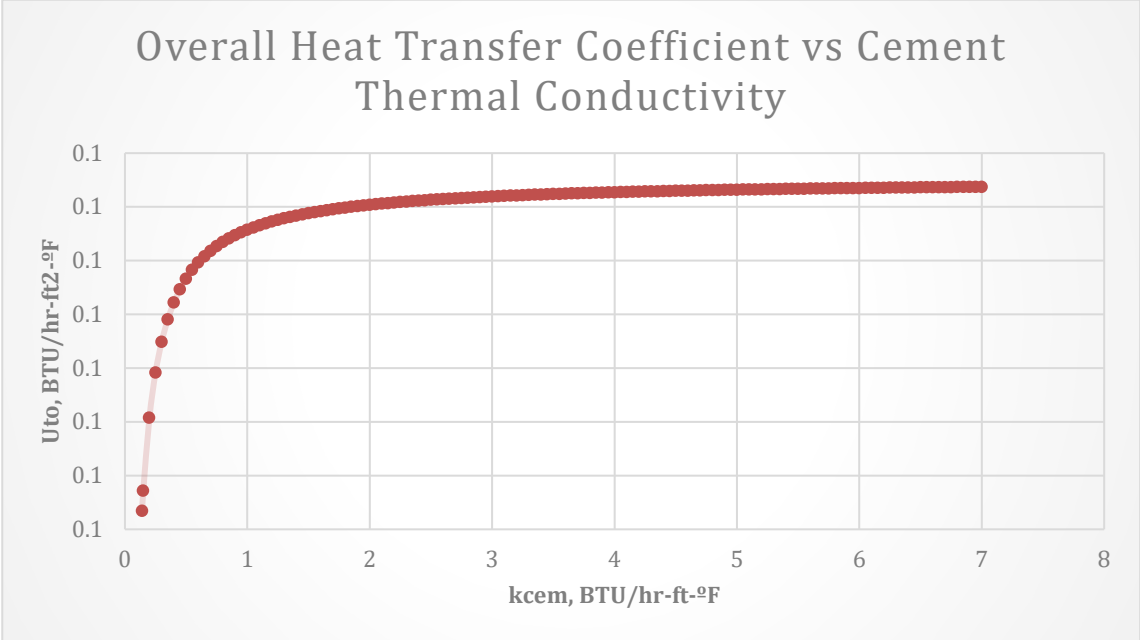

Figure 5.10: Overall heat transfer coefficient versus cement thermal conductivity-outer insulated reservoir section.

Figure 5.11 shows a plot of heat exchange versus cement thermal conductivity when the thickness of the outer insulator is 0,175 [ft]. By increasing the thickness of the outer insulator from 0 to 0,3 [ft], there is a huge reduction of heat exchange between the wellbore and the formation when compared with the current practice in the industry. That is for a cement thermal conductivity of 0,14 [BTU/hr-ft-ºF], the heat loss when an insulator of 0,175 [ft] is kept is -5,7 [BTU/hr-ft] while it is -6,3 [BTU/hr-ft] when there is no insulator. Also, a higher cement conductivity of 7 [BTU/hr-ft-ºF], the heat loss is -63 [BTU/hr-ft] when there is an outer insulation and -1532 [BTU/hr-ft] when there is no insulation.

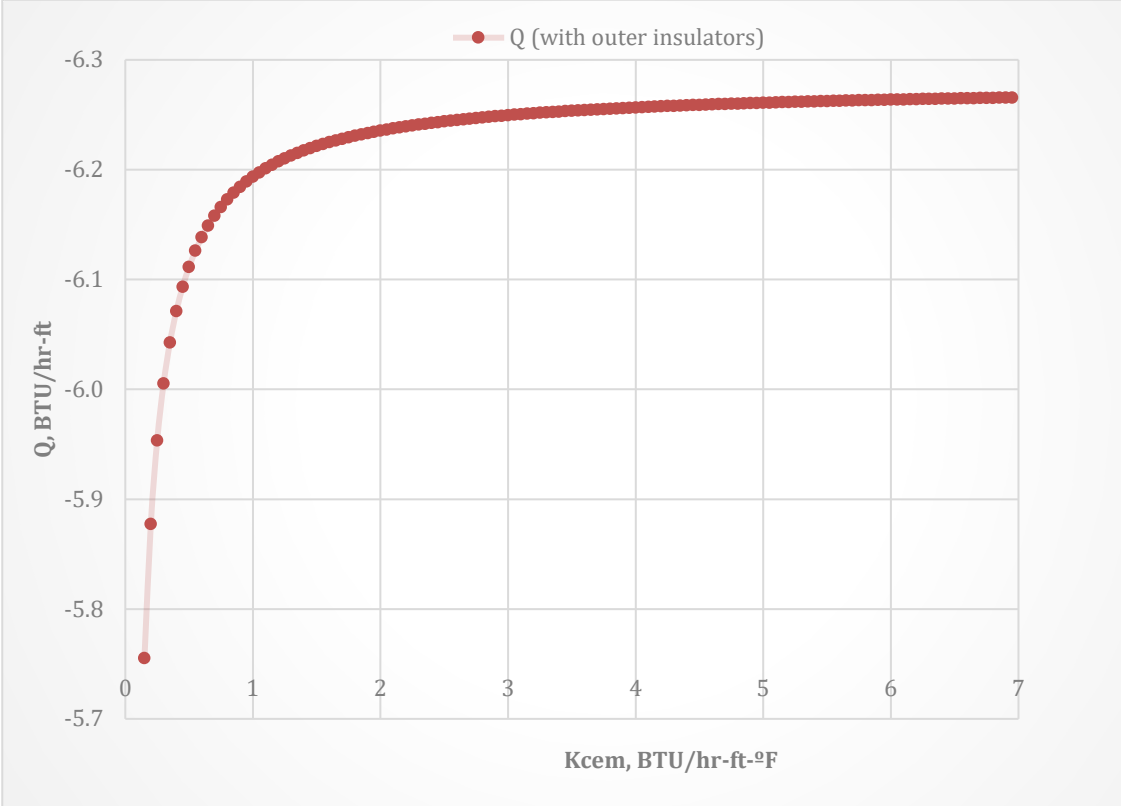

Figure 5.11: Heat exchange versus cement thermal conductivity-outer insulated reservoir section.

5.2.2.1.3 Effect of Thickness of Inner Insulator

To study the effect of inner insulator on the overall heat exchange, the thickness of the outer insulator is kept at zero while that of the inner insulator is varied from 0 to 0,3 [ft]. The conductivity of the insulators where kept constant at 0,02 [W/mK].

At a value of 0,175 [ft], graphs of the cement thermal conductivity against the overall thermal resistance and the overall heat transfer coefficient are shown in Figures 5.12 and 5.13 below. As similar behavior can be observed as in the previous graphs but this time around, the overall thermal resistance declines slowly at a higher value of approximately 14,2 [BTU/hr-ft-ºF].

On Figure 5.14, the overall heat transfer coefficient has a constant value of 0,1 [BTU/hr-ft^2-ºF] as the cement conductivity increases from 0,14 to 7 [BTU/hr-ft-ºF].

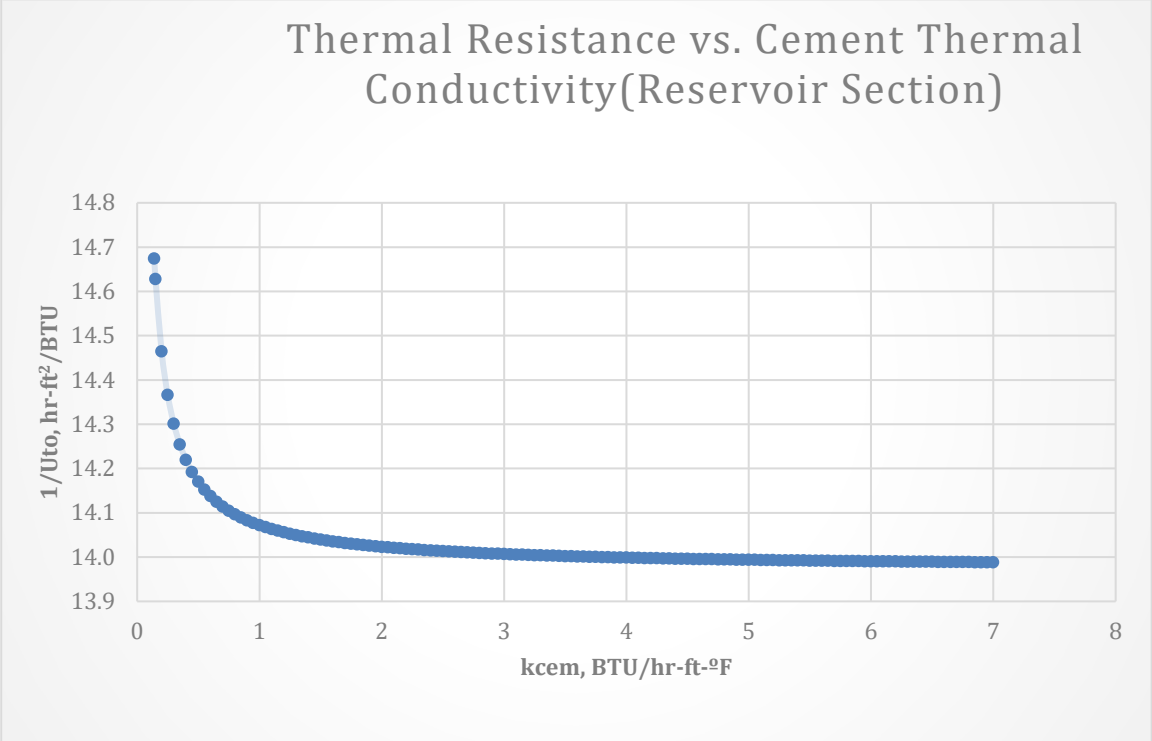

Figure 5.12: Thermal resistance versus cement thermal conductivity-inner insulated reservoir section.

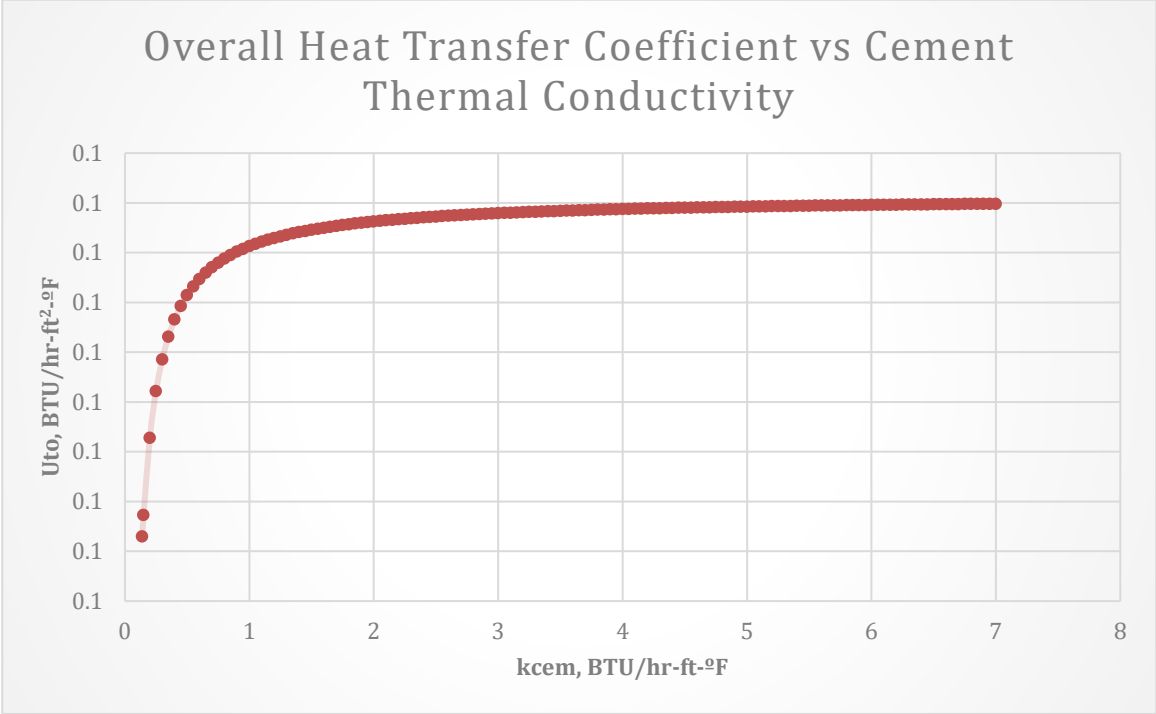

Figure 5.13: Overall heat transfer coefficient versus cement thermal conductivity-inner insulated reservoir section.

When we plotted a graph cement thermal conductivity against heat exchange (Figure 5.14), we observed that at a thickness of 0,175 [ft] for the inner insulator, there is less heat loss to the wellbore as compared to the same thickness for the outer insulator. At a low cement thermal conductivity of 0,14 [BTU/hr-ft-ºF], the heat loss is -3,1 [BTU/hr-ft] and for a higher cement thermal conductivity of 7 [BTU/hr-ft-ºF], the heat loss is -3,2 [BTU/hr-ft]. This shows that there is 50% less heat loss when the inner insulation is used.

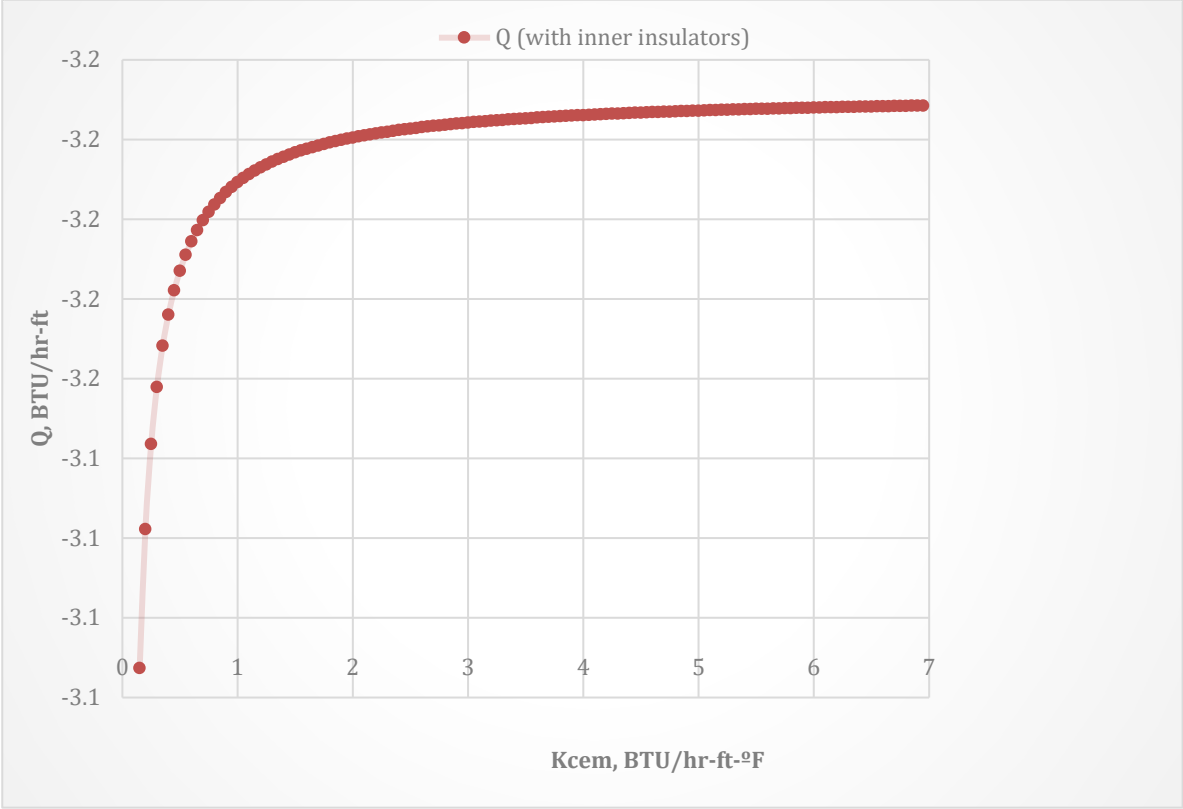

Figure 5.14: Heat exchange versus cement thermal conductivity-inner insulated reservoir section.

5.2.2.1.4 Effect of Completing with both Inner and Outer Insulators

To further determine the effect of installing an inner and outer insulator when completing a geothermal well, the thicknesses of both insulators where varied simultaneously to see their combined effect. The results presented below represents shows when the thickness of both insulators is 0,175 [ft].

At a value of 0,175 [ft] for thickness of both insulators, graphs of the cement thermal conductivity against the overall thermal resistance and the overall heat transfer coefficient are shown in Figures 5.15 and 5.16 below. Similar behavior can be observed as in the previous graphs but this time around, the overall thermal resistance declines slowly at a higher value of approximately 21,4 [BTU/hr-ft-ºF].

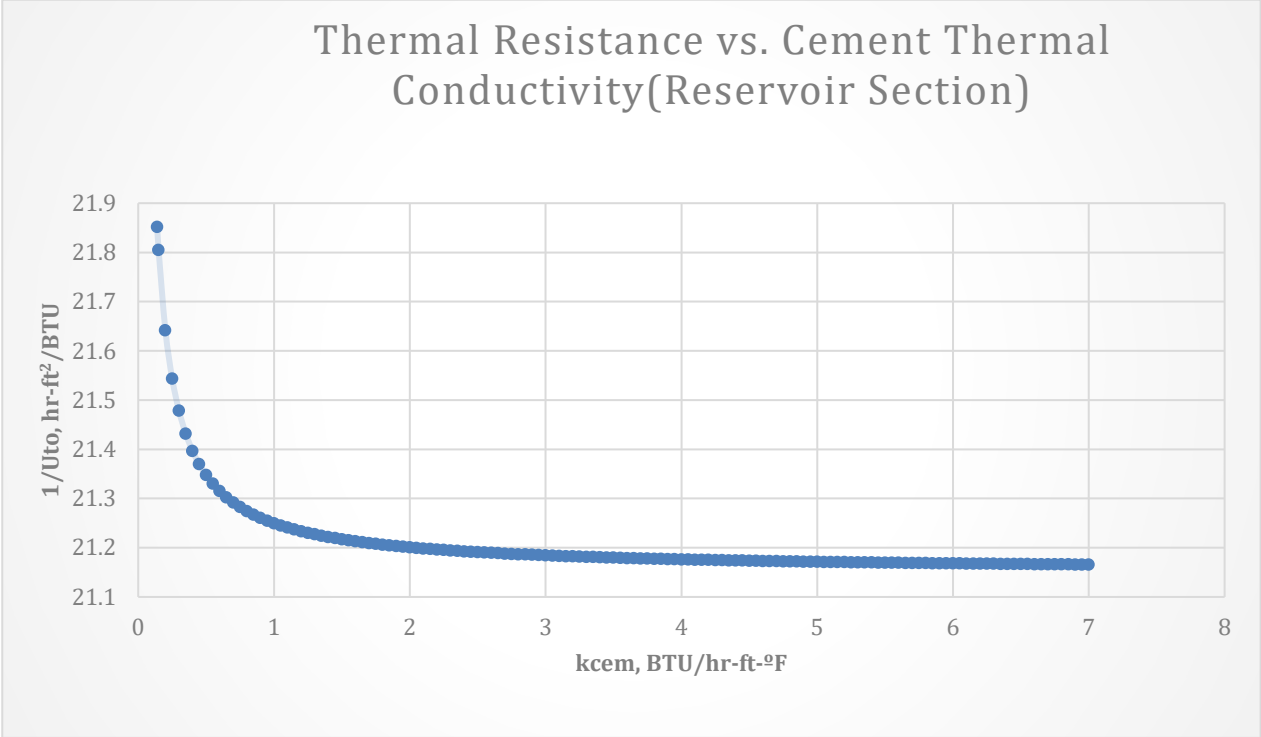

Figure 5.15: Thermal resistance versus cement thermal conductivity-outer and inner insulated reservoir section.

On Figure 5.16, the overall heat transfer coefficient has a constant value of zero as the cement conductivity increases from 0,14 to 7 [BTU/hr-ft-ºF].

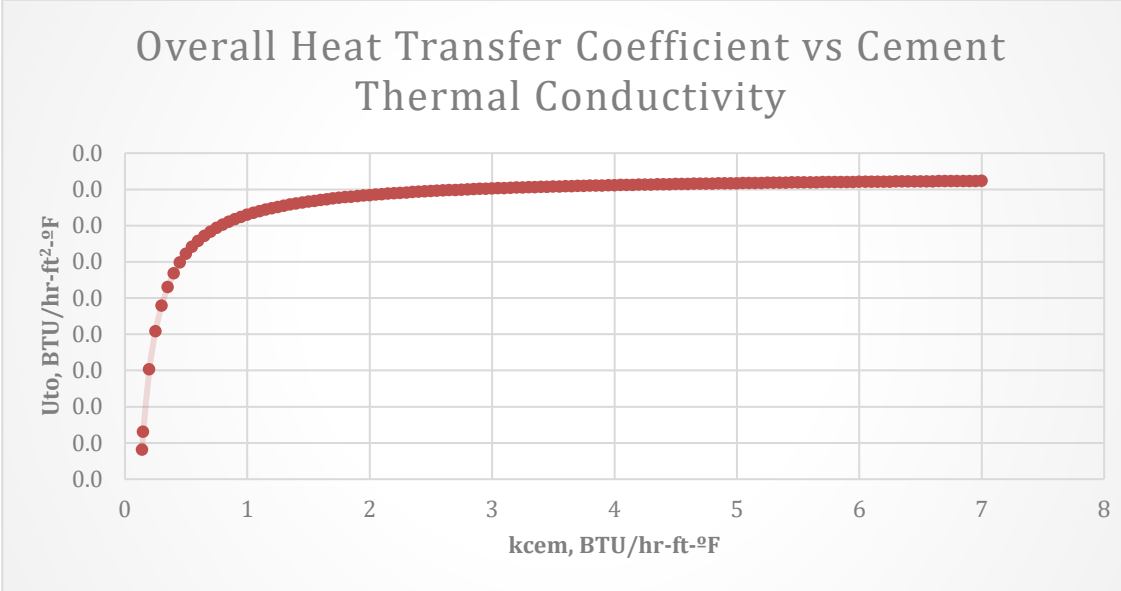

Figure 5.16: Overall heat transfer coefficient versus cement thermal conductivity-outer and inner insulated reservoir section.

When we plotted a graph cement thermal conductivity against heat exchange (Figure 5.17), we observed that there is almost no heat loss to the wellbore as compared to the previous cases. The overall heat loss remained constant at a value of -2,1 [BTU/hr-ft] for all values of cement thermal conductivity. This shows that there is; 33,3% less heat loss when both insulators are used as compared to when only the inner insulator is used. insulation is used, 65% less heat loss when compared to using only the outer insulator and 95% less heat loss when compared to completing the well without insulators in the reservoir section.

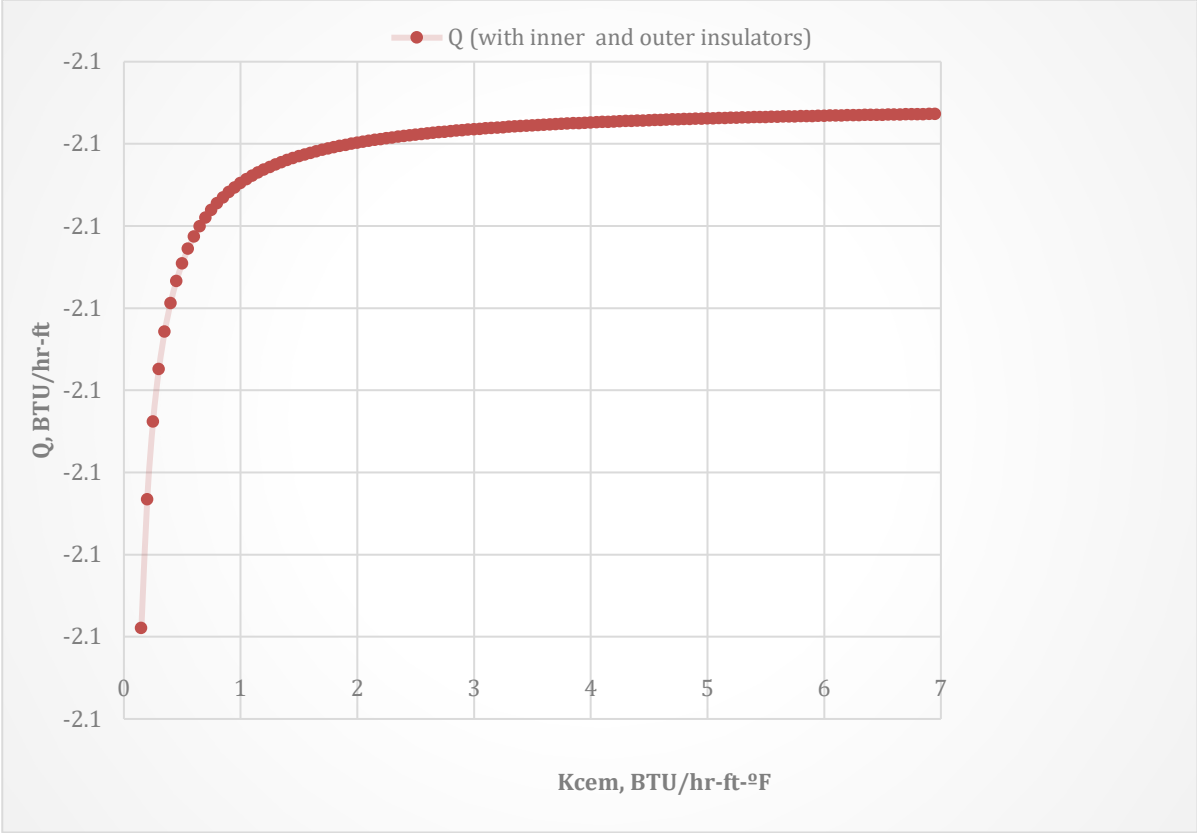

Figure 5.17: Heat exchange versus cement thermal conductivity-outer and inner insulated reservoir section.

5.2.2.1.5 Effect of Thermal Conductivity of Insulators

The effect of thermal conductivity of the outer and inner insulators where studied by varying the conductivity of both insulators while maintaining constant values for their thicknesses. The thicknesses of the inner and outer insulator were kept constant at 0,175 [ft]. This value is chosen because it gave an overall thermal heat transfer coefficient of approximately zero with a constant thermal conductivity.

The graph of the thermal conductivity of the cement and the overall thermal resistance of the wellbore in Figure 5.18 shows an exponential decline followed by a slow linear decline at approximately 14,3 [BTU/hr-ft^2-ºF] when the conductivity of the outer insulator is kept at 5 [BTU/hr-ft-ºF] and that of the inner insulator at 0,02 [BTU/hr-ft-ºF].

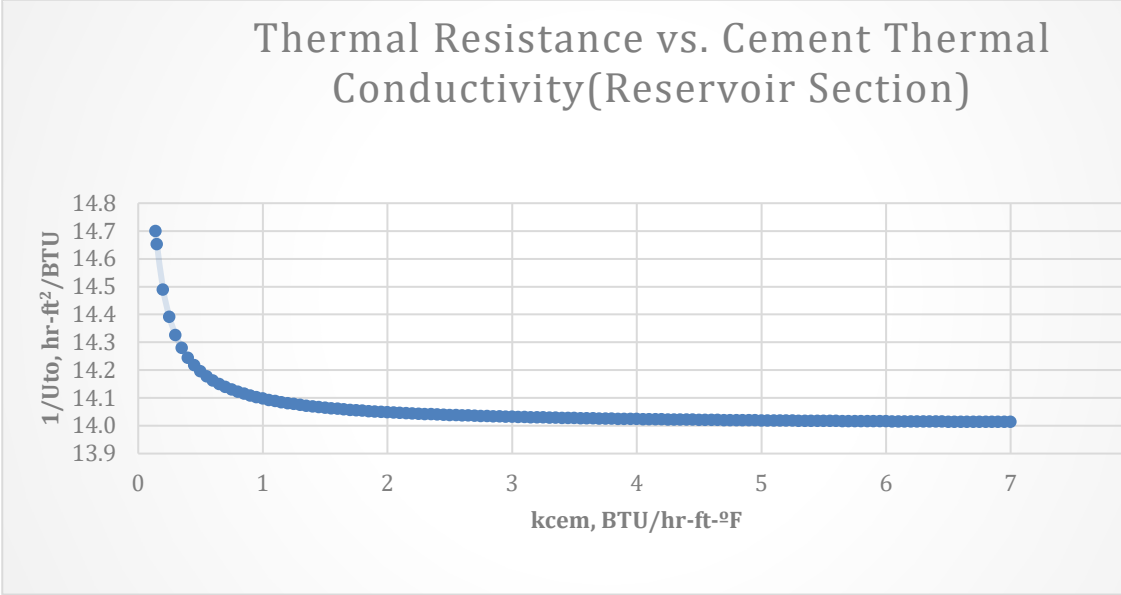

Figure 5.18: Effect of conductivity of insulators at the reservoir section.

The overall thermal heat transfer coefficient remains constant at 0,1 [BTU/hr-ft^2-ºF] at a higher value of thermal conductivity of the outside insulator as shown in Figure 5.19.

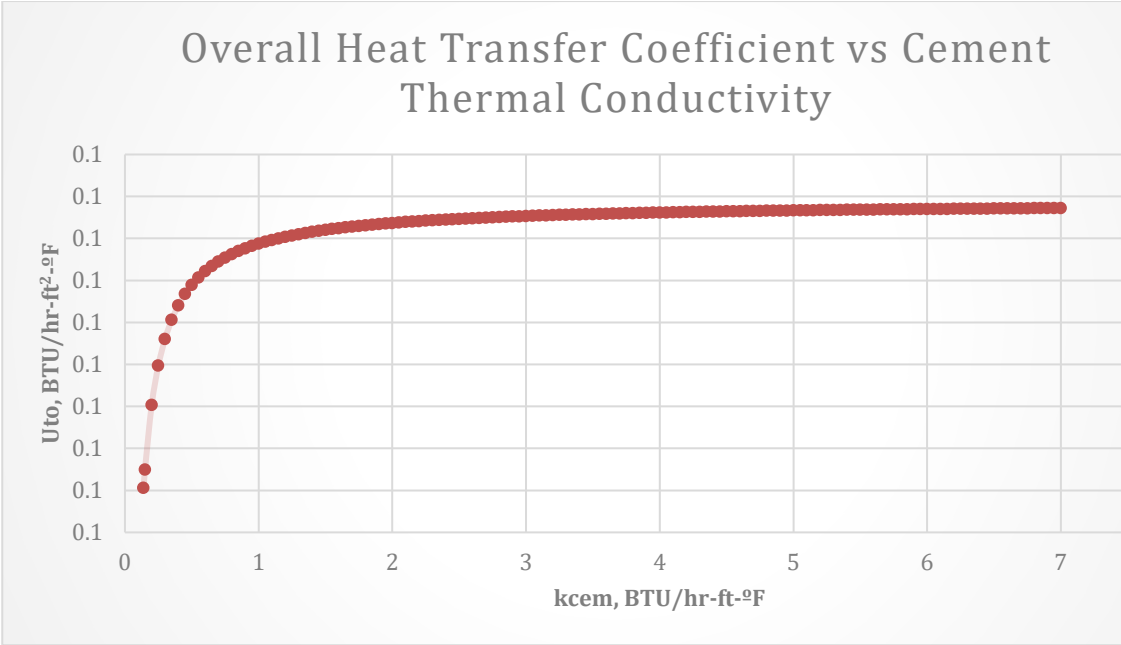

Figure 5.19: Effect of conductivity of insulators at the reservoir section.

Heat exchange in this scenario does not have a real significant change as compared to when we simulated with only an inner insulation which had a lower thermal conductivity of about 0,02 [BTU/hr-ft-ºF]. This is shown in Figure 5.20 below. Overall heat exchange ranged from -3,1 to -3,2 [BTU/hr-ft].

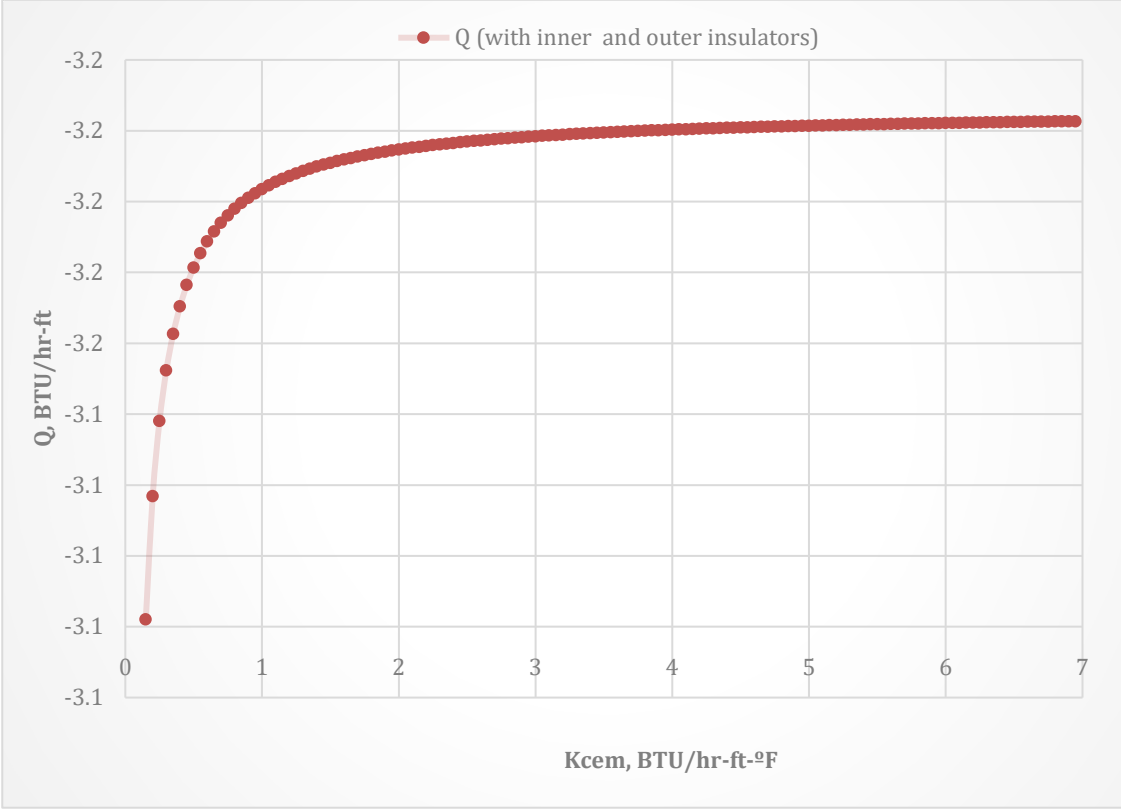

Figure 5.20: Effect of conductivity of insulators at the reservoir section.

When the thermal conductivity of the inner insulator is increased to 5 [BTU/hr-ft-ºF] and that of the outer insulator is decreased to 0,02 [BTU/hr-ft-ºF], the result of thermal resistance versus cement conductivity shows a sharp decline at 7,5 [BTU/hr-ft^2-ºF] as compared to 14,3 [BTU/hr-ft^2-ºF] in the previous case. This is shown in Figure 5.21 below.

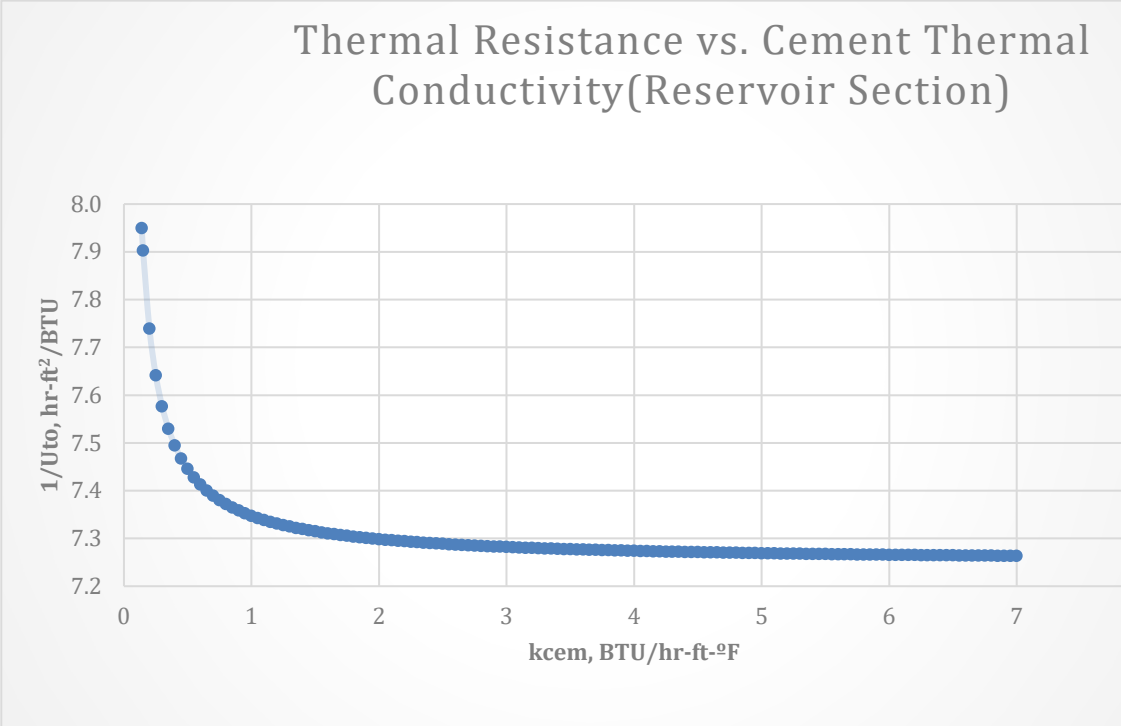

Figure 5.21: Effect of conductivity of insulators at the reservoir section.

The overall heat transfer coefficient in this case remained 0,1 [BTU/hr-ft^2-ºF] when plotted against thermal conductivity of cement as shown in Figure 5.22. This is the same as in the previous case.

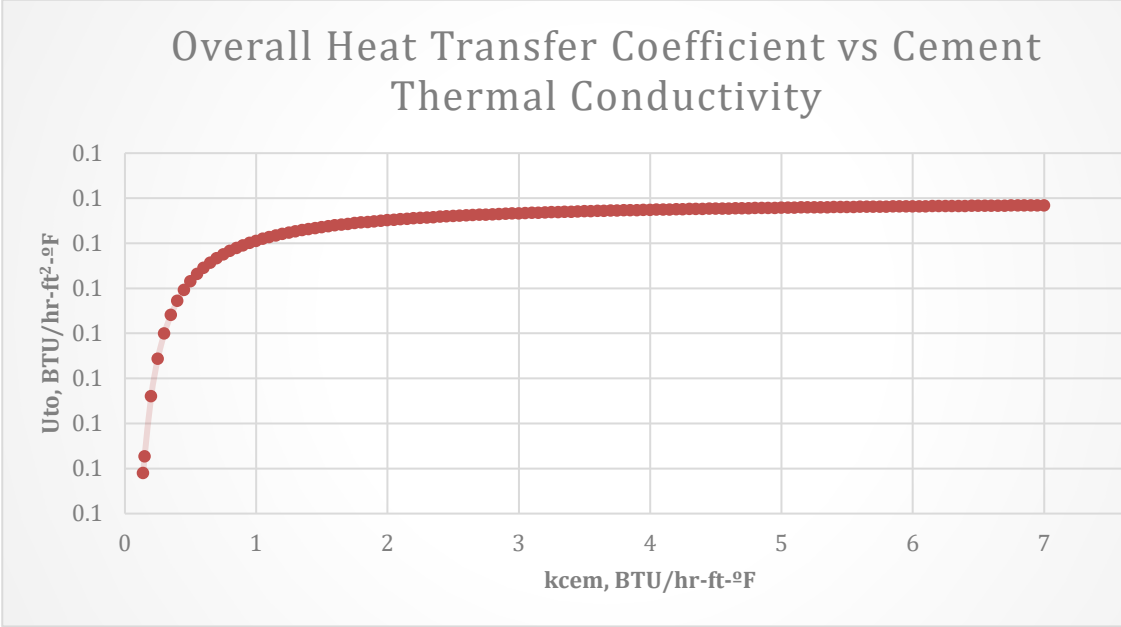

Figure 5.22: Effect of conductivity of insulators at the reservoir section.

When we plotted a graph of cement thermal conductivity against heat exchange (Figure 5.23), we observed that there is almost no heat loss to the wellbore as compared to the previous cases. The overall heat loss remained constant at a value of -5,7 to -6,2 [BTU/hr-ft] for all values of cement thermal conductivity. This shows that a high thermal conductivity for the outer insulator and low thermal conductivity for the inner insulators will significantly reduce heat loss between the formation and the wellbore as compared to the opposite scenario. But the effect of the conductivities of both insulators in reducing heat loss to the wellbore is less when compared to installing an inner insulator with low conductivity as previously seen.

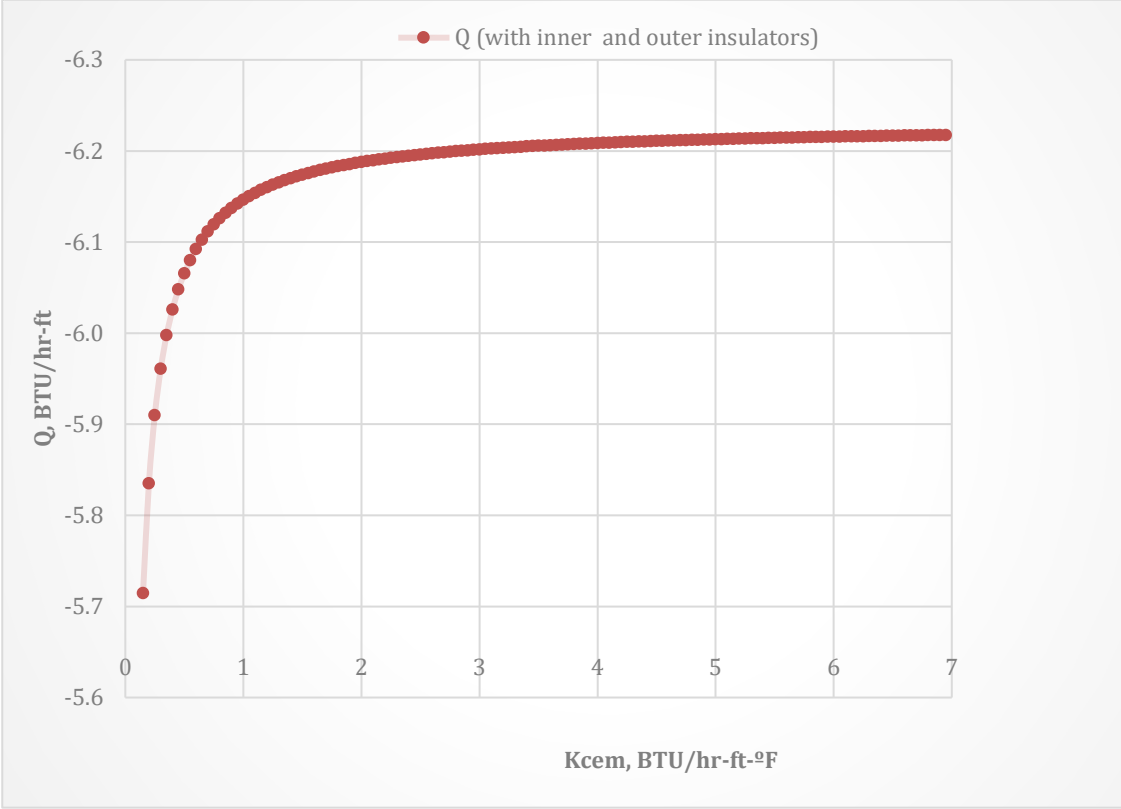

Figure 5.23: Effect of conductivity of insulators at the reservoir section.

5.2.2.2 Middle Section

The middle section consists of the zone just above the reservoir section and the simulations are done with a consideration for the effect of the intermediate casing and the production casing with the help of equation 4.17 and as shown in Figure 5.5. The same simulations where done like in the reservoir section to study the effect of adding more casings to the overall heat transfer coefficient and heat exchange. The assumed fluid temperature for this section is 440[ºC] and that of the wellbore temperature is 340[ºC]. The same change in parameters done in the reservoir section, will also be done in the middle section.

5.2.2.2.1 Heat Transfer without Insulators

In this simulation, the middle/intermediate section of the well is completed with no inner or outer insulators. That is, their thicknesses are zero. The graphs of the overall thermal resistance and the overall heat transfer coefficient plotted against cement thermal conductivity are shown in Figures 5.24 and 5.25 below.

The thermal conductivity of cement and the overall thermal resistance of the wellbore are inversely proportional, and the decrease in resistance shows an exponential decline behavior initially, followed by a slow decline which begins at approximately 0,6 [BTU/hr-ft-ºF].

The reverse is achieved when plotting the same cement thermal conductivities against overall heat transfer coefficient. There is an exponential increase in the overall heat transfer coefficient as the conductivity of cement increases. This is due to the fact that high cement thermal conductivities lead to higher heat loss in the reservoir.

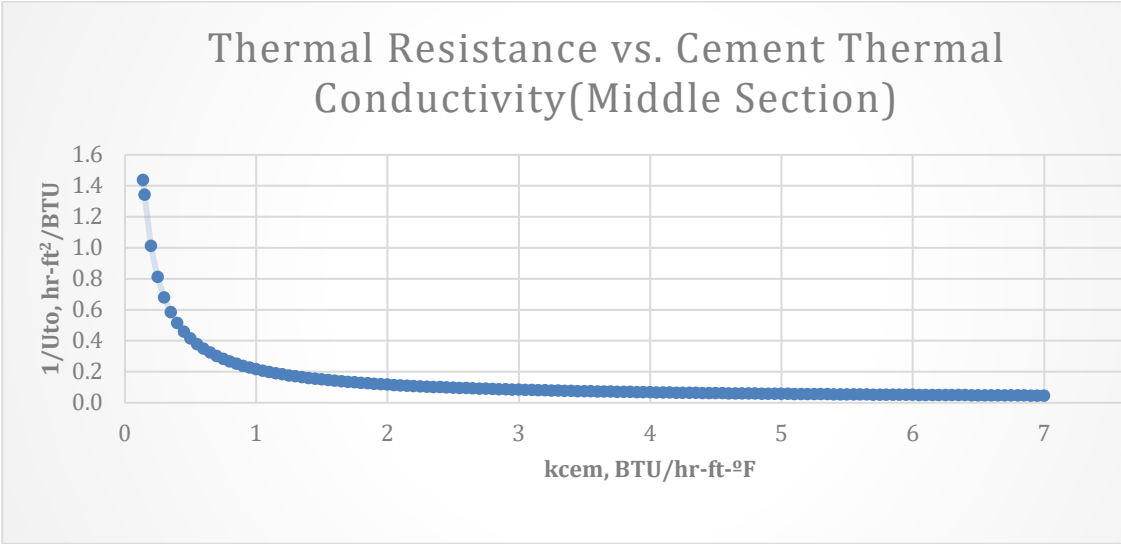

Figure 5.24: Thermal resistance versus cement thermal conductivity-uninsulated middle section.

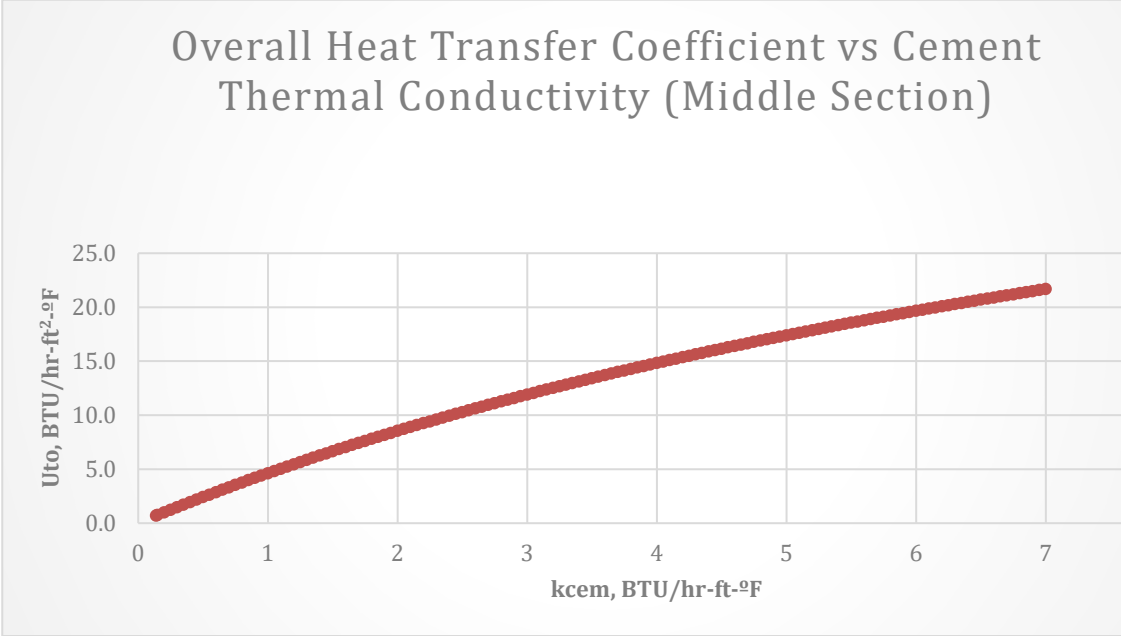

Figure 5.25: Overall heat transfer coefficient versus cement thermal conductivity-uninsulated middle section.

Figure 5.26 shows a plot of heat exchange versus cement thermal conductivity when there are no insulators. The graph shows an exponential loss of heat to the wellbore from 0 to -10000 [BTU/hr-ft] as cement thermal conductivity increases from 0,14 to 7 [BTU/hr-ft-ºF]. This is to confirm that high cement thermal conductivity leads to a higher rate of heat loss to the wellbore.

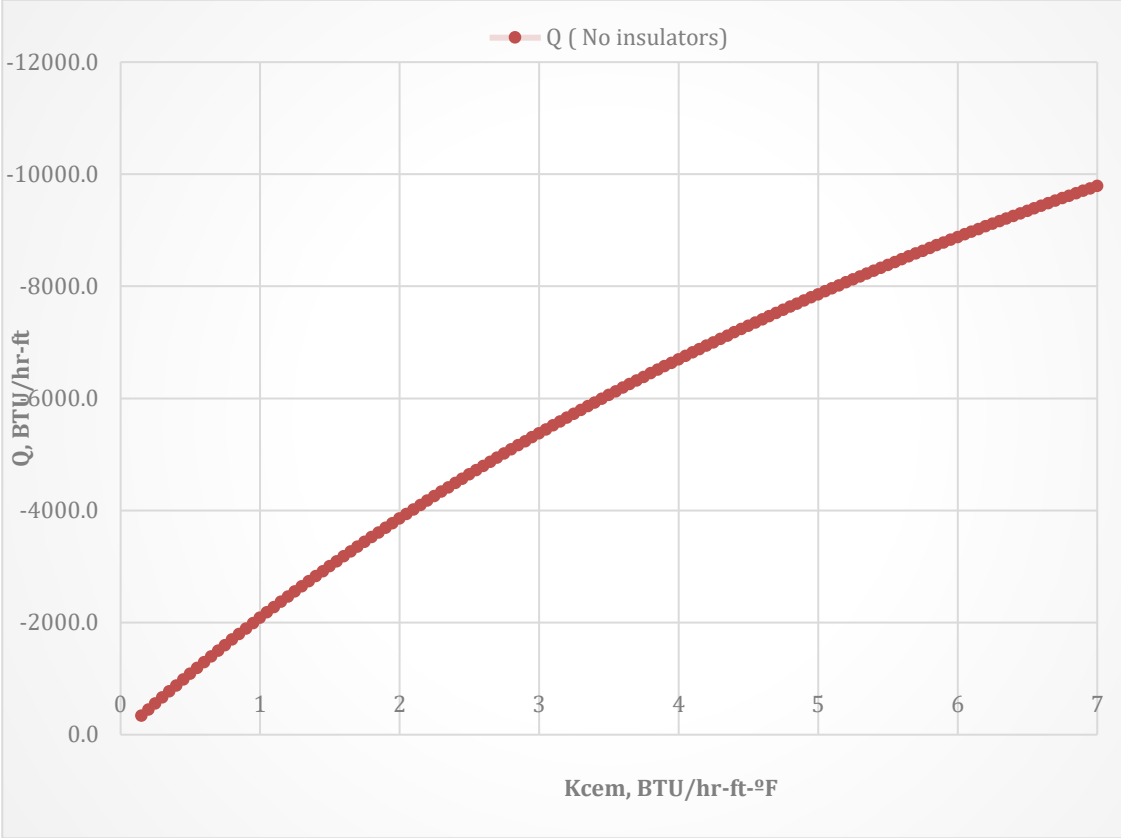

Figure 5.26: Heat exchange versus cement thermal conductivity-uninsulated middle section.

5.2.2.2.2 Effect of Thickness of the Outer Insulator

The effect of the thickness of the outer insulator was simulated by varying the thickness of the outer insulator from 0 to 0,3 [ft]. The thermal conductivity of the insulator is set at 0,02 [W/mK].

At a value of 0,175 [ft], graphs of the cement thermal conductivity against the overall thermal resistance and the overall heat transfer coefficient are shown in Figures 5.27 and 5.28 below. The thermal conductivity of cement and the overall thermal resistance of the wellbore are inversely proportional, and the decrease in resistance shows an exponential decline behavior initially, followed by a slow decline which begins at approximately 7,8 [BTU/hr-ft-ºF].

The reverse is seen when plotting the same cement thermal conductivities against overall heat transfer coefficient. Unlike in Figure 5.24, the overall heat transfer coefficient remains constant at 0,1 [BTU/hr-ft-ºF] for cement thermal conductivity ranging from 0,14 to 7 [BTU/hr-ft-ºF].

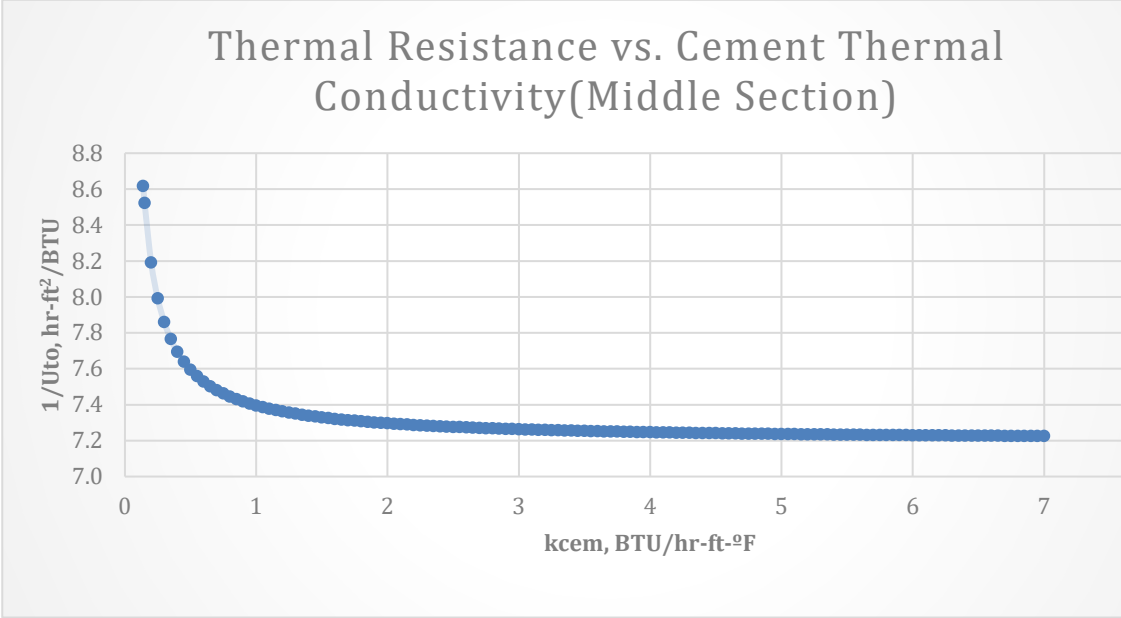

Figure 5.27: Thermal resistance versus cement thermal conductivity-outer insulated middle section.

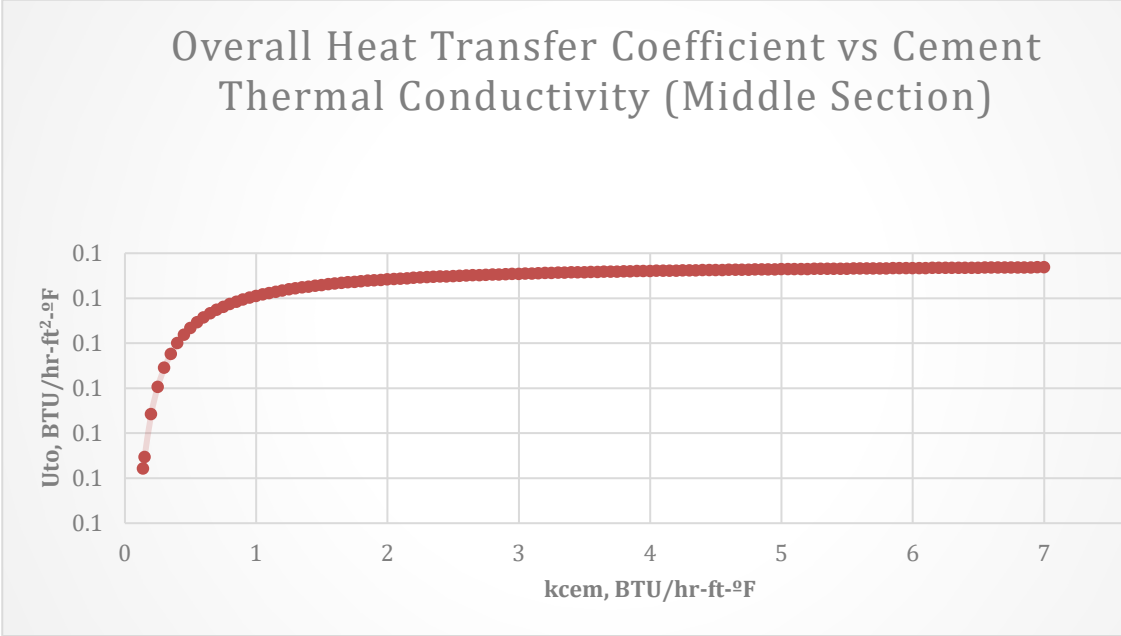

Figure 5.28: Overall heat transfer coefficient versus cement thermal conductivity-outer insulated middle section.

A graph of the cement thermal conductivity against the heat exchange also shows a similar trend like in the reservoir section as shown in Figure 5.29. The result for the heat exchange shows a significant change as compared to the reservoir section. Heat exchange ranges increases exponentially from -52,4 [BTU/hr-ft] and then slows down rapidly at -60 [BTU/hr-ft] for cement thermal conductivity of 0,14 to 0,85 [BTU/hr-ft-ºF]. The exponential increase slows down from -60 to -62,5 [BTU/hr-ft] and then remain constant.

There is more heat loss in this section of the wellbore when compared to the reservoir section at an approximate value of 89% more.

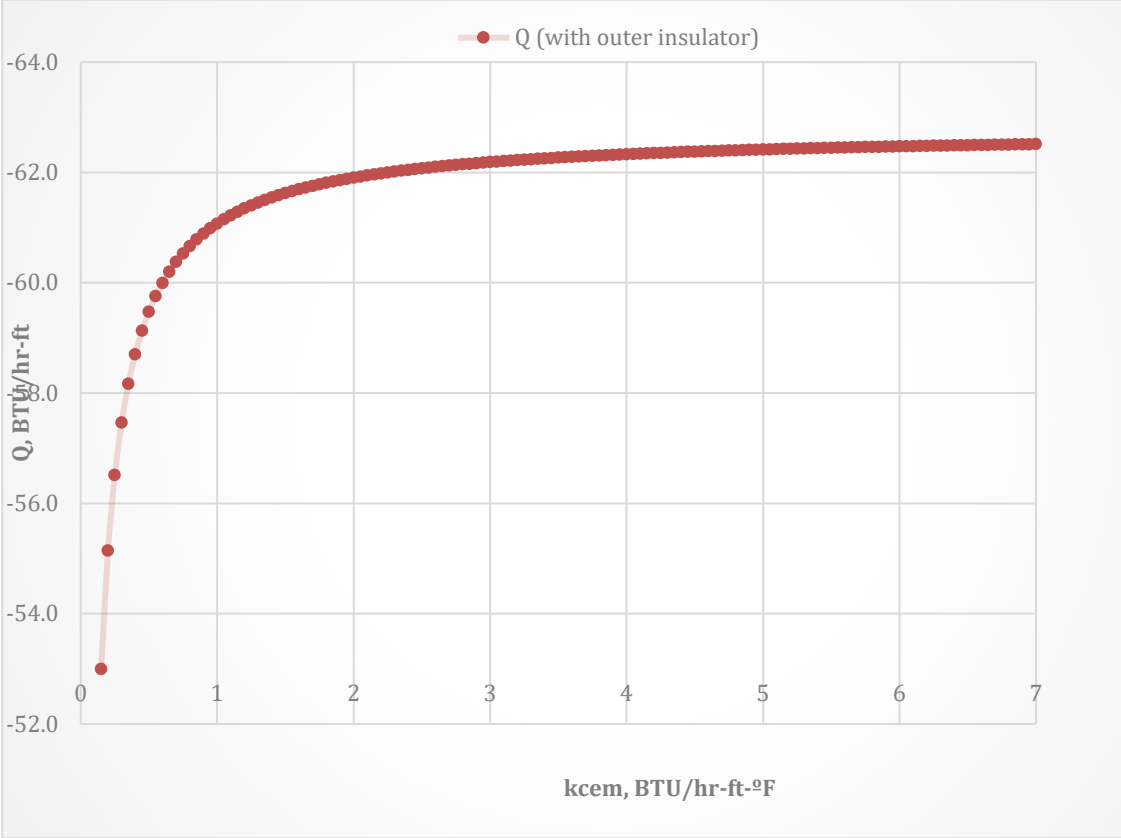

Figure 5.29: Heat exchange versus cement thermal conductivity-outer insulated middle section.

5.2.2.2.3 Effect of Thickness of Inner Insulator

To study the effect of inner insulator on the overall heat exchange, it's thickness is varied from 0 to 0,3 [ft] while the outer thickness remains zero. The conductivity of the insulator is kept constant at 0,02 [W/mK]. A similar behavior of the parameters can be seen in Figures 5.30 and 5.31 as seen previously. However, in this case, the overall thermal resistance declines slowly at a higher value of 14,8 [BTU/hr-ft-ºF].

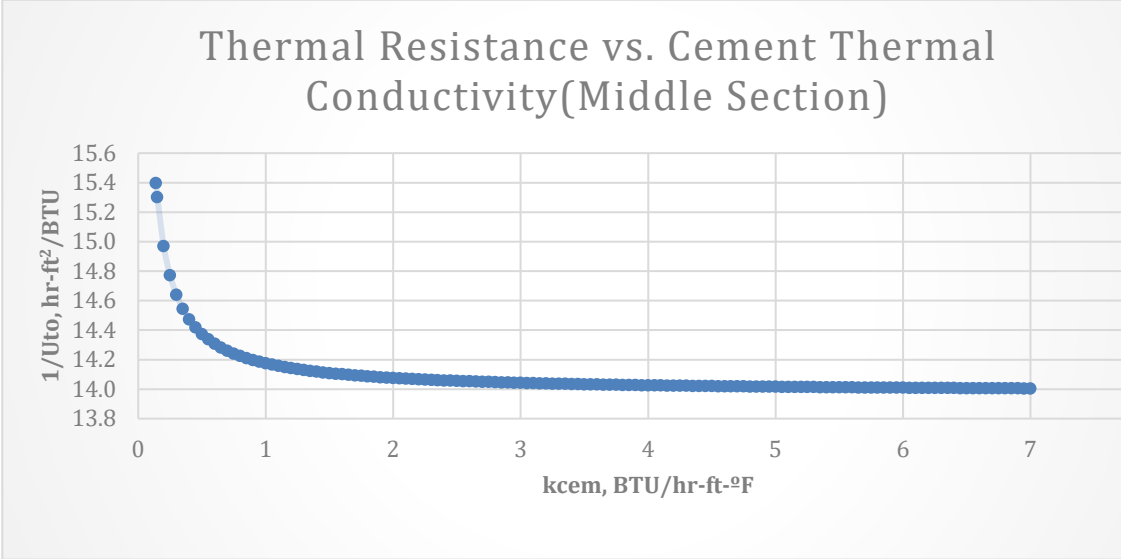

Figure 5.30: Thermal resistance versus cement thermal conductivity-inner insulated middle section.

The overall heat transfer just as in the previous section, remains constant at 0,1 [BTU/hr-ft^2-ºF] for all values of cement thermal conductivity.

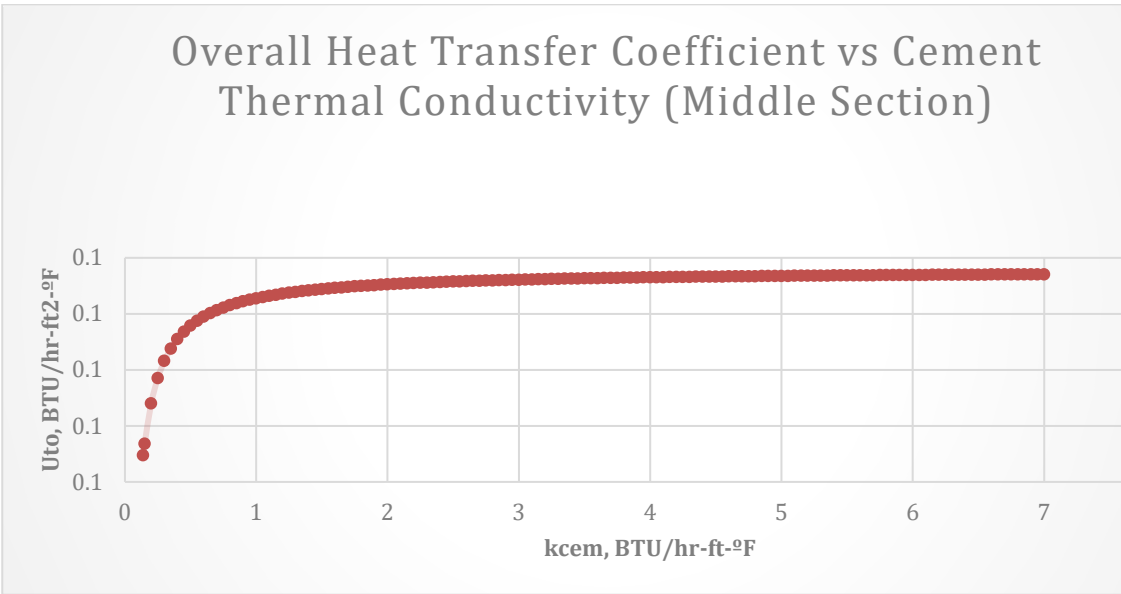

Figure 5.31: Overall heat transfer coefficient versus cement thermal conductivity-inner insulated middle section.

However, the effect of thickness of the outer insulator in reducing the heat exchange between the wellbore and the formation was significant in this scenario. The overall heat exchange when an inner insulator is installed ranges from -29,5 to -32,25 [BTU/hr-ft] for values of cement thermal conductivity that range from 0,14 to 7 [BTU/hr-ft-ºF] as shown in Figure 5.32.

This reveals that, 58% less heat is lost when compared with geothermal well completion at the intermediate section by insulating from the outside.

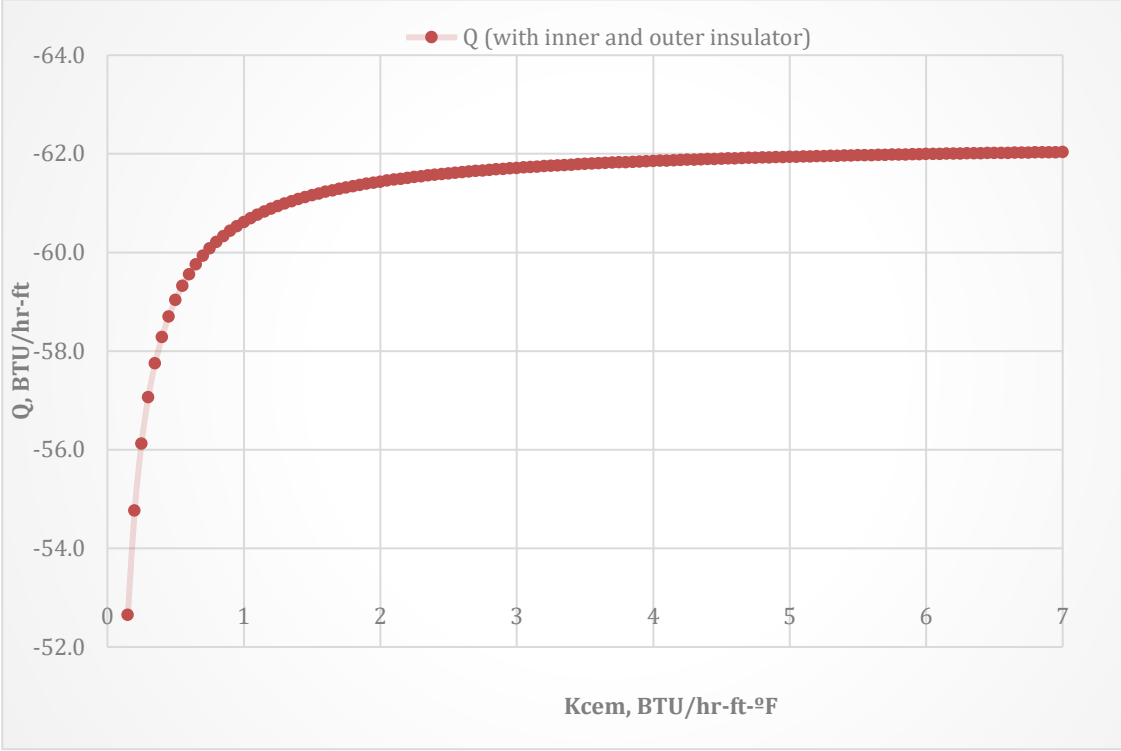

Figure 5.32: Heat exchange versus cement thermal conductivity-inner insulated middle section.

5.2.2.2.4 Effect of Completing with both Inner and Outer Insulators

To further determine the effect of installing an inner and outer insulator when completing the intermediate section of a geothermal well, the thicknesses of both insulators where varied simultaneously to see their combined effect. The results presented below represents the thickness of both insulators at 0,175 [ft].

At a value of 0,175 [ft] for thickness of both insulators, graphs of the cement thermal conductivity against the overall thermal resistance and the overall heat transfer coefficient are shown in Figures 5.33 and 5.34 below. Similar behavior can be observed as in the previous graphs but this time around, the overall thermal resistance declines slowly at a higher value of approximately 21,8 [BTU/hr-ft-ºF].

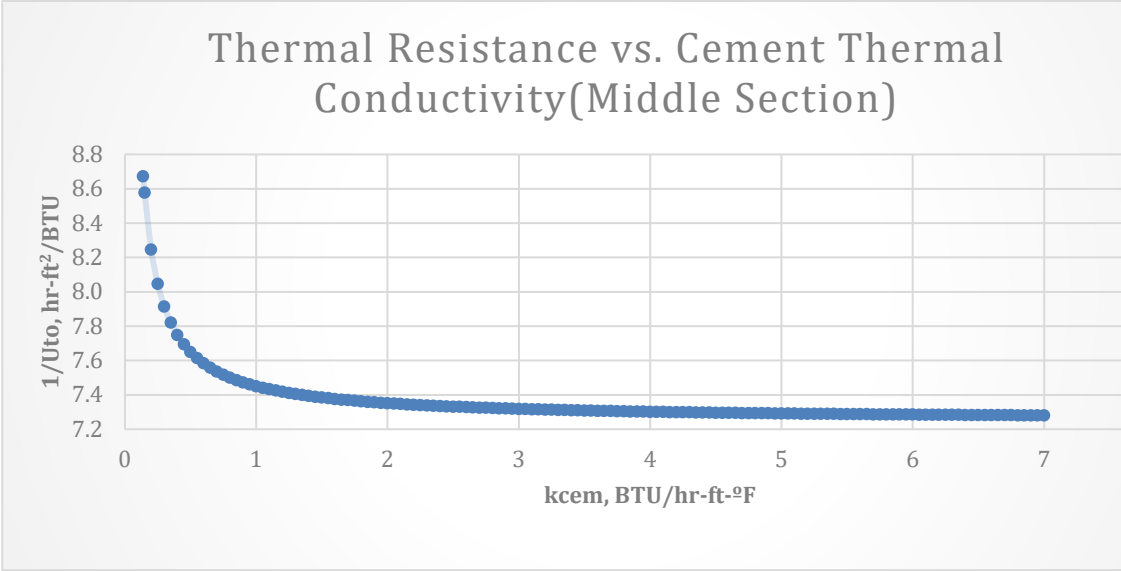

5.33: Thermal resistance versus cement thermal conductivity-inner insulated middle section.

The overall heat transfer coefficient however, remains zero for cement thermal conductivities ranging from 0,14 to 7 [BTU/hr-ft-ºF]. This shows that there is almost no heat lost to the wellbore in the intermediate section.

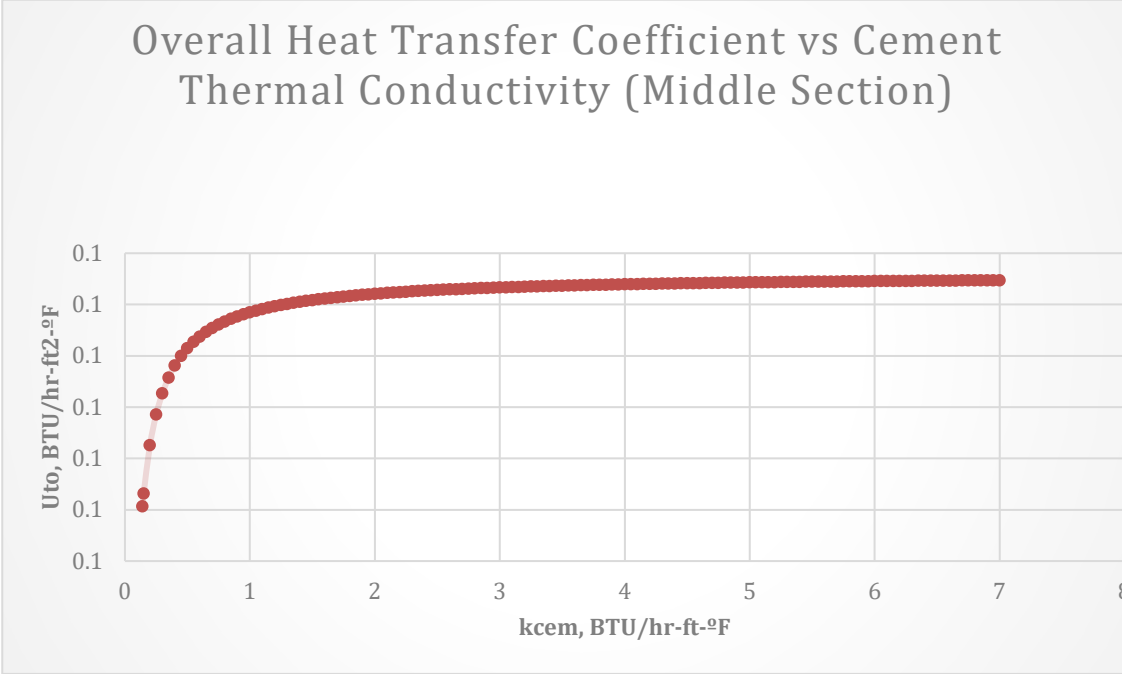

5.34: Overall heat transfer coefficient versus cement thermal conductivity-inner insulated middle section.

When we plotted a graph of cement thermal conductivity against heat exchange (Figure 5.35), we observed that there is less heat loss to the wellbore as compared to the previous cases. The overall heat loss varied slightly from a value of -20 to -21,3 [BTU/hr-ft] for all values of cement thermal conductivity.

This shows that there is; 32% less heat loss when both insulators are used as compared to when only the inner insulator is used, 61,8% less heat loss when compared to using only the outer insulator and 93,6% less heat loss when compared to completing this section of the well without insulators. It can also be determined that, additional casing does not have an effect on the heat transfer of the fluid to the surface.

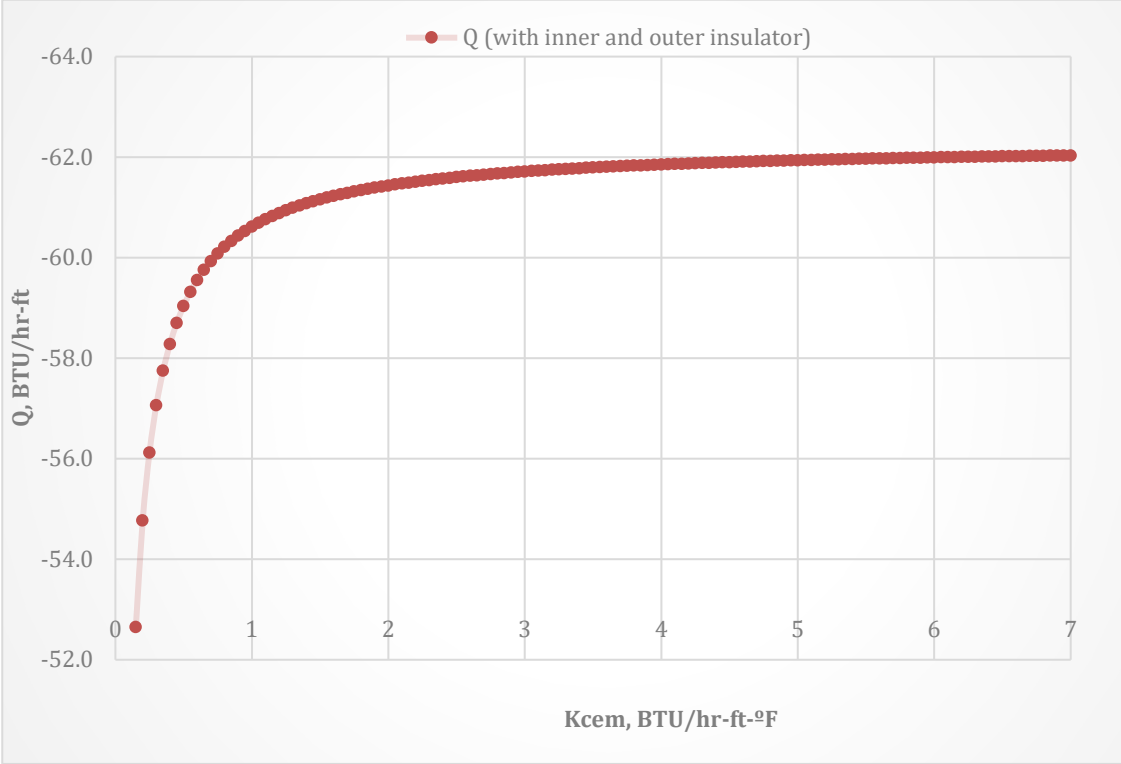

Figure 5.35: Heat exchange versus cement thermal conductivity-inner insulated middle section.

5.2.2.2.5 Effect of Thermal Conductivity of Insulators

This section of the study was to help us study the effect of adding one more casing (intermediate casing), to determine its importance in the overall heat transfer of the fluid. The effect of thermal conductivity of the outer and inner insulators where studied by varying the conductivity of both insulators while maintaining constant values for their thicknesses. The thickness of the insulators was kept constant at 0,175 [ft] for both inner and outer layers.

The graph of the thermal conductivity of the cement and the overall thermal resistance of the wellbore in Figure 5.36 shows an exponential decline followed by a slow linear decline at approximately 21,8 [BTU/hr-ft^2-ºF] when the conductivity of the outer insulator is kept at 5 [BTU/hr-ft-ºF] and that of the inner insulator at 0,02 [BTU/hr-ft-ºF].

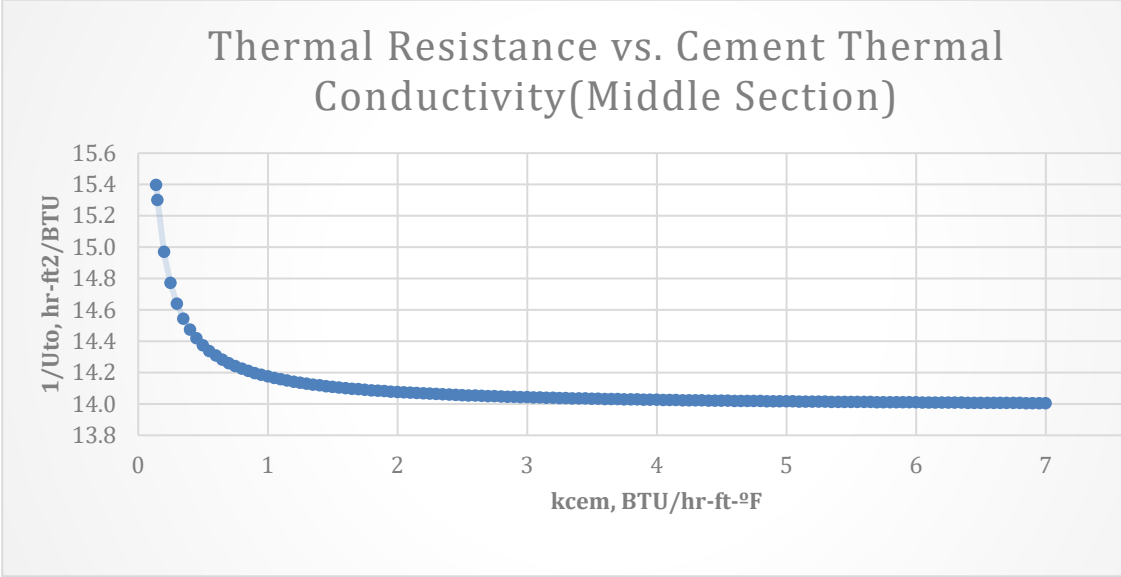

Figure 5.36: Effect of conductivity of both insulators-Middle Section.

The overall heat transfer coefficient is constant at 0,1 [BTU/hr-ft^2-ºF] in this case (Figure 5.37). This is a sign that no heat or less heat is loss.

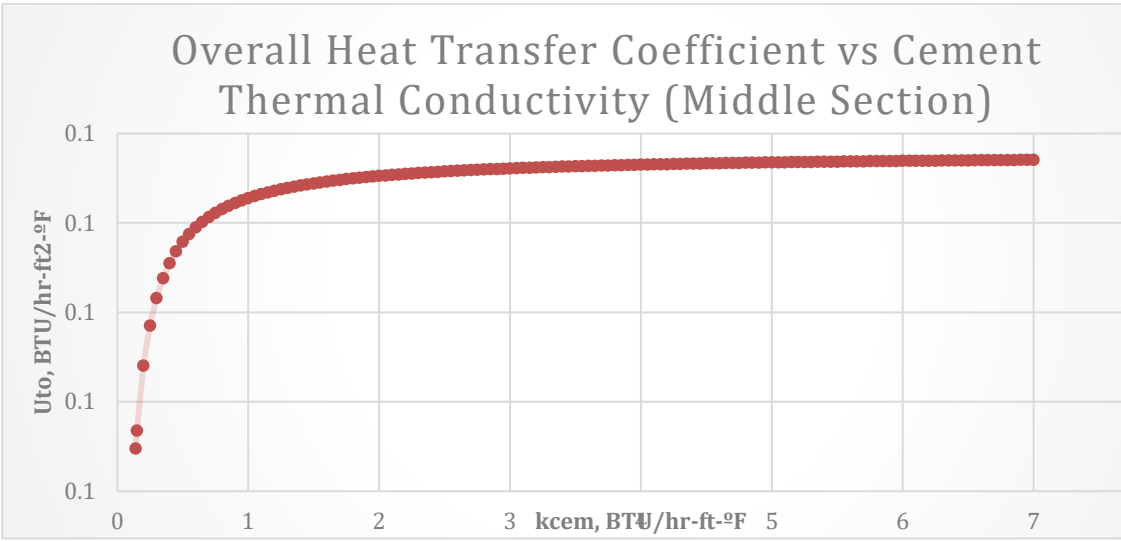

Figure 5.37: Effect of conductivity of both insulators-Middle Section.

Heat exchange when plotted against cement thermal conductivity does not have a real significant change as compared to when we simulated with only an inner insulation which

had a lower thermal conductivity of about 0,02 [BTU/hr-ft-ºF]. This is shown in Figure 5.38 below. Overall heat exchange ranged from -29,3 to -32,2 [BTU/hr-ft].

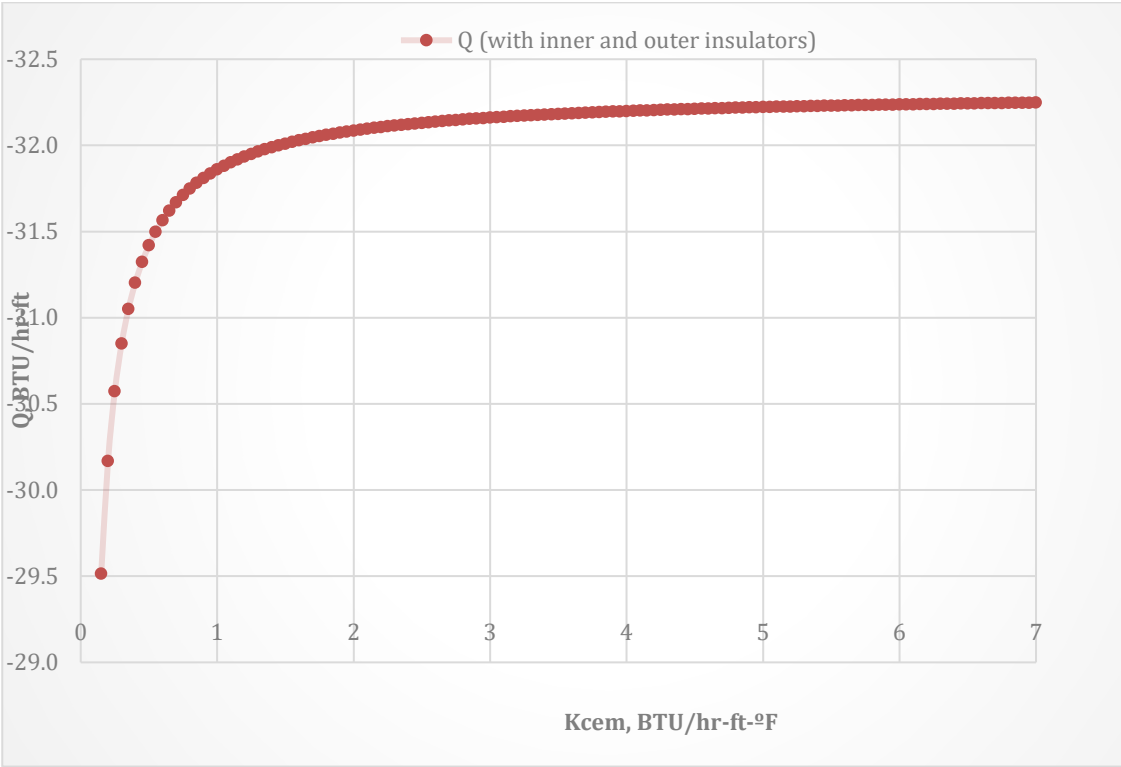

Figure 5.38: Effect of conductivity of both insulators-Middle Section.

When the thermal conductivity of the inner insulator is increased to 5 [BTU/hr-ft-ºF] and that of the outer insulator is decreased to 0,02 [BTU/hr-ft-ºF], the result of thermal resistance versus cement conductivity shows a sharp decline at 7,8 [hr-ft^2-ºF/BTU] as compared to 21,8 [hr-ft^2-ºF/BTU] in the previous case. This is shown in Figure 5.39 below. A similar trend of results is observed when cement thermal conductivity is plotted against overall heat transfer coefficient (Figure 5.40). The overall heat transfer coefficient remains constant at 0,1 [BTU/hr-ft^2-ºF].

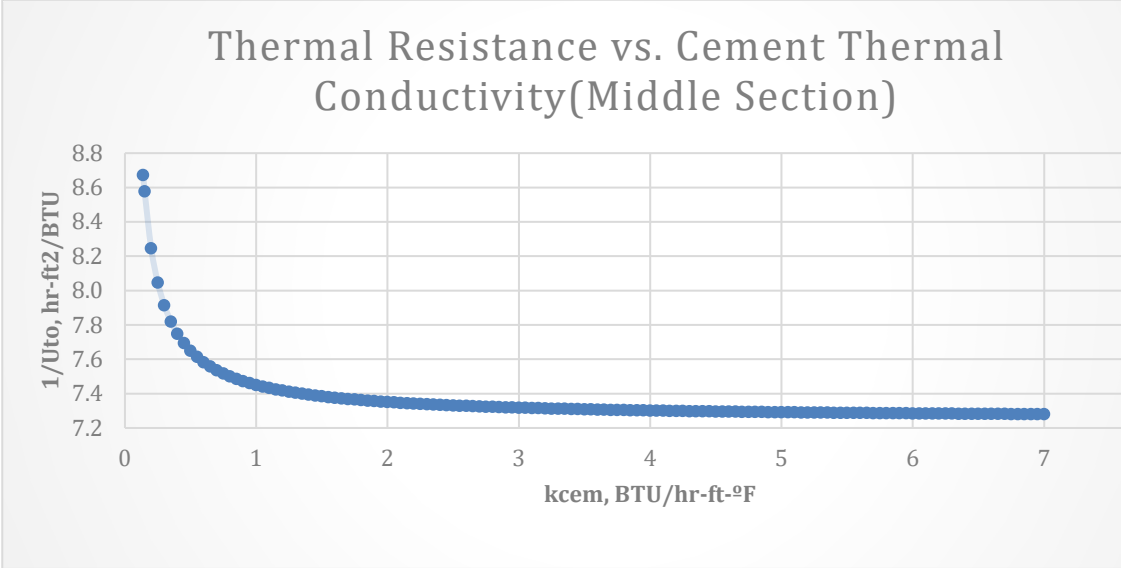

Figure 5.39: Effect of conductivity of both insulators-Middle Section.

The overall heat transfer coefficient, just as in the previous case remains constant at 0,1 [BTU/hr-ft^2-ºF] in this case (Figure 5.40).

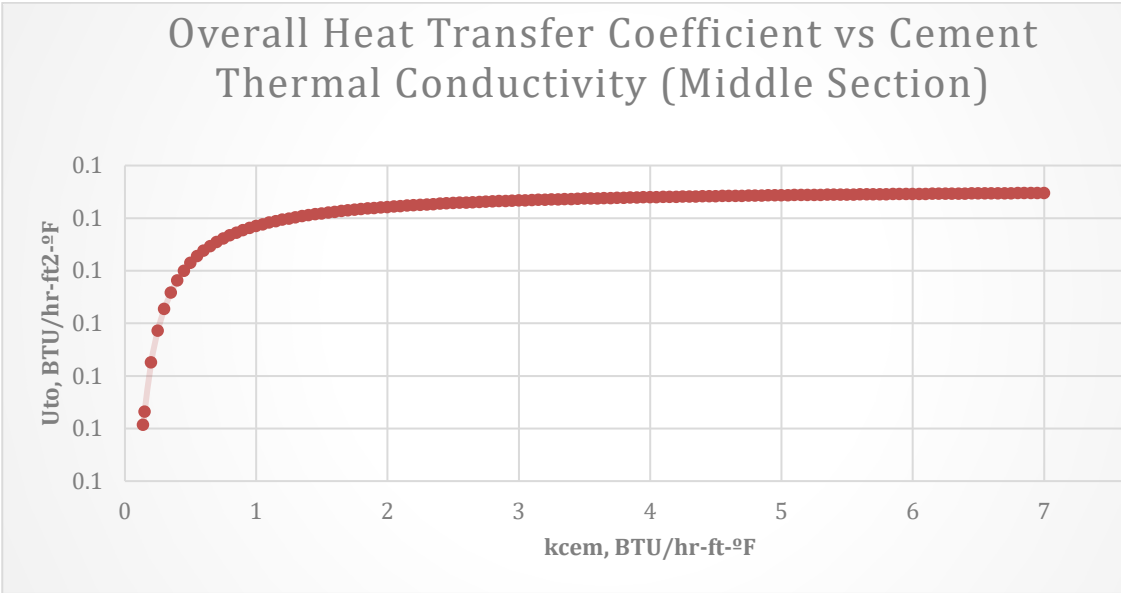

Figure 5.40: Effect of conductivity of both insulators-Middle Section.

When we plot cement thermal conductivity against heat exchange, there is no significant change as compared to when we simulated with only an inner insulation which had a

lower thermal conductivity of 0,02 [BTU/hr-ft-ºF]. This is shown in Figure 5.41 below. Overall heat exchange ranged from -52,1 to -62 [BTU/hr-ft].

These results show that, a higher thermal conductivity of the inner insulator and a lower thermal conductivity of the outer insulator or vice versa, does not have significant change in the overall heat exchange of the fluid between the wellbore and the fluid. Also, the addition of an intermediate casing does not have a significant effect on the overall heat exchange between the fluid and the formation at the intermediate/middle section of the well.

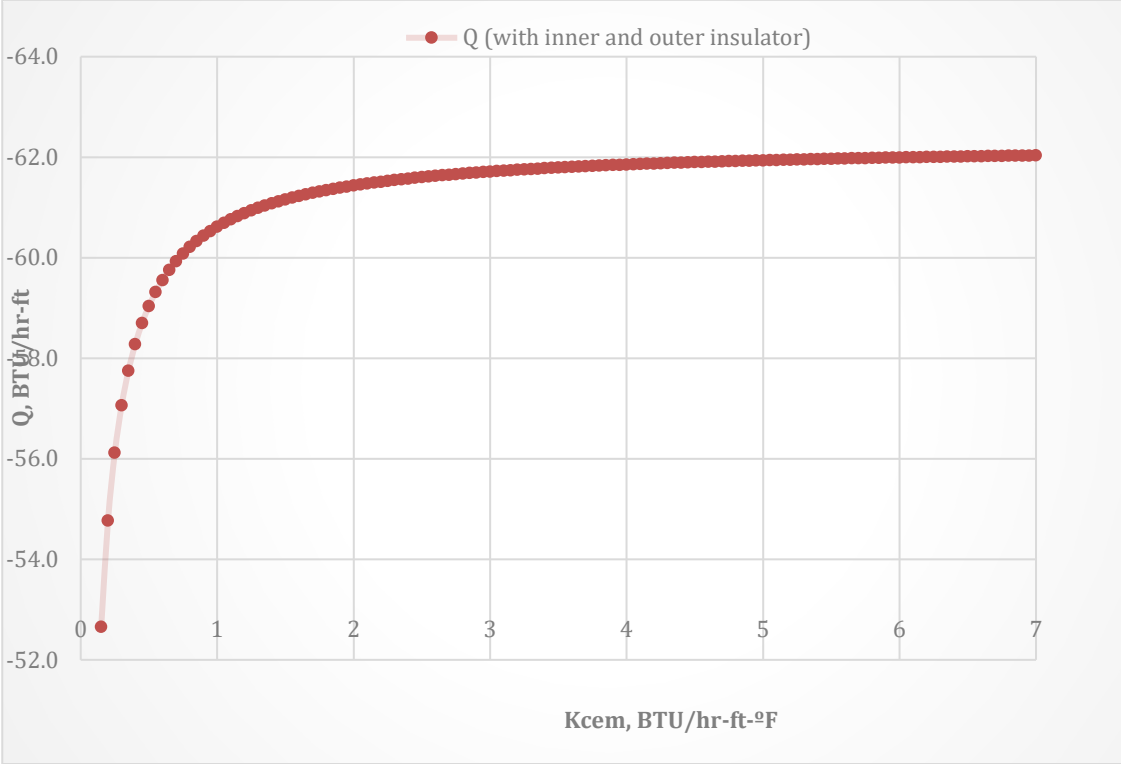

Figure 5.41: Effect of conductivity of both insulators-Middle Section.

5.2.2.3 Top Section

The top section consists of the zone above the middle section. The simulations are done with a consideration for the effect of the production, intermediate, surface, conductor casing with the help of equation 4.20. The same simulations where done like in the reservoir and middle section to study the effect of adding more casings to the overall heat transfer coefficient and heat exchange. Temperature of the fluid for this section is assumed to be 410 [ºC] and that of the wellbore 170 [ºC] (From Table 4.6 and Figure 5.5).

5.2.2.3.1 Heat Transfer without Insulators

In this simulation, the top section of the well is completed with no inner or outer insulators. The graphs of the overall thermal resistance and the overall heat transfer coefficient plotted against cement thermal conductivity are shown in Figures 5.42 and 5.43 below.

The thermal conductivity of cement and the overall thermal resistance of the wellbore are inversely proportional, and the decrease in resistance shows an exponential decline behavior initially, followed by a slow decline which begins at approximately 1,6 [BTU/hr-ft-ºF].

The reverse is achieved when plotting the same cement thermal conductivities against overall heat transfer coefficient. There is an exponential increase in the overall heat transfer coefficient as the conductivity of cement increases. This is due to the fact that high cement thermal conductivities lead to higher heat loss in the reservoir.

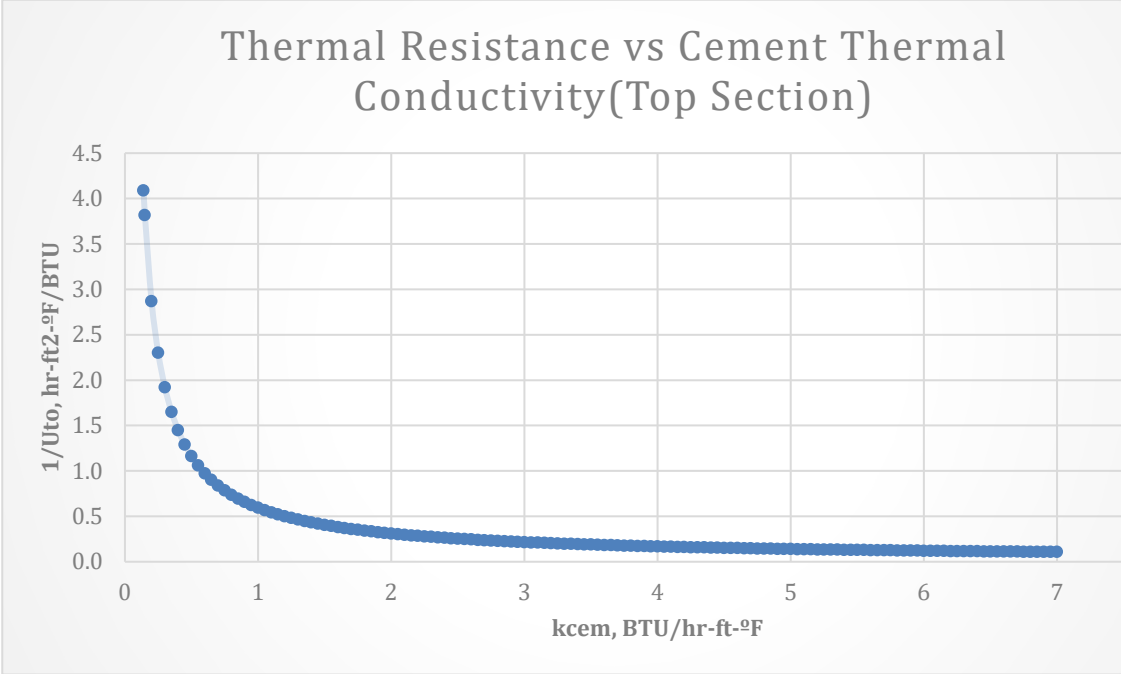

Figure 5.42: Thermal resistance versus cement thermal conductivity-uninsulated top section.

The results at the top section of the well show that, a low amount of heat loss can be achieved if the cement thermal conductivity is less than 1 [BTU/hr-ft-ºF] in this scenario.

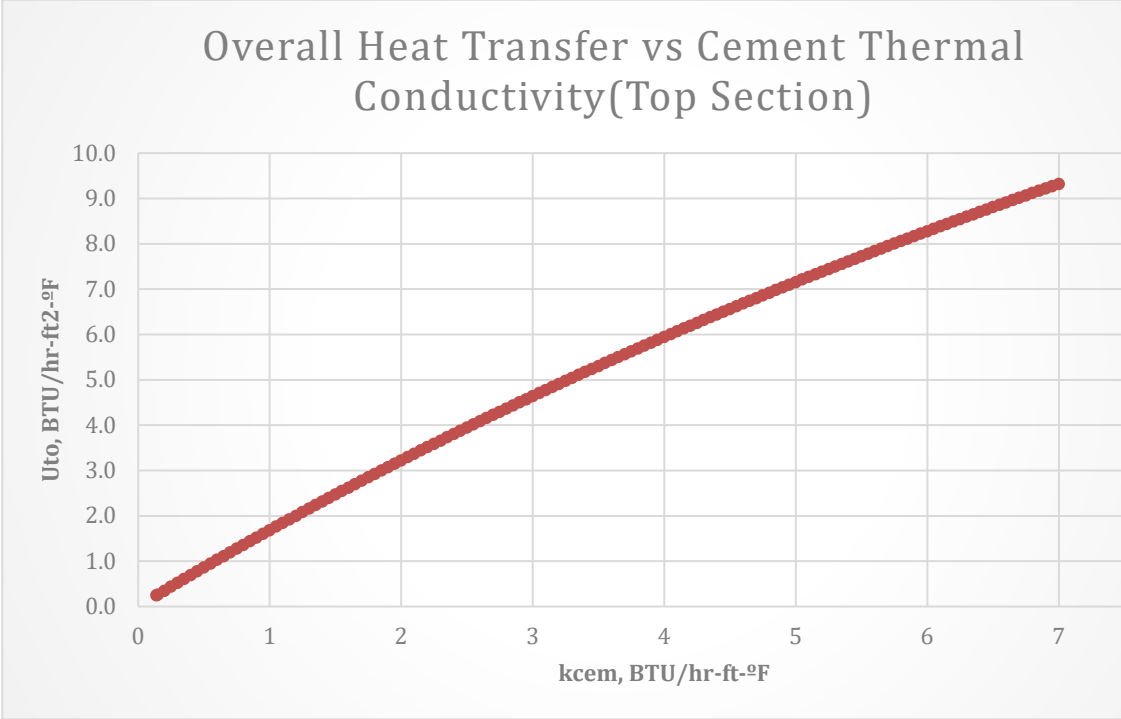

Figure 5.43: Overall heat transfer versus cement thermal conductivity-uninsulated Top Section.

An exponential increase in heat exchange between the fluid and the wellbore as shown on Figure 5.44. This is still to confirm that, to minimize the amount of heat loss to the formation, cement of very low thermal conductivity needs to be used for the geothermal well. It also shows that the addition of more casings in our simulations does not have a significant effect on the overall heat exchange because the heat exchange for both the middle and the top section varies from 0 to -10000 [BTU/hr-ft] when plotted against a range of cement thermal conductivity of 0,14 to 7 [BTU/hr-ft-ºF].

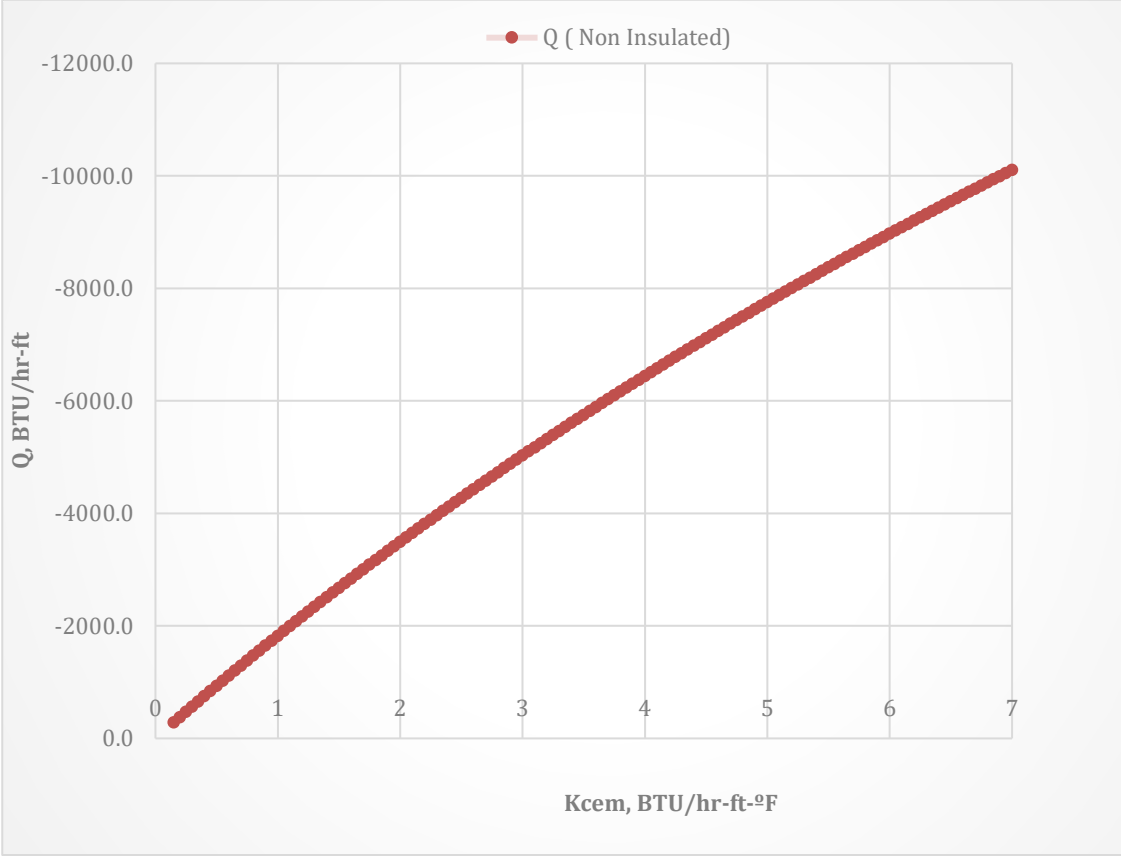

Figure 5.44: Heat exchange versus cement thermal conductivity-uninsulated Top Section.

5.2.2.3.2 Effect of Thickness of Outer Insulator

The effect of the thickness of the outer insulator on the top section of the well was simulated by varying the thickness of the outer insulator from 0 to 0,3[ft] while maintaining the inner thickness at zero.

The results plotted on a thermal resistance versus cement thermal conductivity shows when the outer thickness is simulated at 0,175 [ft] (Figure 5.45). It shows exponential decline of thermal resistance when cement thermal conductivity range from 0 to 0,2 [BTU/hr-ft-ºF] and a slow decline at about from 0,2 to 7 [BTU/hr-ft-ºF]. This is similar to the results for both the reservoir and middle section presented already.

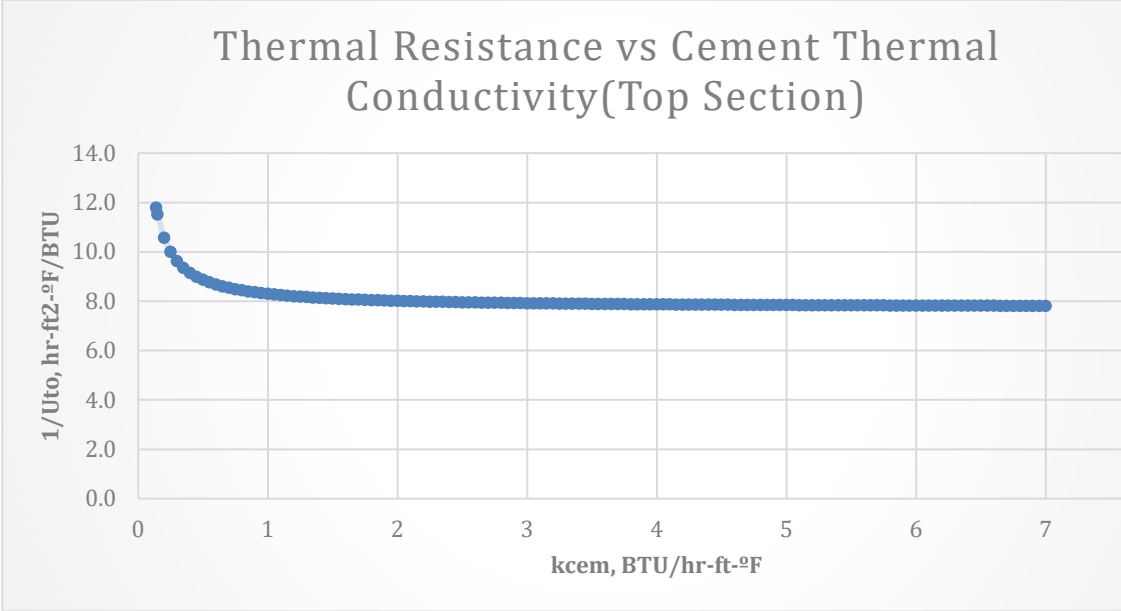

Figure 5.45: Thermal resistance versus cement thermal conductivity-outer Insulated Top Section.

The overall heat transfer coefficient remains constant at 0,1 [BTU/hr-ft^2-ºF] as shown in Figure 5.46 below.

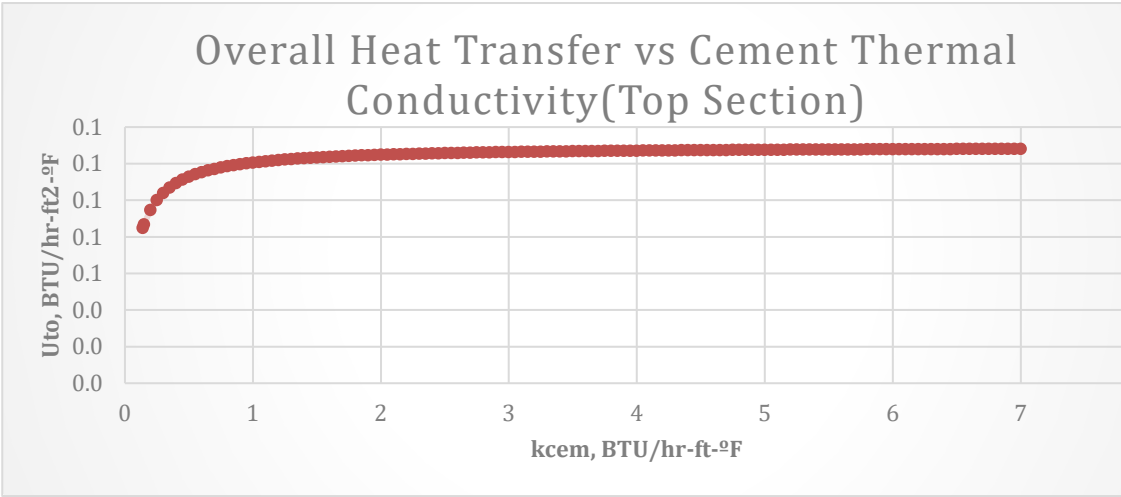

Figure 5.46: Overall heat transfer coefficient versus cement thermal conductivity-outer insulated Top Section.

Figure 5.47 shows the plot of heat exchange versus cement thermal conductivity. The results show that, heat exchange when the outer insulator thickness is 0,175 [ft], ranges from -92,3 to -139,7 [BTU/hr-ft]. This is a significant 65% reduction in heat exchange between the formation and the fluid compared to when there are no insulators at all. Heat exchange between the fluid and the formation however, shows a gradual increase from the reservoir to the surface when an outer insulator is placed.

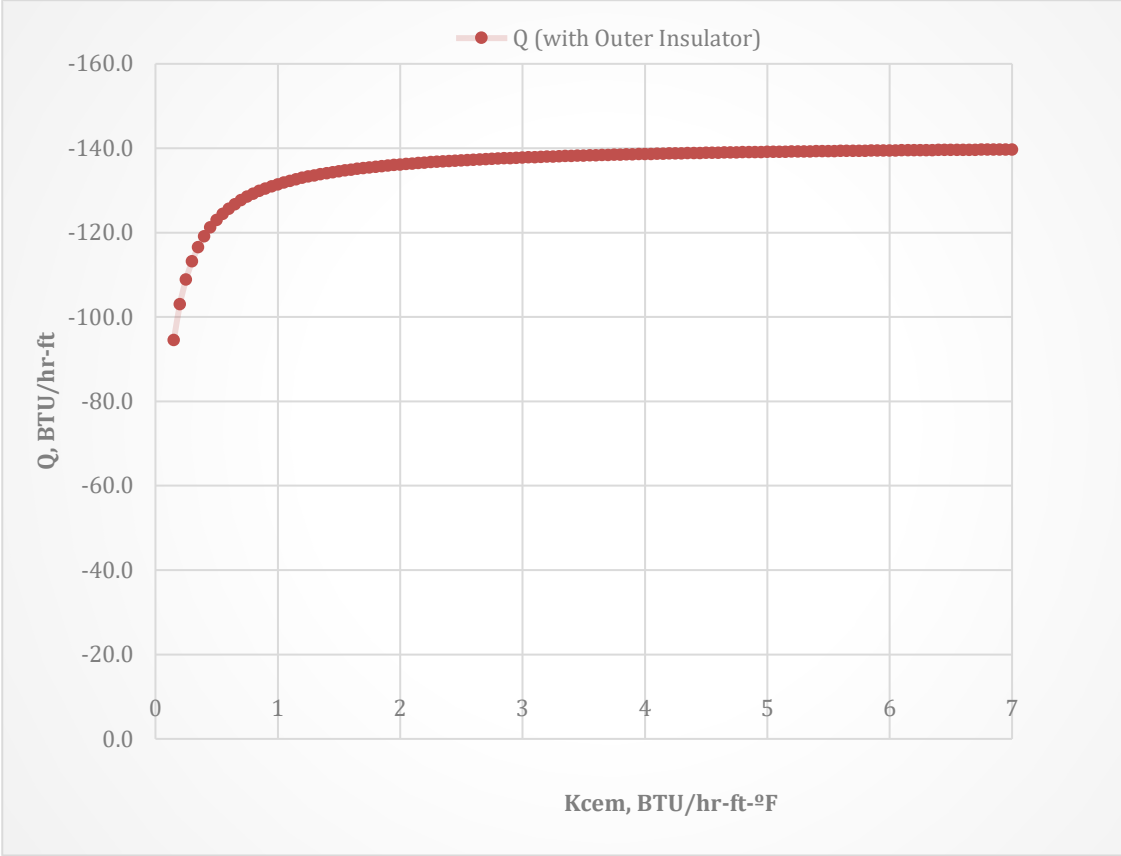

Figure 5.47: Heat exchange versus cement thermal conductivity-outer insulated Top Section.

5.2.2.3.3 Effect of Thickness of Inner Insulator

To study the effect of inner insulator on the overall heat exchange, the thickness of the outer insulator is kept at zero while varying the thickness of the inner insulator from 0 to 0,3 [ft]. At a thickness of 0,175 [ft], a similar behavior of the parameters can be seen in

Figures 5.48 and 5.49 as seen previously. However, in this case, the overall thermal resistance declines slowly at a higher value of 14 [BTU/hr-ft-ºF].

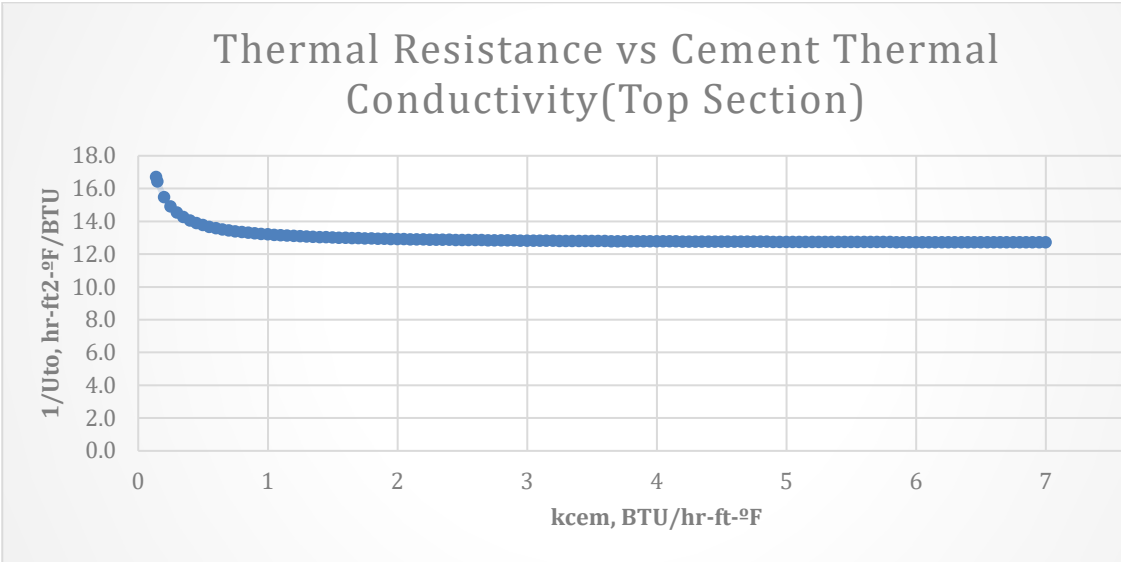

Figure 5.48: Thermal resistance versus cement thermal conductivity-inner insulated Top Section.

The overall heat transfer coefficient remains constant at 0,1 [BTU/hr-ft^2-ºF] as shown below.

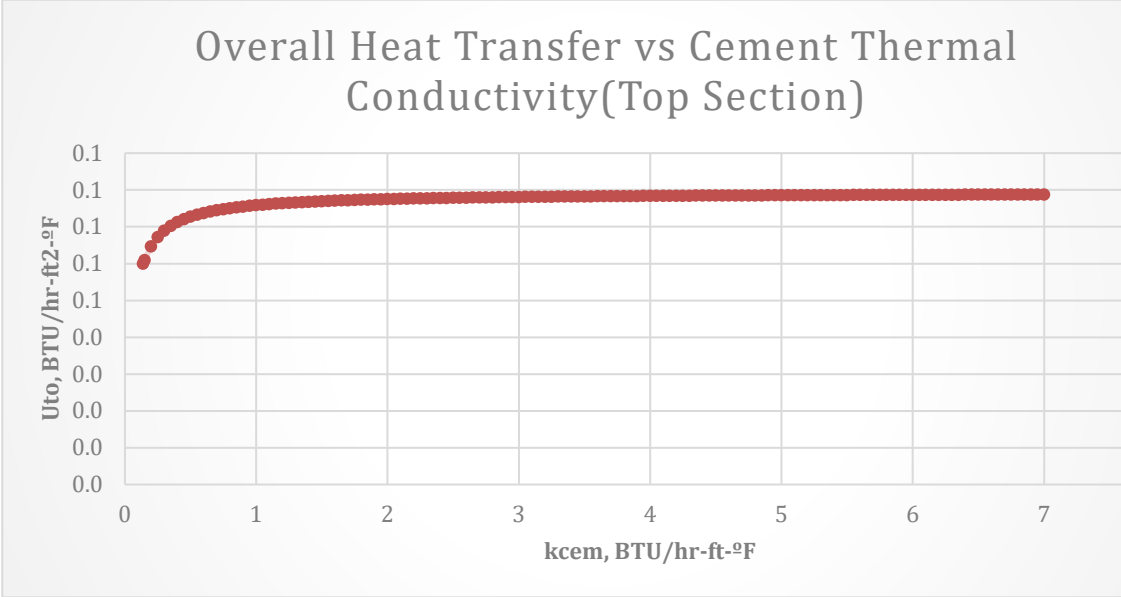

Figure 5.49: Overall heat transfer versus cement thermal conductivity-inner insulated Top Section.

However, figure 5.50 shows the plot of heat exchange versus cement thermal conductivity. The results show that, heat exchange when the inner insulator thickness is 0,175 [ft], ranges from -65 to -85,5 [BTU/hr-ft]. There is a significant 29% less heat loss to the wellbore at the reservoir section when an inner insulator is used compared to the same thickness of the outer insulator. It also shows that, placing an inner insulation is going to be much efficient in preventing heat loss between the wellbore and the formation.

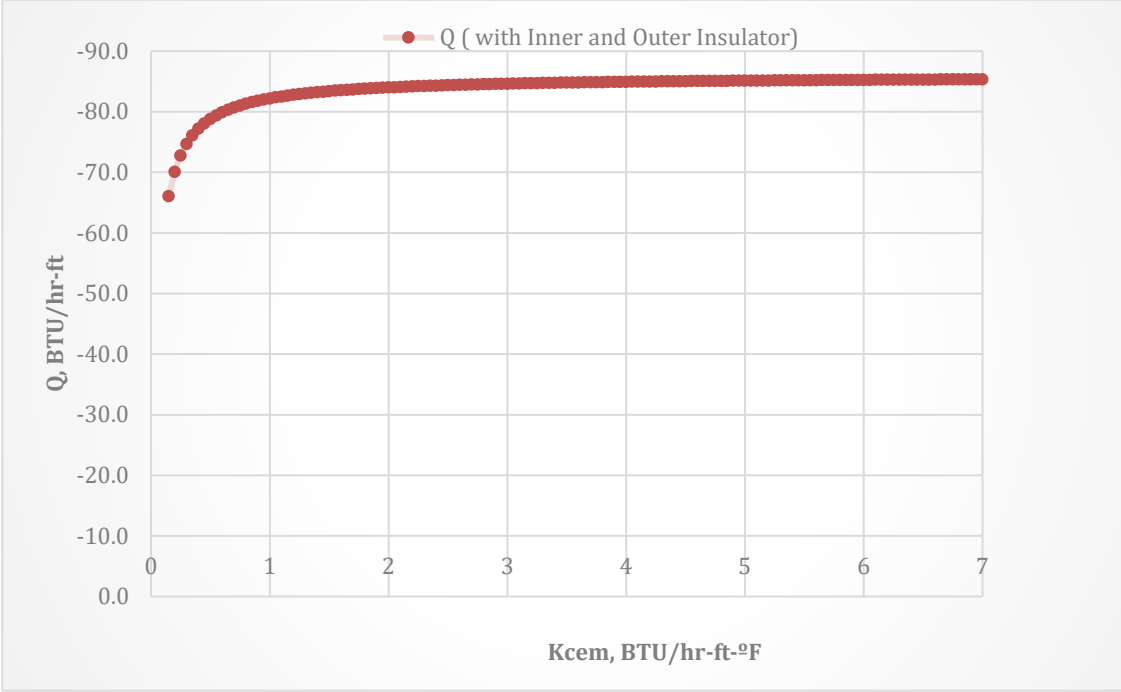

Figure 5.50: Heat exchange versus cement thermal conductivity-inner insulated Top Section.

5.2.2.3.4 Effect of Completing with both Inner and Outer Insulators

To determine the effect of installing an inner and outer insulator when completing the top section of the well, the thicknesses of both insulators where varied simultaneously to see their combined effect. The results presented below represents the thickness of both insulators at 0,175 [ft].

At a value of 0,175 [ft] for thickness of both insulators, graphs of the cement thermal conductivity against the overall thermal resistance and the overall heat transfer coefficient are shown in Figures 5.51 and 5.52 below. Similar behavior can be observed as in the previous graphs but this time around, the overall thermal resistance declines slowly at a higher value of approximately 21,5 [BTU/hr-ft-ºF].

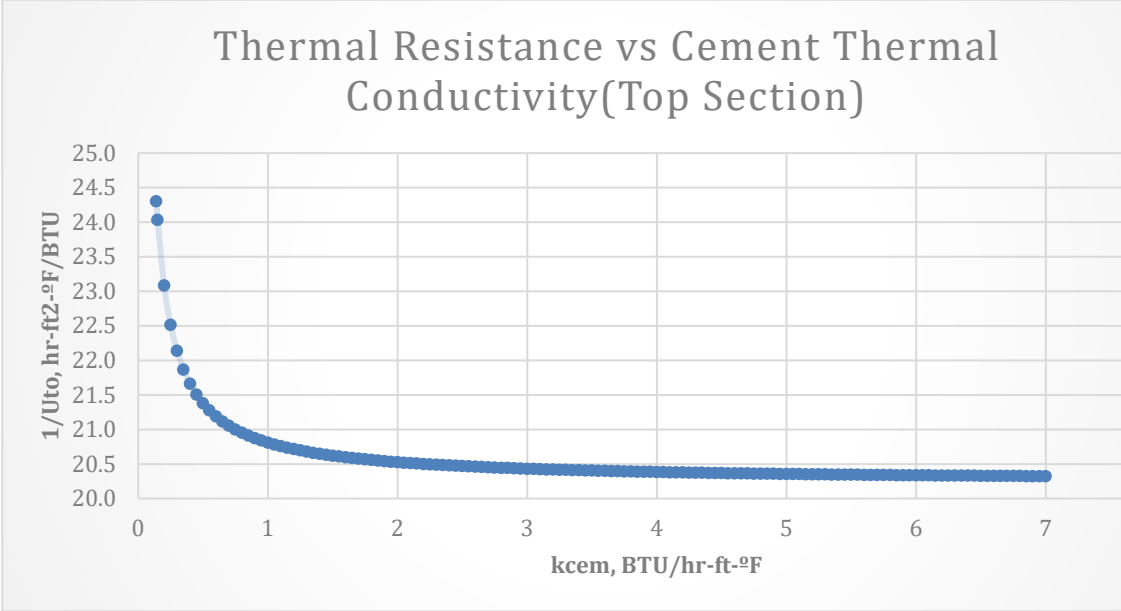

Figure 5.51: Thermal resistance versus cement thermal conductivity-inner and outer insulated Top Section.

The overall heat transfer coefficient however, remains zero for cement thermal conductivities ranging from 0,14 to 7 [BTU/hr-ft-ºF]. This shows that there is almost no heat lost to the wellbore in the top section.

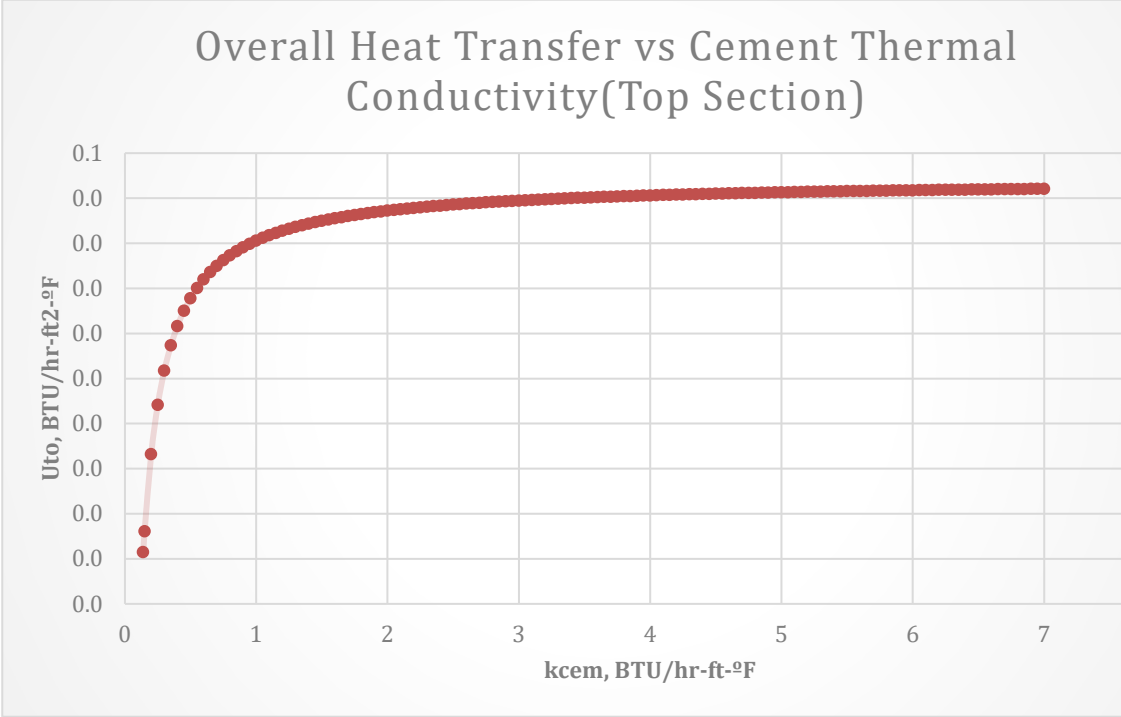

Figure 5.52: Overall heat transfer coefficient versus cement thermal conductivity-inner and outer insulated Top Section.

When we plotted a graph of cement thermal conductivity against heat exchange (Figure 5.53), we observed that there is almost no heat loss to the wellbore as compared to the previous cases. The overall heat loss ranges from -44,6 to -53,3 [BTU/hr-ft] for all values of cement thermal conductivity. This shows that there is; 31,4% less heat loss when both insulators are used as compared to when only the inner insulator is used, 51,7% less heat loss when compared to using only the outer insulator and 83% less heat loss when compared to completing the well without insulators in the top section.

It can be concluded that, heat loss at the surface can best be reduced when both insulators are placed in the well. Also, the effect of more casings is insignificant in reducing heat loss to the formation.

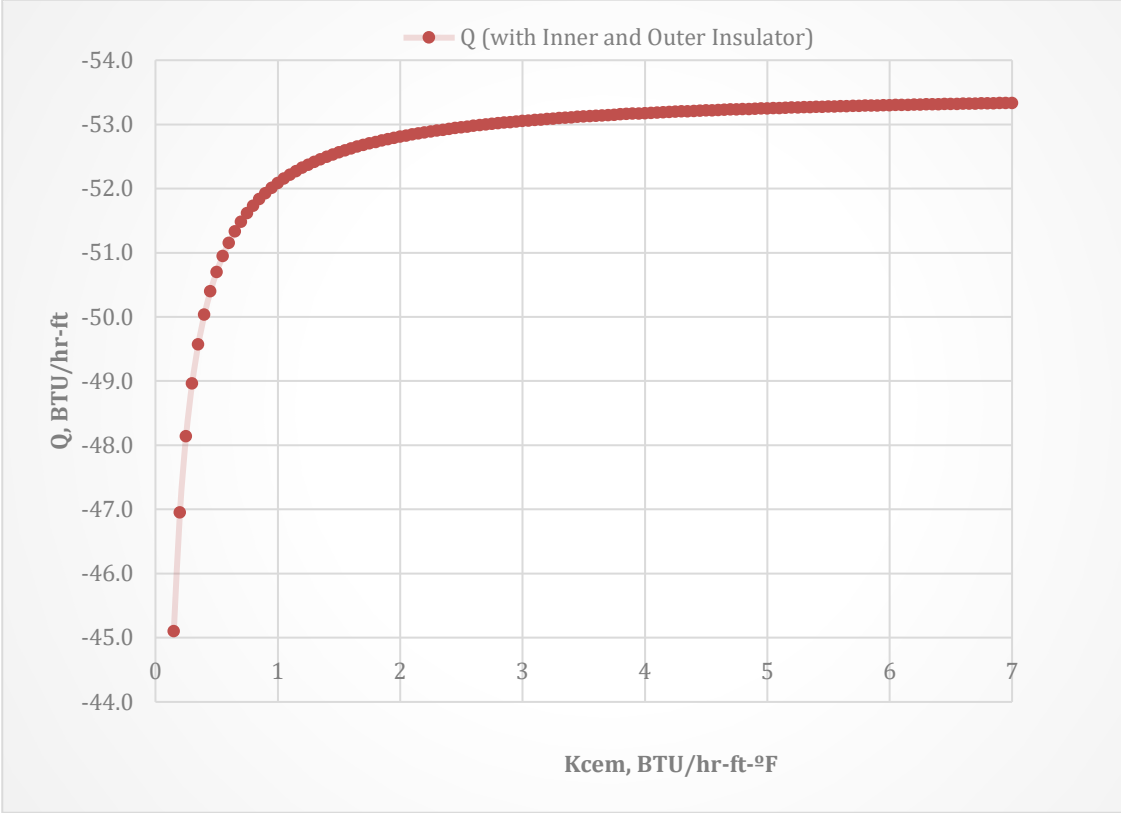

Figure 5.53: Heat exchange versus cement thermal conductivity-inner and outer insulated Top Section.

5.2.2.3.5 Effect of Thermal Conductivity of Insulators

As mentioned earlier in this thesis, this section of the simulation is to determine the effect of thermal conductivity of the outer and inner insulators on the overall heat transfer of fluid in the top section of our well. The thickness of the inner and outer insulators is kept at 0,175 [ft].

The graph of the thermal conductivity of the cement and the overall thermal resistance of the wellbore in Figure 5.54 shows an exponential decline followed by a slow linear decline at approximately 14 [BTU/hr-ft^2-ºF] when the conductivity of the outer insulator is kept at 5 [BTU/hr-ft-ºF] and that of the inner insulator at 0,02 [BTU/hr-ft-ºF].

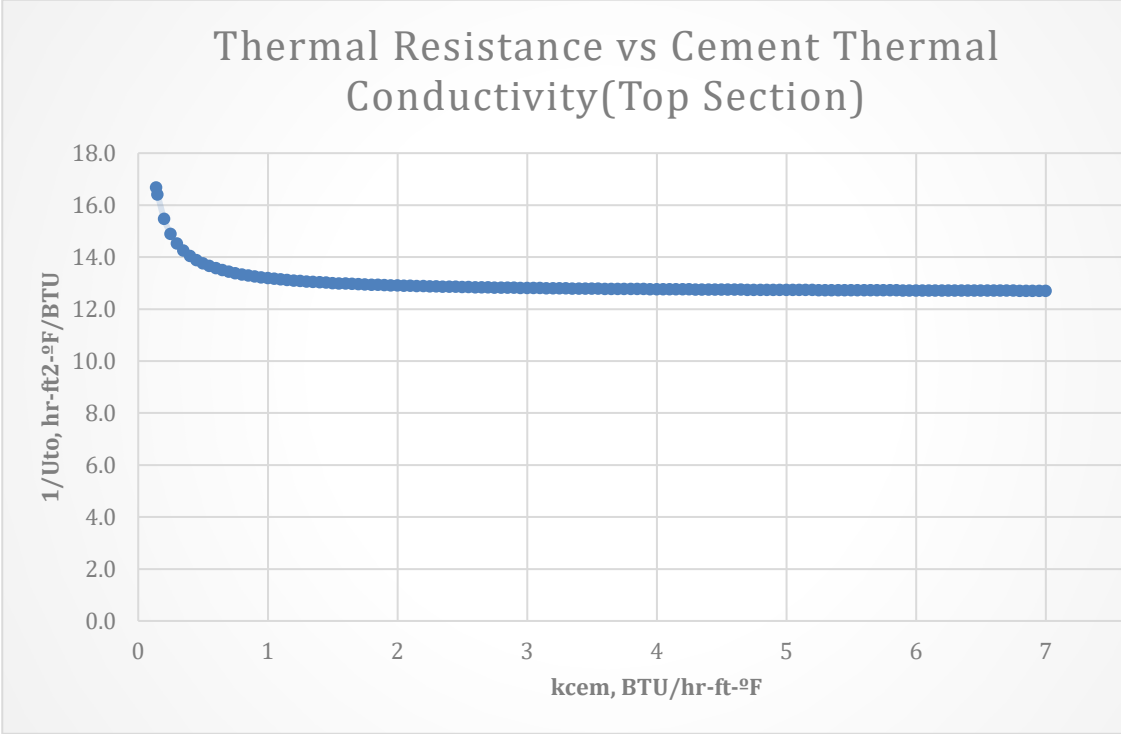

Figure 5.54: Thermal resistance versus cement thermal conductivity-inner and outer insulated Top Section.

The overall heat transfer remains at a constant value of 0,1 [BTU/hr-ft^2-ºF] just as in the scenario for the reservoir section and middle section. This is shown in the graph (Figure 5.55) plotted below.

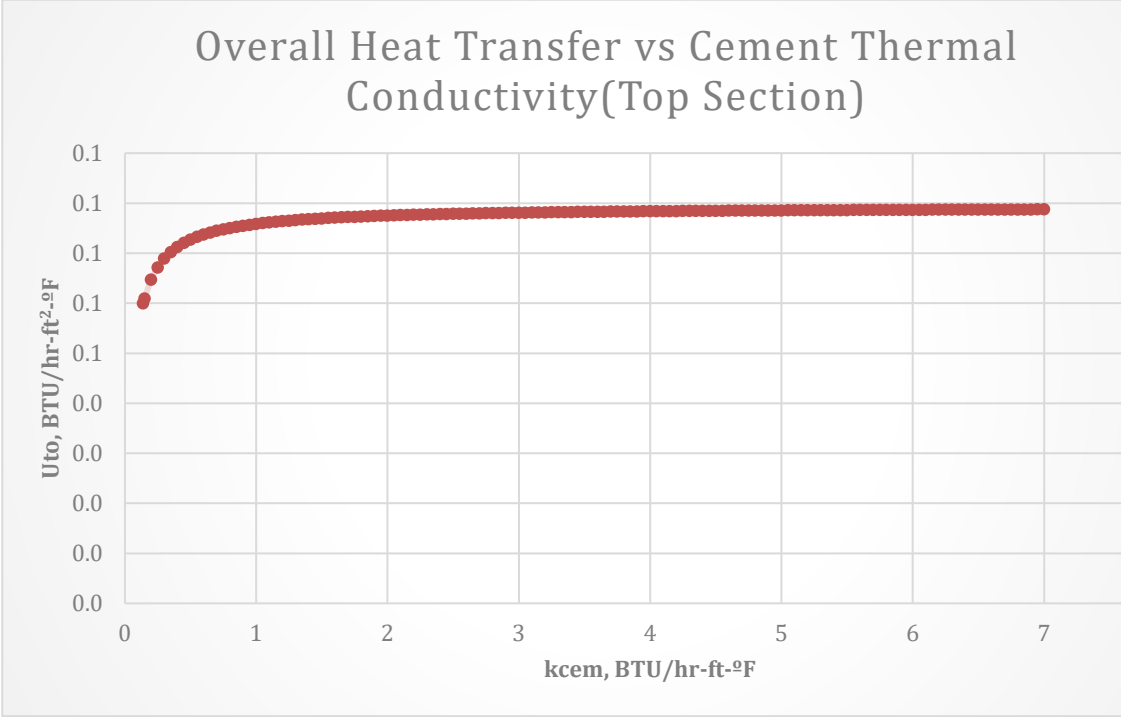

Figure 5.55: Overall heat transfer versus cement thermal conductivity-inner and outer insulated Top Section.

Heat exchange when plotted against cement thermal conductivity does not have a real significant change as compared to when we simulated with only an inner insulation which had a lower thermal conductivity of about 0,02 [BTU/hr-ft-ºF]. This is shown in figure 5.56. Overall heat exchange ranged from -65 to -85,3 [BTU/hr-ft].

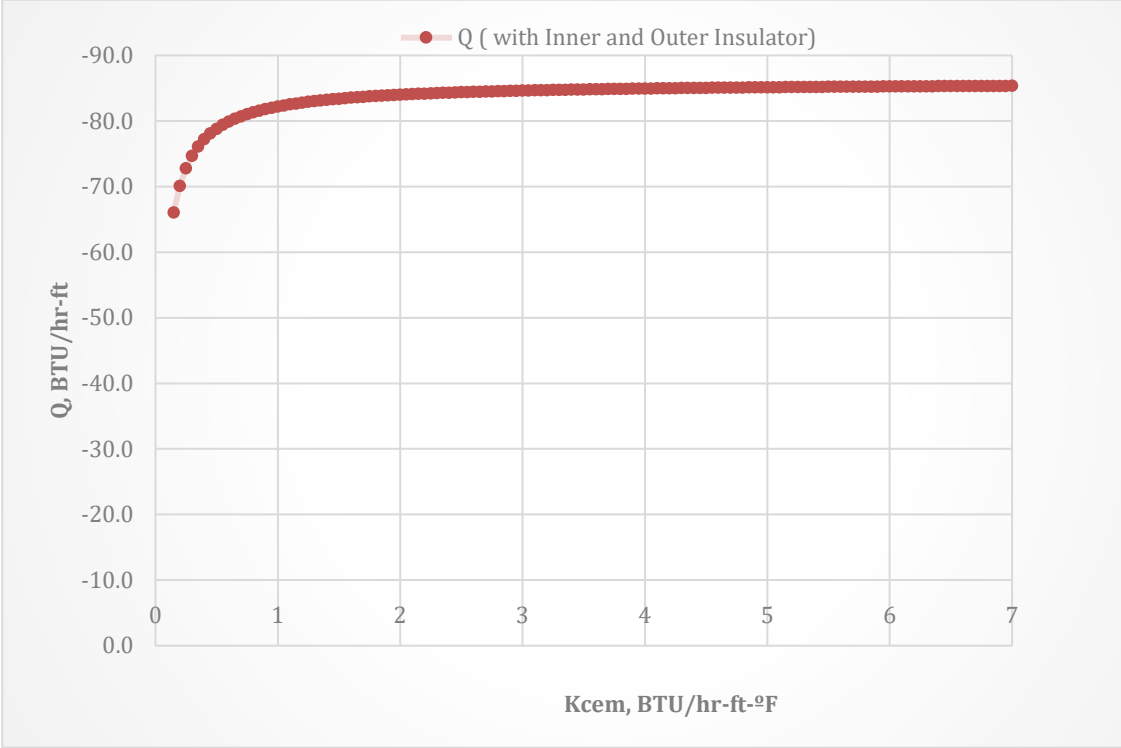

Figure 5.56: Heat exchange versus cement thermal conductivity-inner and outer insulated Top Section.

When the thermal conductivity of the inner insulator is increased to 5 [BTU/hr-ft-ºF] and that of the outer insulator is decreased to 0,02 [BTU/hr-ft-ºF], the result of thermal resistance versus cement conductivity shows a sharp decline at 9 [BTU/hr-ft^2-ºF] as compared to 7 and 26 [BTU/hr-ft^2-ºF] in the previous cases. This is shown in Figure 5.57.

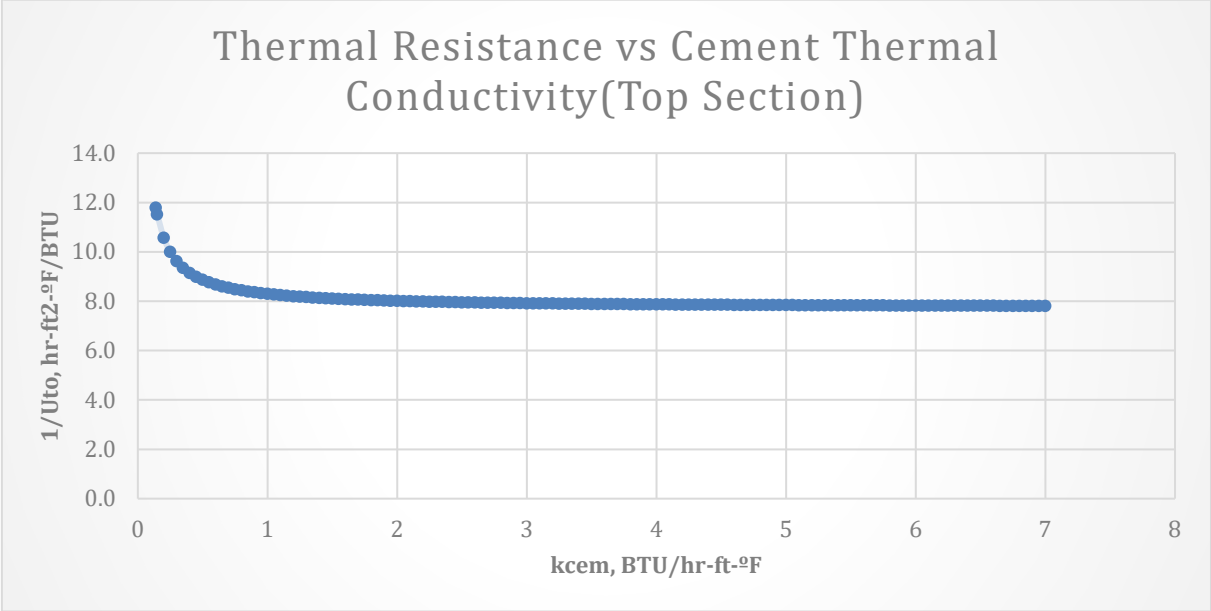

Figure 5.57: Thermal resistance versus cement thermal conductivity-inner and outer insulated Top Section.

A similar trend of results is observed when cement thermal conductivity is plotted against overall heat transfer coefficient (Figure 5.58) and overall heat exchange (Figure 5.59).

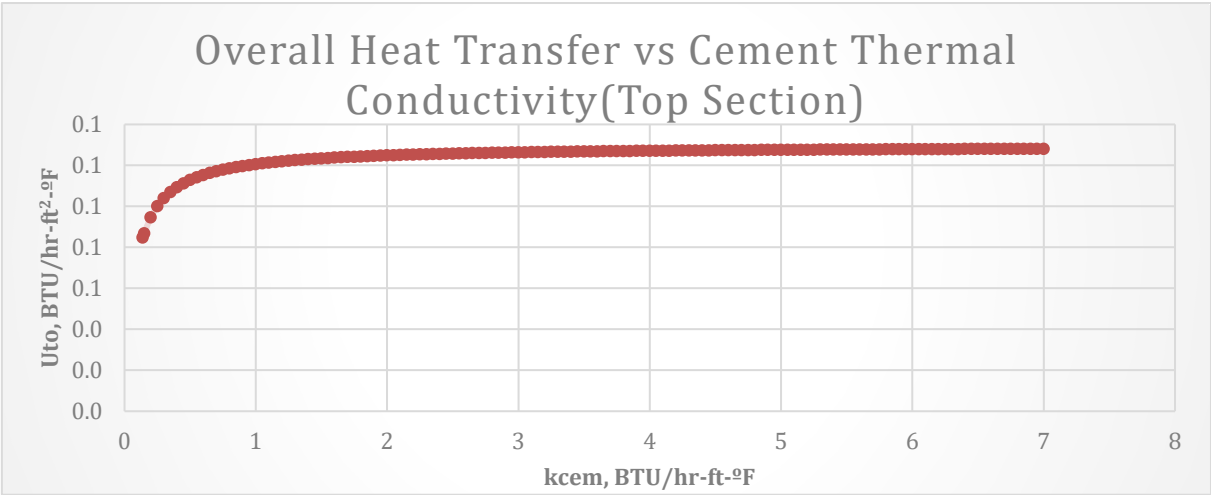

Figure 5.58: Overall heat transfer coefficient versus cement thermal conductivity-inner and outer insulated Top Section.

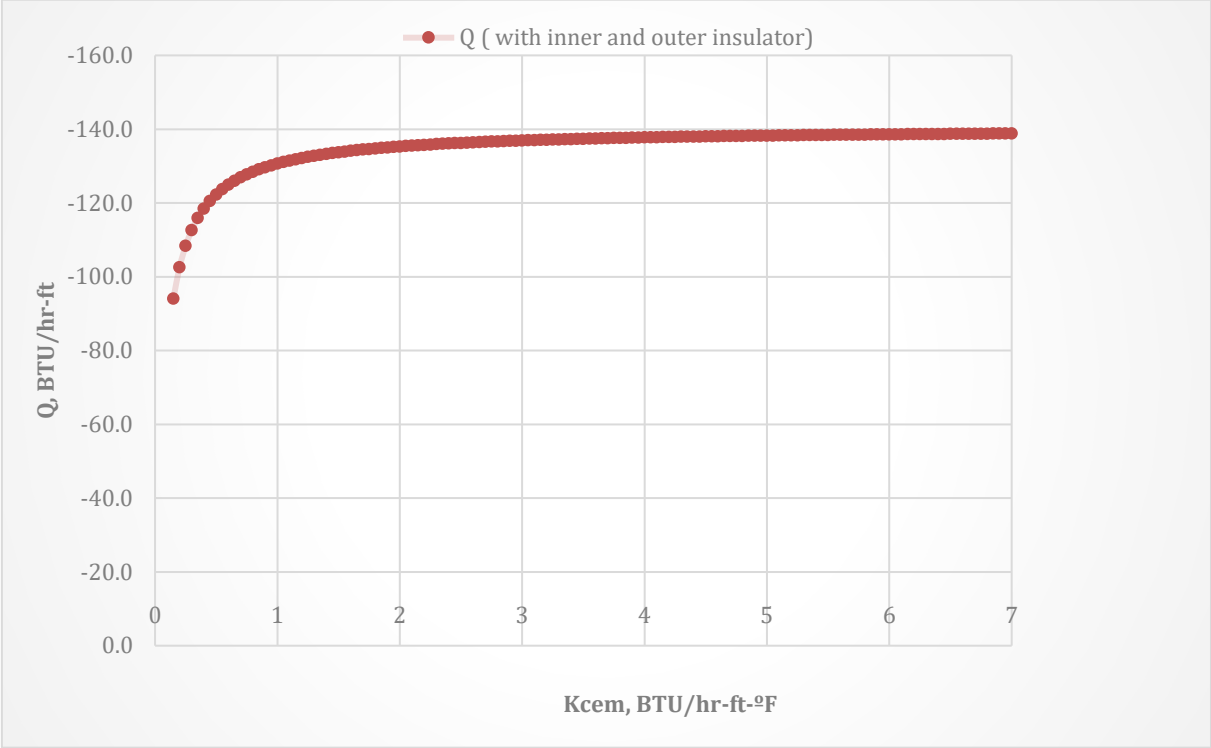

Figure 5.59: Heat exchange versus cement thermal conductivity-inner and outer insulated Top Section.

It can be observed that, the overall heat exchange in this scenario is the same as when the top section is completed with just the outer insulator with a thickness of 0,175 [ft] and thermal conductivity of 0,02 [BTU/hr-ft-ºF], Figure 5.59.

These results show that there is a greater need for an inner insulator than outer insulator if heat produced from the reservoir is to be maximize. Also, higher thermal conductivity of the inner insulator is preferred to that of the outer insulator.

6 Discussion

6.1 Heat Transfer Model

Geothermal well design and engineering is a major challenge in the industry. The main objective in well design process is to provide a functional, productive and cost-effective wellbore for successful exploration and production. The properties of materials used in this design process have to play a major role in maximizing the energy that is produced for further use. The efficiency and maximization of power plants in geothermal wells relies on the amount of heat that is produced at the surface.

In this thesis we assessed the effect of designing a geothermal well with an inner insulator and compare with the current practice of placing an outer insulator or no insulator at all by the industry with the help of an ideal geothermal well we developed. Sensitivity analysis was also done on some material properties to know their impact on heat transfer to the surface of the wellbore with a new model and simulation in Excel and commercial WellCAT™.

The results show that, all these parameters affect the overall heat exchange between the wellbore and the formation and in turn affect the overall heat of the fluid produced at the surface. For the case of high production rate, the higher the rate production of reservoir fluid to the surface, the lesser the heat loss to the formation. Lower cement thermal conductivity also gives better results in all cases most especially when the wellbore is not insulated at all. In insulated wellbores, cement thermal conductivity greater than 1 [BTU/hr-ft-^{o}F] does not give a significant change in the heat exchange in the wellbore. Inner insulation proved to be better in all cases when compared to outer insulation and non-insulated wells. Also, heat loss depends on the geothermal gradient of the well. Low thermal conductivity of the inner insulator has a positive impact on the overall heat exchange in the wellbore even if the well is not completed without an outer insulator. Large heat loss at the surface and middle section of the well due to low geothermal

gradient indicates that, insulators can be efficiently used in these sections compared to the reservoir section. Below are graphical comparisons and analysis of the effect the various parameters studied in this thesis.

6.1.1 Effect of Insulators

Insulators play a very important part in reducing heat loss to the formation during production. The introduction of an inner insulation gives a better percentage reduction of heat loss as compared to using just the outer insulation. Further combination of the two insulators in one completion gives the best percentage reduction in heat loss. As it can be seen in Figures 6.1, 6.2 and 6.3, the effect of cement conductivity is only significant when it is less than 0,85 [BTU/hr-ft-^{o}F]. Above this value, heat loss is almost linear.

The average percentage heat loss when the inner insulation is compared to the outer insulation (current practice) is 48,3%. When the inner insulation is compared to the heat exchange when the well is completed with both insulators, the percentage is 65,8% for the reservoir section.

For the middle section, the average percentage loss for the previous is 48% and 65,6% while that of the top section values are 38,7% and 61,8% respectively.

Reservoir section

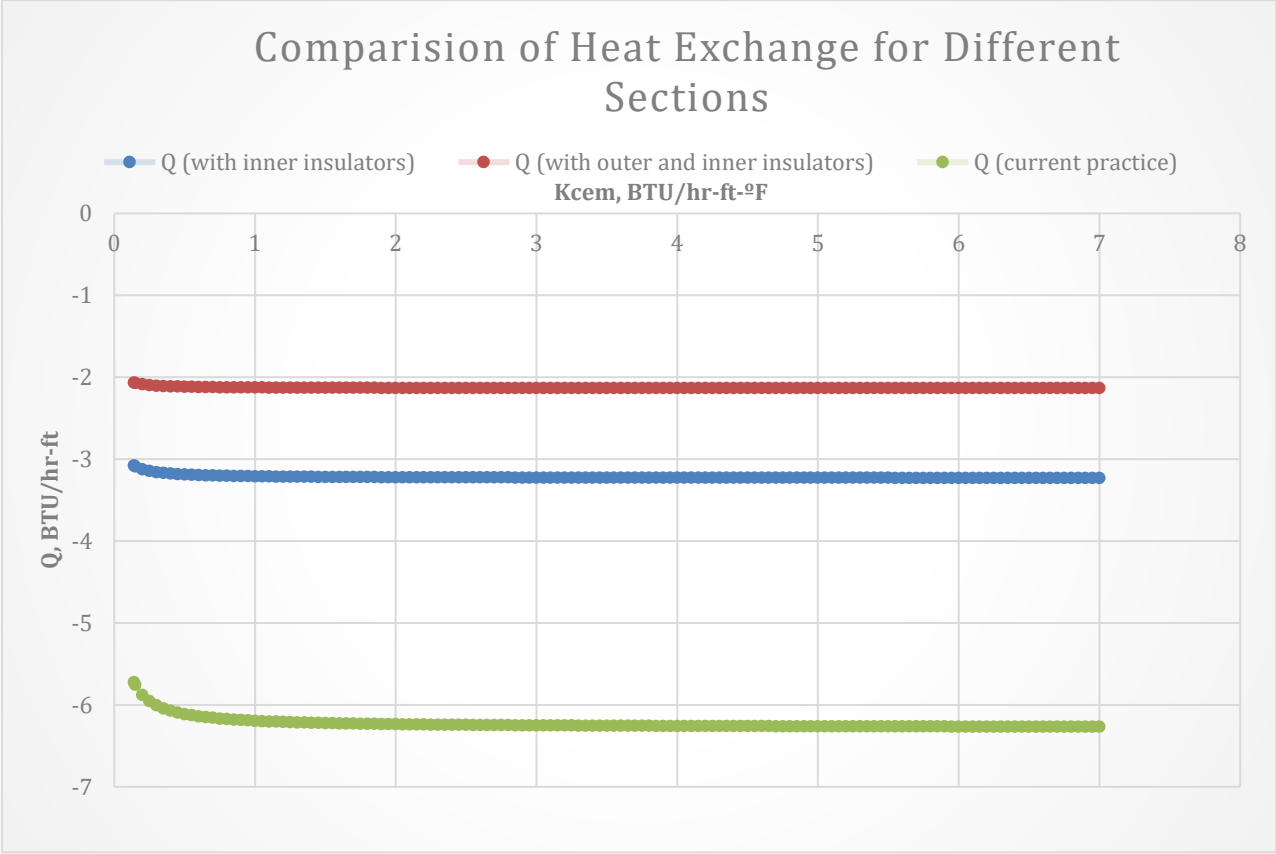

Figure 6.1: Heat exchange versus cement thermal conductivity of reservoir section.

Middle Section

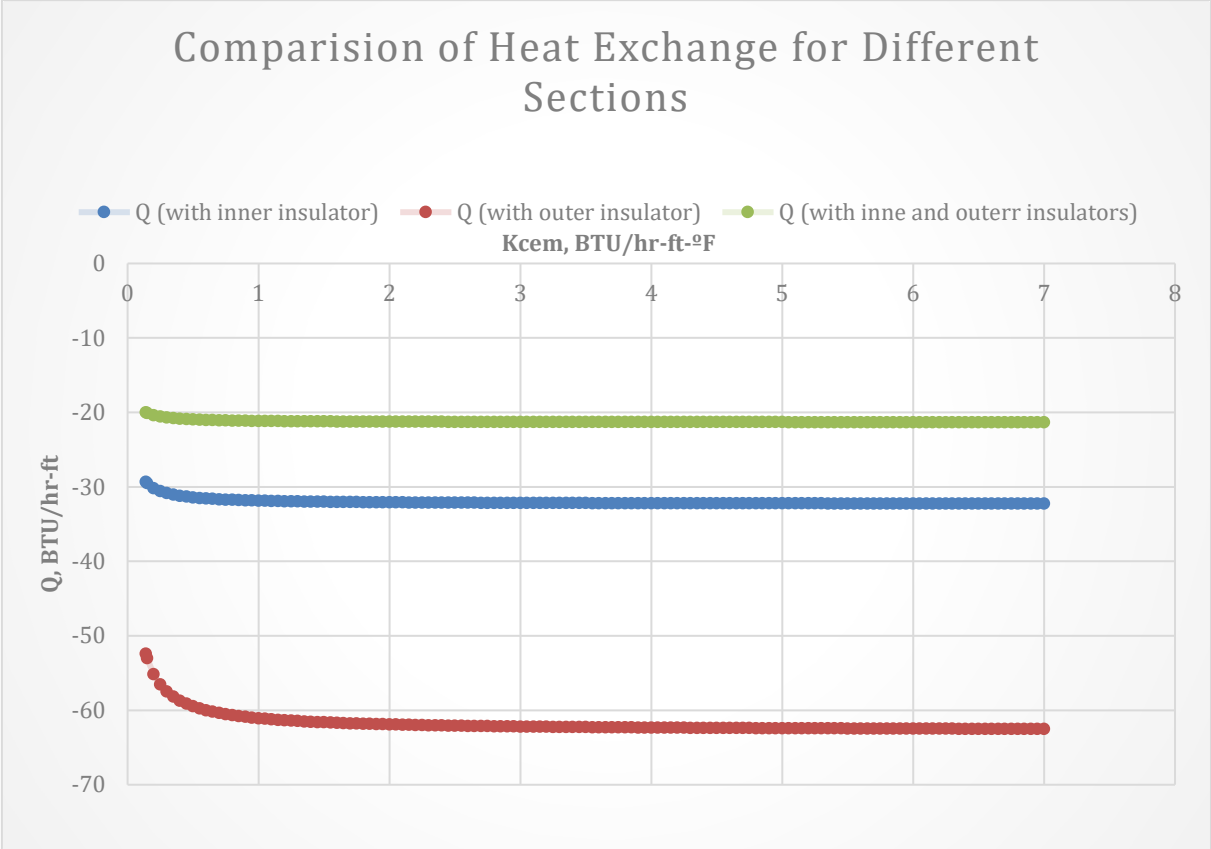

Figure 6.2: Heat exchange versus cement thermal conductivity of middle section.

Top Section

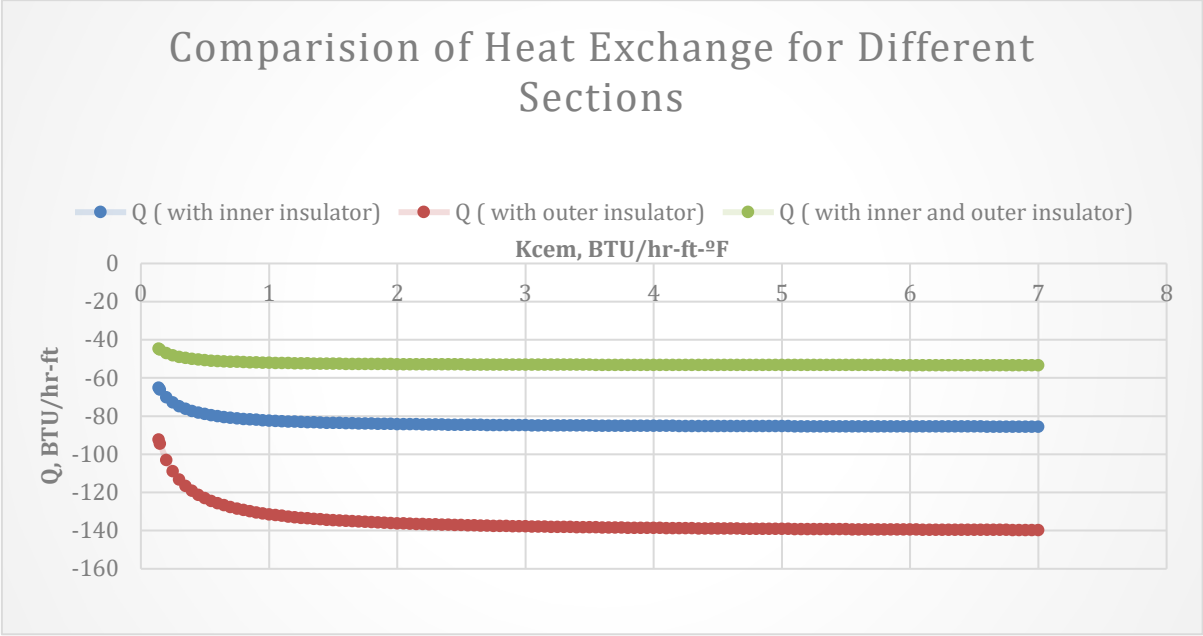

Figure 6.3: Heat exchange versus cement thermal conductivity of top section.

6.1.2 Effect of Non-insulation

Heat exchange in the geothermal well when it is not insulated, increases exponentially with increasing cement thermal conductivity. However, it can be observed from Figure 6.4 that, les heat is loss in reservoir section. This is due to high geothermal gradient in this section. The effect of multiple conductors can also be seen when the middle section is compared to the top section. In this case, though the geothermal gradient is lowest at the surface, the casings at the top section has slightly reduced the amount of heat loss. Hence less heat loss at the top section compared to the middle section.

Also, for a geothermal well to maximize the heat produced from the reservoir, cement with very low thermal conductivity of about 1 [BTU/hr-ft-ºF] have to be used for completion. Conventional oil and gas wells do not have insulators attached to the

production casing/tubing. Therefore, when converting these wells to geothermal wells, a lot of heat will be loss during production.

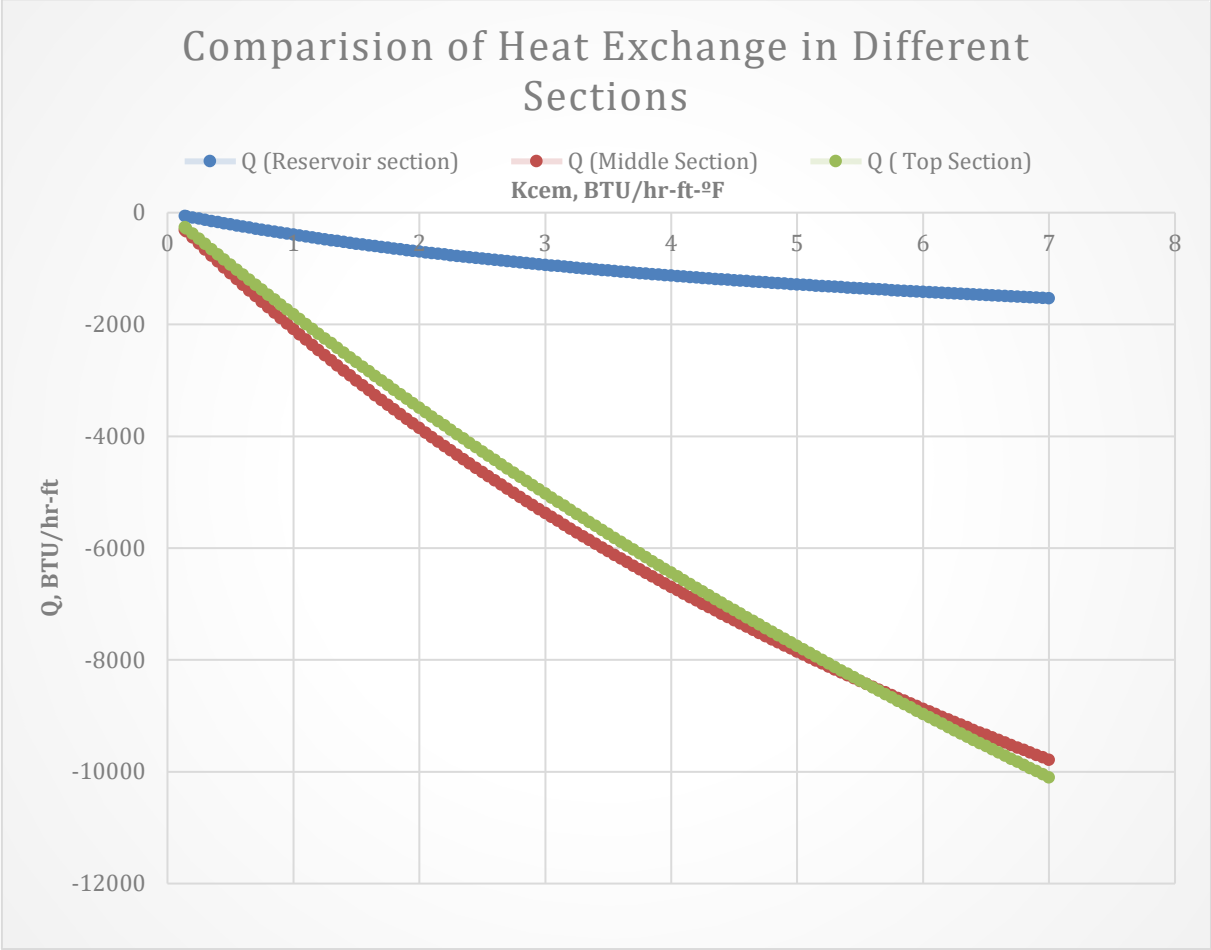

Figure 6.4: Heat exchange versus cement thermal conductivity for uninsulated well.

6.1.3 Effect of Cement Thermal Conductivity

Analysis of the cement thermal conductivity reveals that heat exchange is sensitive at very low values. Cement thermal conductivity above 1 [BTU/hr-ft-ºF] does not give significant changes in the heat exchange in all sections of our case study. A good comparison can be seen in the Figure 6.5 below where the heat exchange when the well has both insulators and when the well has just the outer insulator (current practice in the industry).

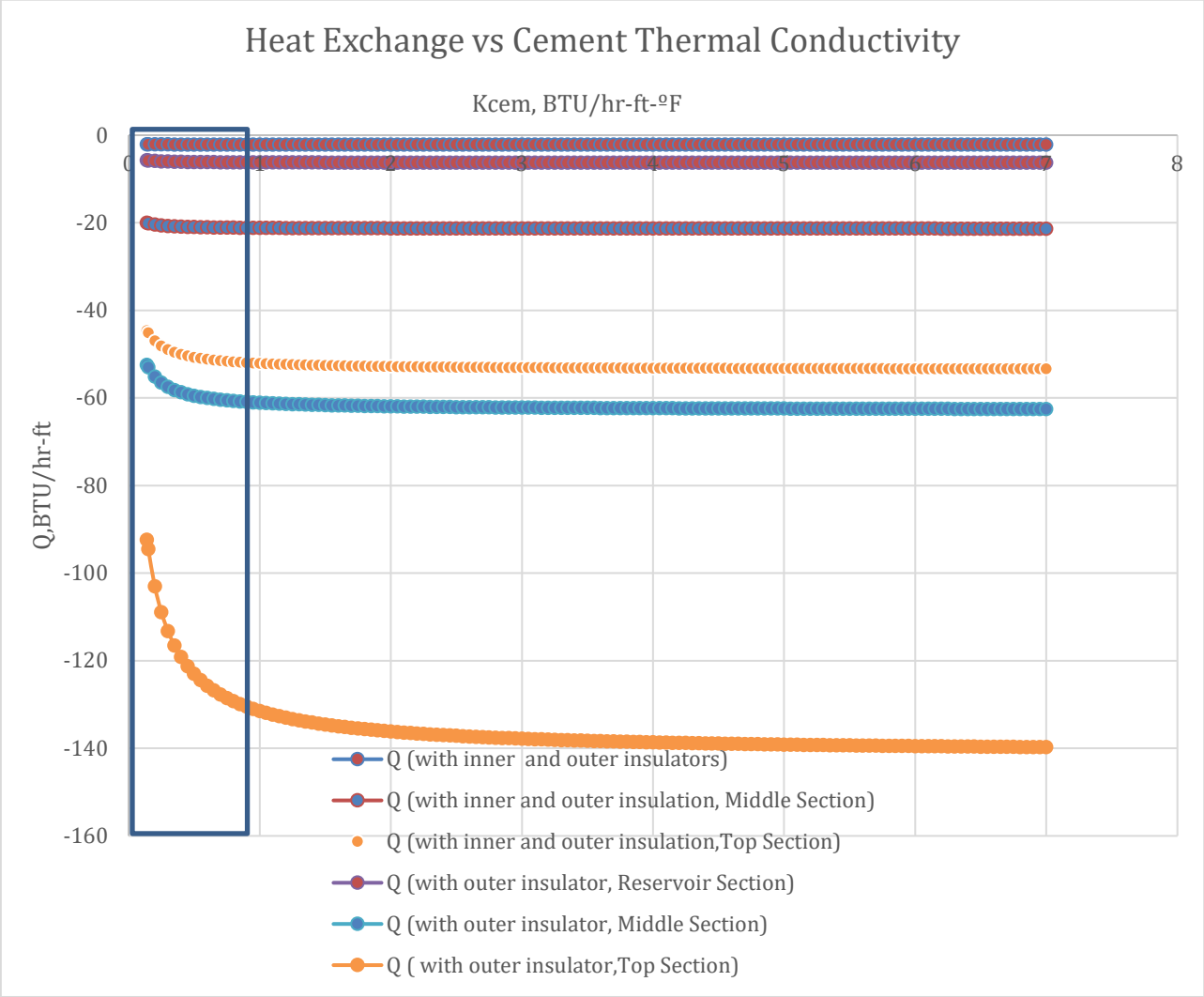

Figure 6.5: Comparison heat exchange versus cement thermal conductivity between outer insulated wells and inner and outer insulated wells.

6.1.4 Effect of Thickness of Insulators

In analyzing the effect of the thickness of the insulators on the overall heat exchange, their thickness was varied between 0,01[ft] to 0,3[ft] with a constant conductivity of 0,02 [BTU/hr-ft-ºF]. We observed that, then the inner insulator is thicker than the outer insulator, heat loss is reduced better than when their thicknesses are of the same value. When the outer insulator is thicker than the inner insulator, heat loss is highest. Figures

6.6, 6.7 and 6.8 show the thickness against the average heat exchange in each section of the well.

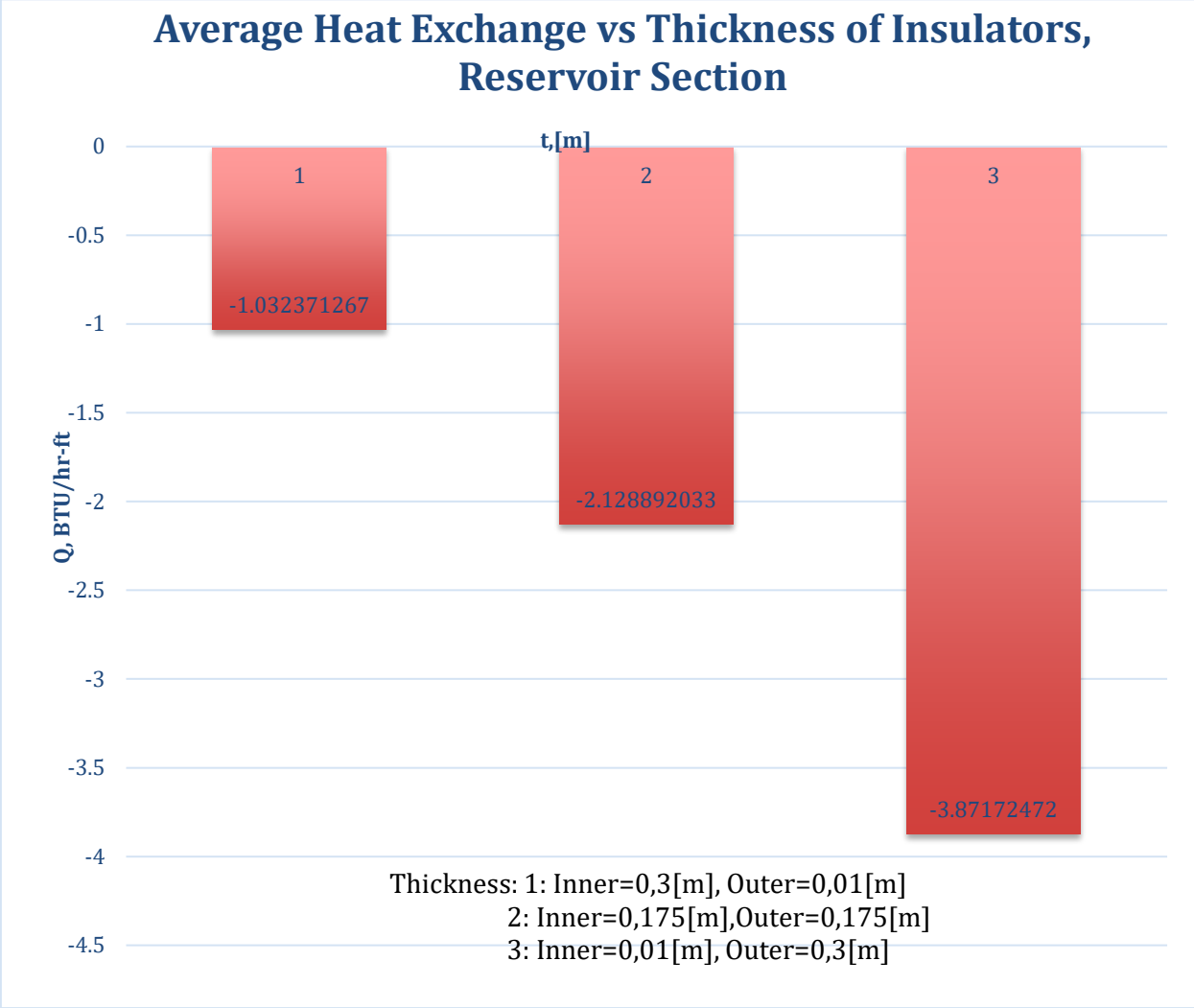

Figure 6.6: Average heat exchange versus thickness of insulators –Reservoir Section

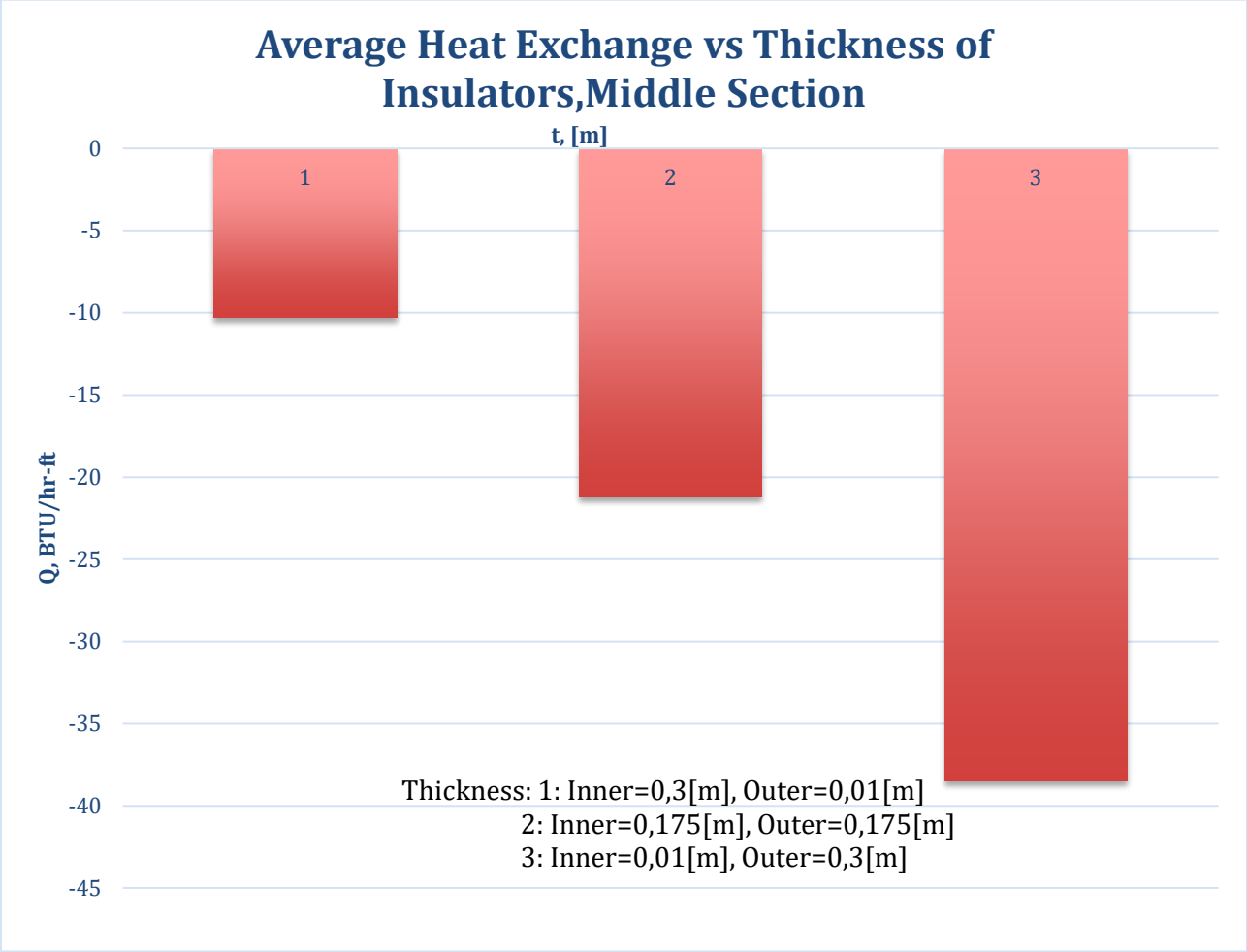

Figure 6.7: Average heat exchange versus thickness of insulators –Middle Section

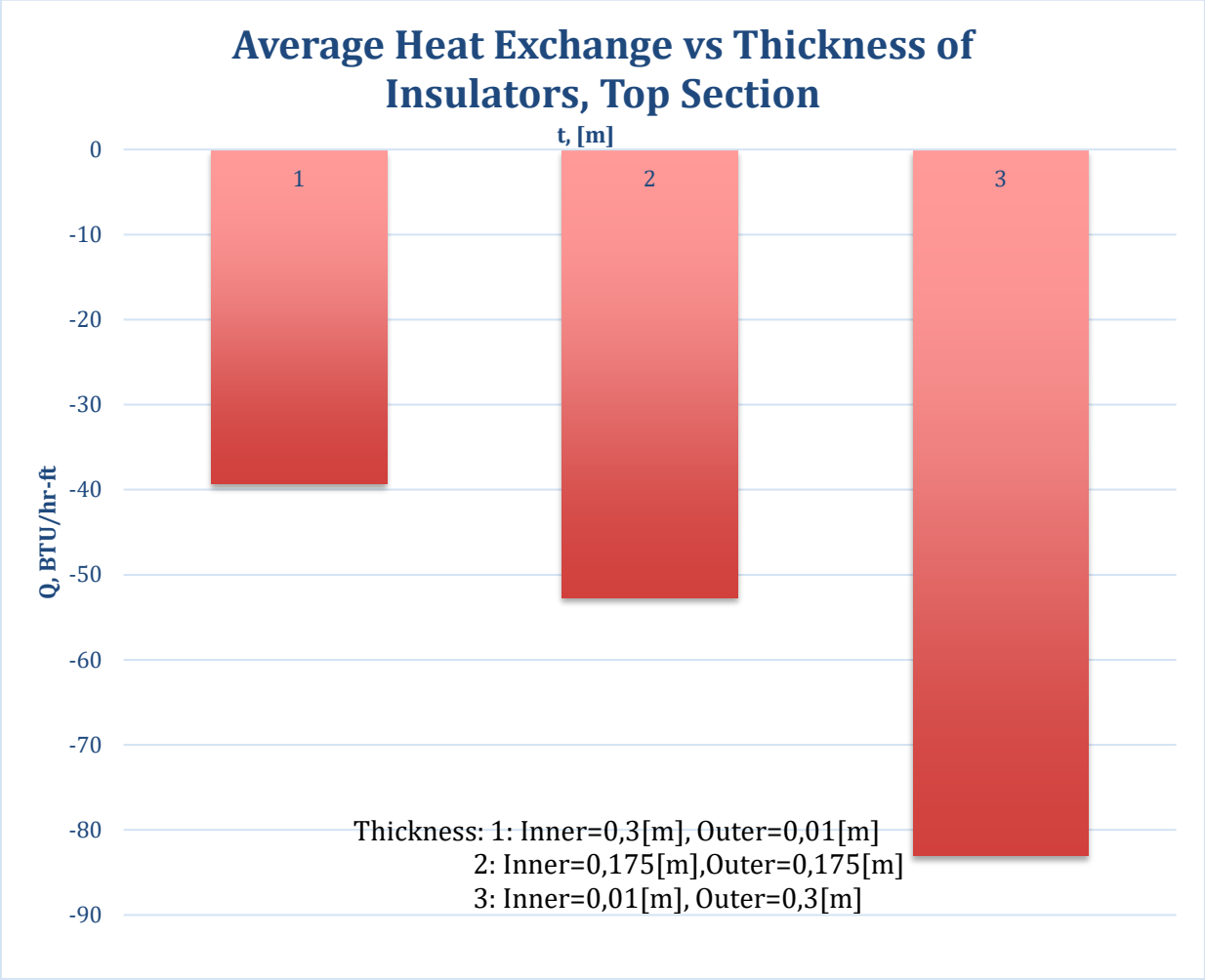

Figure 6.8: Average heat exchange versus thickness of insulators –Top Section

6.1.5 Effect of Varying the Conductivity of the Insulators

To determine the effect of varying the conductivity of the inner and outer insulators on the heat exchange, the conductivities of both insulators were varied from 0 to 5 [BTU/hr-ft-°F]. The results showed that, a very low conductivity of 0,02 [BTU/hr-ft-°F] for the inner insulator and a higher value of more than 1[BTU/hr-ft-°F] for the outer insulator, gives less average heat loss to the formation. At a conductivity of 1[BTU/hr-ft-°F] for both insulators, there is a very large amount of heat exchange in the formation as shown on figures 6.9, 6.10 and 6.11. However, at a lower conductivity of less than 0,85 [BTU/hr-ft-°F] for both insulators, there is a significant improvement in the average heat exchange

in the well. The higher the conductivities of both insulators, the greater the amount of heat loss. The lower the conductivity of the inner insulator, the smaller the amount of heat loss for all sections of the well. The best results is when both insulators have a conductivity of less than 1[BTU/hr-ft-°F].

Reservoir Section

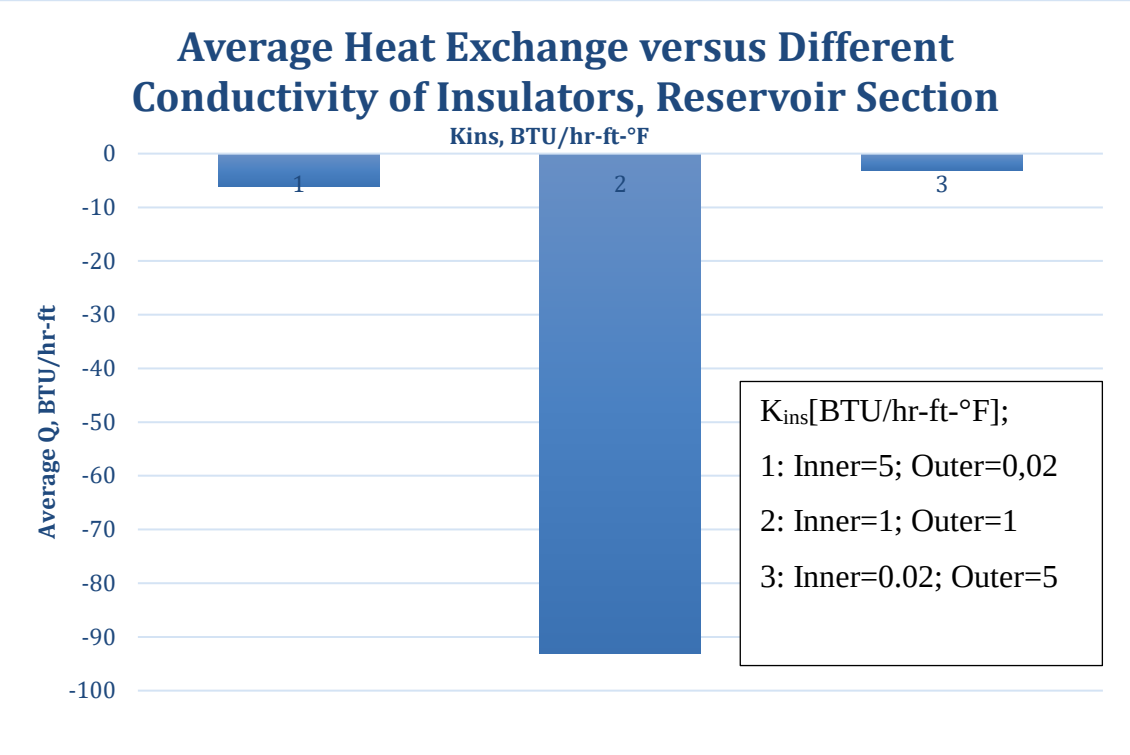

6.9: Average heat exchange versus different conductivity of insulators-Reservoir Section

Middle Section

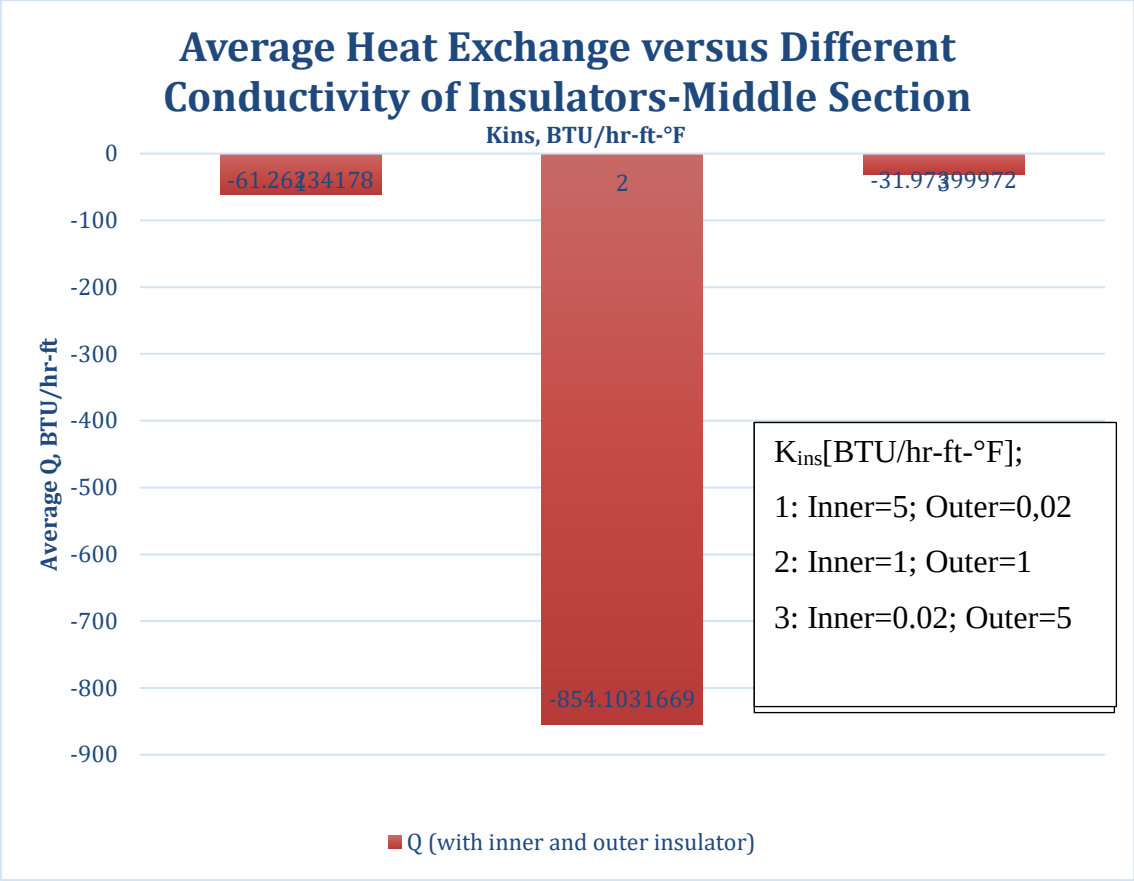

6.10: Average heat exchange versus different conductivity of insulators-Middle Section.

Top Section

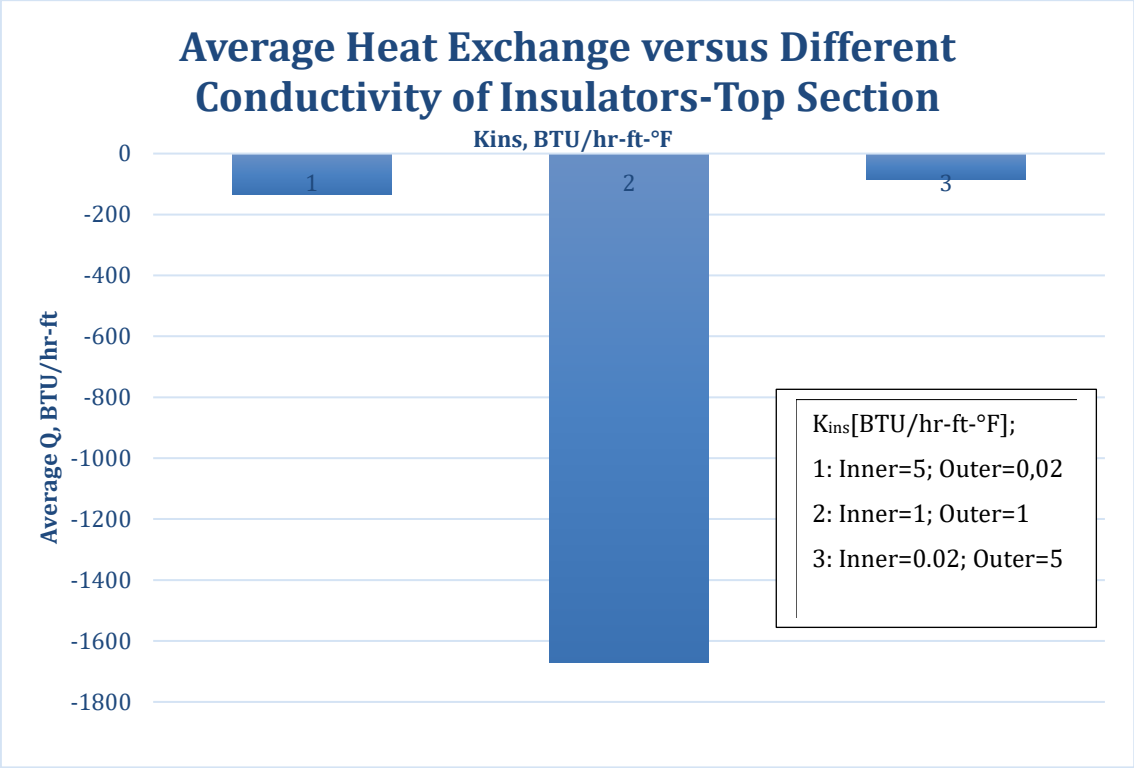

6.11: Average heat exchange versus different conductivity of insulators-Top Section.

6.2 Effect of Flowrate on Fluid Heat Loss

High flowrate in our geothermal well simulation had less heat loss as fluid move from the reservoir to the surface. At a flowrate of 76 [bbl/d], there was 84% reduction in fluid temperature at the surface. A flowrate of 2000 [bbl/d] gave a reduction of 22% which is a better improvement than the previous case. This can be seen in the Figure 6.12 shown below. The higher the flowrate, the smaller the heat loss to the formation.

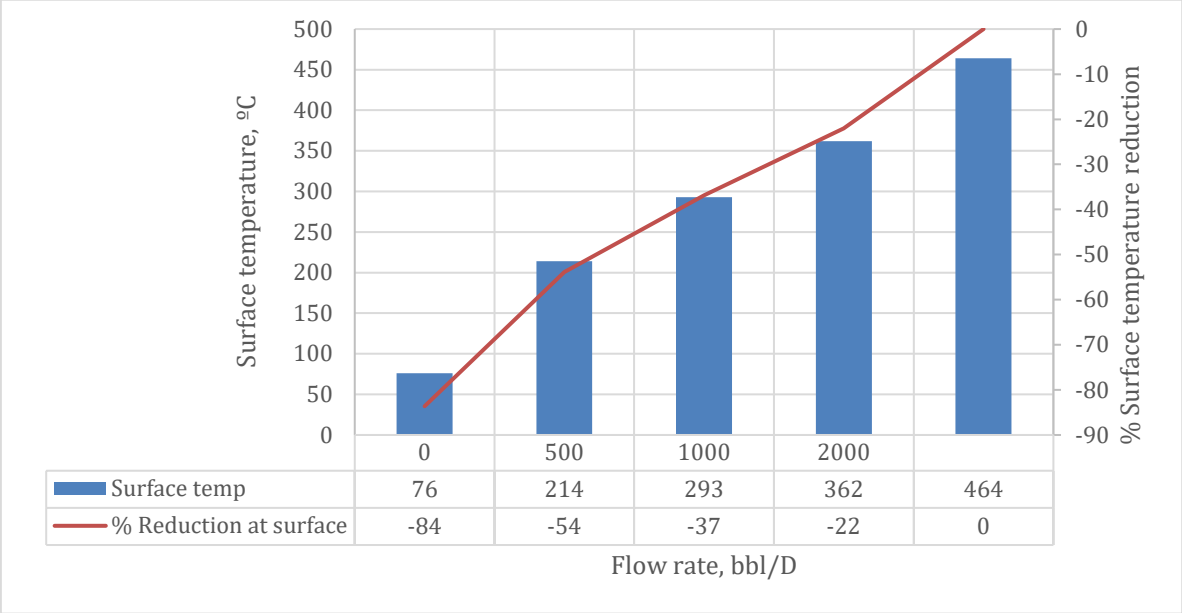

Figure 6.12: Comparison of the percentage heat loss in the wellbore with different flowrates.

7 Summary and Conclusion

In this study, the inclusion of inner insulation in geothermal well completion gave better results in reducing heat loss during production as compared to the current practice in the industry where wells are completed with either outer insulations or without insulations at all. The use of inner insulations would help reduce geothermal well production problems like scaling, erosion and corrosion of the production casing. The effect of the thickness of both insulators also proved to be important in maximizing heat production especially when the cost benefit analysis of the material to be used in the well is considered. Conductivity of the cement is only essential when the value is less than 1 [BTU/hr-ft-^{o}F] in uninsulated wells. Its effect is not significant when there is an insulation. Also, inner insulations with low conductivity are essential in preventing heat loss to the formation.

We also observed that, high flowrates are essential in reducing heat exchange in the well. Since geothermal wells have higher flowrates than conventional oil and gas wells, the potential for erosion of the production could be reduced with the inner insulation. Fluids produced from geothermal wells contain corrosive and radioactive elements (Southon, 2005) and by completing the well with inner and/or outer insulators would help in prolonging the life of these wells. Thermal cycling could also be prevented by introducing this type of well design. We can draw the following conclusions:

- Inner insulation is very essential in reducing heat loss to the formation in geothermal wells
- Inner insulation gives better results compared to outer insulation or non-insulated wells.
- Well completion with both inner and outer insulation gives the best results in heat loss reduction
- Thickness of both insulators is essential in maximizing heat produced at the surface with thicker inner insulation giving the best results
- Conductivity of the insulators is only significant when only the outer or inner insulator is used in the well completion.

- High flow rates reduce heat loss significantly
- Conductivity of the casings is only essential in non-insulated wells with more heat loss taking place at the middle/intermediate section
- Cement thermal conductivity is very important in non-insulated wells and less significant when an inner insulator is present.

The new model could prove to be revolutionize how geothermal wells are designed in the industry. The main concern in the industry is the financial risk and we believe that if further studies is done on possible materials to use for this type of well completion, common well problems like corrosion, scaling, erosion, and thermal cycling and heat loss could be solved.

References

Ármannsson, H., Fridriksson, T., Gudfinnsson, G. H., Ólafsson, M., Óskarsson, F., & Thorbjörnsson, D. (2014). IDDP—The chemistry of the IDDP-01 well fluids in relation to the geochemistry of the Krafla geothermal system. *Geothermics, 49*, 66-75.

Baghban, M. H., Hovde, P. J., & Jacobsen, S. (2013). Analytical and experimental study on thermal conductivity of hardened cement pastes. *Materials and structures, 46*(9), 1537-1546.

Belayneh, M. A. (2018). *Grading, Tube Stress and Failure Analysis*. Petroleum Engineering University of Stavanger Norway.

Bellarby, J. (2009). *Well completion design* (Vol. 56): Elsevier.

Bioenergy, I. (2015). IEA Bioenergy Task 37–Country Reports Summary 2014. *IEA Bioenergy, International Energy Agency: Paris, France*.

BORES, A. P., & SCHMIDT, R. J. (2003). ADVANCED MECHANICS OF MATERIALS.

Byars, H., & Gallop, B. (1972). *Injection Water+ Oxygen= Corrosion and/or Well Plugging Solids.* Paper presented at the SPE Symposium on Handling of Oilfield Water.

Carvalho, M., Forjaz, V., & Almeida, C. (2006). Chemical composition of deep hydrothermal fluids in the Ribeira Grande geothermal field (São Miguel, Azores). *Journal of Volcanology and Geothermal Research, 156*(1-2), 116-134.

Community, G. (2016). Chemistry of Thermal Fluids. In Geothermal Systems and Technologies (pp. 11). Website: Geothermal Communities. Retrieved from http://www.geothermalcommunities.eu/assets/elearning/3.2.Corrosion&Scalling.pdf.

Conover, M. F. (1982). *Designing geothermal power plants to avoid reinventing the corrosion wheel*. Retrieved from

Dickson, M., & Fanelli, M. (2001). Hidden resources-power from geothermal energy. *Renewable Energy World, 4*(4), 210-212, 214.

Elders, W., Friðleifsson, G., & Albertsson, A. (2014). Drilling into magma and the implications of the Iceland Deep Drilling Project (IDDP) for high-temperature geothermal systems worldwide. *Geothermics, 49*, 111-118.

Ellis, P. (1985). Companion study guide to short course on geothermal corrosion and mitigation in low temperature geothermal heating systems. *Radian Corporation prepared for The Geo - Heat Center Oregon Institute of Technology. Klamath Falls, OR*.

Field, C. B., Barros, V., Stocker, T., Qin, D., Dokken, D., & Ebi, K. (2012). IPCC 2012. *Managing the risks of extreme events and disasters to advance climate change adaptation. A special report of the intergovernmental panel on climate change*.

Filippov, A., Mack, R., Cook, L., York, P., Ring, L., & McCoy, T. (1999). *Expandable tubular solutions.* Paper presented at the SPE Annual Technical Conference and Exhibition.

Finger, J., & Blankenship, D. (2010). Handbook of best practices for geothermal drilling. *Sandia National Laboratories, Albuquerque*.

Friðleifsson, G. Ó., Elders, W. A., Zierenberg, R. A., Stefánsson, A., Fowler, A. P., Weisenberger, T. B., . . . Mesfin, K. G. (2017). The Iceland Deep Drilling Project 4.5 km deep well, IDDP-2, in the seawater-recharged Reykjanes geothermal field in SW Iceland has successfully reached its supercritical target. *Scientific Drilling, 23*, 1.

Fridleifsson, I. B. (2001). Geothermal energy for the benefit of the people. *Renewable and Sustainable Energy Reviews, 5*(3), 299-312.

Fridriksson, T., & Thórhallsson, S. Geothermal utilization: scaling and corrosion.

Gehringer, M., & Loksha, V. (2012). Geothermal handbook: planning and financing power generation. *Washington DC: World Bank Group, Energy Sector Management Assistance Program*.

Gunnlaugsson, E., Ármannsson, H., Þórhallsson, S., & Steingrímsson, B. (2014). Problems in geothermal operation-scaling and corrosion.

Hasan, A., & Kabir, C. (1994). Aspects of wellbore heat transfer during two-phase flow (includes associated papers 30226 and 30970). *SPE Production & Facilities, 9*(03), 211-216.

Hashmi, G. M. (2014). *Heat Transfer Modeling and Use of Distributed Temperature Measurements to Predict Rate.*

Hochstein, M. (1990). Classification and assessment of geothermal resources. *Small geothermal resources: A guide to development and utilization, UNITAR, New York*, 31-57.

Hodson-Clarke, A., Rudolf, R., Bour, D., & Russell, P. (2016). *Key factors to successful drilling and completion of EGS well in Cooper Basin.* Paper presented at the Proceedings of the 41st Workshop on Geothermal Reservoir Engineering Stanford University, Stanford, California.

Ichim, A., Teodoriu, C., & Falcone, G. (2016). *Influence of Cement Thermal Properties on Wellbore Heat Exchange.* Paper presented at the 41st Workshop on Geothermal Reservoir Engineering, Stanford, California, USA.

IEA. (2017). *World Energy Outlook 2017*: Organisation for Economic Co-operation and Development, OECD.

Ingason, K., Árnason, A. B., Bóasson, H. Á., Sverrisson, H., Sigurjónsson, K. Ö., & Gislason, Ţ. (2015). *IDDP-2, Well design.* Paper presented at the Proceedings World Geothermal Congress.

Initiative, M. E. (2006). The Future of Geothermal Energy". *Report to the US Department of Energy, Idaho National Laboratory, Idaho Falls, Idaho*.

Kaasalainen, H., Stefánsson, A., Giroud, N., & Arnórsson, S. (2015). The geochemistry of trace elements in geothermal fluids, Iceland. *Applied Geochemistry, 62*, 207-223.

Kaldal, G. S., Jonsson, M. T., Palsson, H., & Karlsdottir, S. N. (2015). Structural modeling of the casings in high temperature geothermal wells. *Geothermics, 55*, 126-137.

Kalvenes, K. L. (2017). *Investigation of Corrosion in Geothermal Wells-A Qualitative Risk Assessment.* University of Stavanger, Norway,

Karlsdottir, S., Ragnarsdottir, K., Moller, A., Thorbjornsson, I., & Einarsson, A. (2014). On-site erosion–corrosion testing in superheated geothermal steam. *Geothermics, 51*, 170-181.

Kaya, T., & Hoshan, P. (2005). *Corrosion and material selection for geothermal systems.* Paper presented at the Proceedings World Geothermal Congress.

Kristanto, D., Kusumo, L. P., & Abdassah, D. (2005). *Strategy development for corrosion problems in geothermal installation based on corrosion management technology.* Paper presented at the Proceedings of World Geothermal Congress.

Lichti, K. (1989). Development of a Standards Based Expert System for Selecting Materials for Oil and Gas Industry. *K. A. Lichti, et. al., CORROSION 89/476, NACE, Houston, TX. Per Copy$*.

Lopez, D., Perez, T., & Simison, S. (2003). The influence of microstructure and chemical composition of carbon and low alloy steels in CO2 corrosion. A state-of-the-art appraisal. *Materials & Design, 24*(8), 561-575.

Lukawski, M. Z., Anderson, B. J., Augustine, C., Capuano Jr, L. E., Beckers, K. F., Livesay, B., & Tester, J. W. (2014). Cost analysis of oil, gas, and geothermal well drilling. *Journal of Petroleum Science and Engineering, 118*, 1-14.

Lund, J. W., & Boyd, T. L. (2016). Direct utilization of geothermal energy 2015 worldwide review. *Geothermics, 60*, 66-93.

Lund, J. W., Lienau, P. J., & Culver, G. G. (1990). *The current status of geothermal direct use development in the United States.* Paper presented at the 1990 International Symposium on geothermal energy.

Maruyama, K., Tsuru, E., Ogasawara, M., Inoue, Y., & Peters, E. J. (1990). An experimental study of casing performance under thermal cycling conditions. *SPE drilling engineering, 5*(02), 156-164.

Matek, B. (2016). Annual US & global geothermal power production report. *Geothermal Energy Association, USA, pp10*.

Mundhenk, N., Huttenloch, P., Sanjuan, B., Kohl, T., Steger, H., & Zorn, R. (2013). Corrosion and scaling as interrelated phenomena in an operating geothermal power plant. *Corrosion Science, 70*, 17-28.

Nathan Amuri, B. (2017). *Heat Recovery Mechanism for Non Condensable Geothermal Fractured Reservoirs by CO2 Injection and Well Heat Insulating.* University of Stavanger, Norway,

Ocampo-Diaz, J. D. D., Valdez-Salaz, B., Shorr, M., Sauceda, M., & Rosas-González, N. (2005). *Review of corrosion and scaling problems in Cerro Prieto geothermal field over 31 years of commercial operations.* Paper presented at the Proceedings of World Geothermal Congress, International Geothermal Association (IGA), Antalya, Turkey.

Ólafsson, M., Hauksdóttir, S., Thórhallsson, S., & Snorrason, T. (2005). *Calcite scaling at Selfossveitur hitaveita, S-Iceland, when mixing waters of different chemical composition.* Paper presented at the Proceedings of the World Geothermal Congress.

Panwar, N., Kaushik, S., & Kothari, S. (2011). Role of renewable energy sources in environmental protection: a review. *Renewable and Sustainable Energy Reviews, 15*(3), 1513-1524.

Povarov, O., Tomarov, G., & Semenov, V. (2000). *Physical and chemical processes of geothermal fluid impact on metal of geothermal power plant equipment.* Paper presented at the Proceedings of World Geothermal Congress 2000.

Ren, P. (2015). Renewables 2015 global status report. *REN21 Secretariat: Paris, France*.

Sanada, N., Kurata, Y., Nanjo, H., Kim, H.-s., Ikeuchi, J., & Lichti, K. A. (2000). *IEA deep geothermal resources subtask C: Materials, progress with a database for materials performance in deep and acidic geothermal wells.* Paper presented at the Proc World Geothermal Congress, Kyushu, Tohoku, Japan.

Schweitzer, P. A. (1996). *Corrosion Engineering Handbook, -3 Volume Set*: CRC Press.

Shadravan, A., & Shine, J. (2015). *Sustainable Zonal Isolation under Extreme High Temperature Conditions.* Paper presented at the SPE/IATMI Asia Pacific Oil & Gas Conference and Exhibition.

Skimin, C., Snyder, D., & Dickie, D. (1979). Corrosion Characteristics of Zinc Electrodeposits. *Plating and Surface Finishing, 66*(7), 36-40.

Southon, J. N. (2005). *Geothermal well design, construction and failures.* Paper presented at the Proceedings World geothermal congress.

Statoil. (2017). *Sustainability Report* Retrieved from Company's Website: https://www.equinor.com/content/dam/statoil/documents/sustainability-reports/statoil-sustainability-report-2017-23march.pdf

Takabe, H., & Ueda, M. (2001). *The formation behavior of corrosion protective films of low Cr bearing steels in CO2 environments.* Paper presented at the Int. Conf. Corrosion 2001, Paper No.

Teodoriu, C. (2015). *Why and When Does Casing Fail in Geothermal Wells: a Surprising Question.* Paper presented at the Proceedings of World Geothermal Congress 2015.

Teodoriu, C., & Cheuffa, C. (2011). *A comprehensive review of past and present drilling methods with application to deep geothermal environment.* Paper presented at the Proceedings, Thirty-Sixth Workshop on Geothermal Reservoir Engineering, SGP-TR-191, Stanford University, Stanford, California.

Teodoriu, C., & Falcone, G. (2009). Comparing completion design in hydrocarbon and geothermal wells: The need to evaluate the integrity of casing connections subject to thermal stresses. *Geothermics, 38*(2), 238-246.

Þórhallsson, S., Matthíasson, M. H., Gíslason, Þ., Ingason, K., & Palsson, B. (2003). Iceland Deep Drilling Project (IDDP): The challenge of drilling and coring into 350-500 C hot geothermal systems and down to 5 km. *000599234*.

Wenger, S. J., Isaak, D. J., Luce, C. H., Neville, H. M., Fausch, K. D., Dunham, J. B., . . . Rieman, B. E. (2011). Flow regime, temperature, and biotic interactions drive differential declines of trout species under climate change. *Proceedings of the National Academy of Sciences, 108*(34), 14175-14180.

Willhite, G. P. (1967). Over-all heat transfer coefficients in steam and hot water injection wells. *Journal of Petroleum Technology, 19*(05), 607-615.

Willhite, G. P. (1967). Over - all Heat Transfer Coefficients in Steam and Hot Water Injection Wells. 607-615.

Williams, C. F., Reed, M. J., & Anderson, A. F. (2011). *Updating the classification of geothermal resources.* Paper presented at the Proceedings, Thirty-Sixth Workshop on Geothermal Reservoir Engineering.

Appendix

Appendix A: Reviewed Chemistry of Geothermal Fluids

Table 11: Computed chemical composition of the deep fluid supplying the CL3 well, Ribeira Grande geothermal field in the Azores(Carvalho, Forjaz, & Almeida, 2006).

Simulation no.	1	4	6	9	11	16	18	21	23
Ref	CL3-R269/94			CL3-R276/94		CL3-R280/94		CL3-R286/94	
Refer. T (°C)	Well	Na/K	Enthalpy	Na/K	Enthalpy	Na/K	Enthalpy	Na/k	Enthalpy
	240	245	269	250	275	253	275	260	291
Boiling T (°C)		240	240	240	240	240	240	240	240
No. phases	2	2	2	2	2	2	2	2	2
Steam fraction	0.081	0.0126	0.081	0.026	0.098	0.032	0.098	0.054	0.146
Water phase									
pH	8.44	8.05	8.44	6.78	7.2	8.23	8.47	7.01	7.32
E_h (V)	−0.752	−0.708	−0.753	−0.564	−0.614	−0.724	−0.753		
SiO_2 (mg/l)	396	398	396	393	390	394	392	311	308
Na (mg/l)	1725	1735	1725	1643	1633	1724	1714	1560	1547
K (mg/l)	265	266	265	264	263	283	281	275	272
Ca (mg/l)	0.59	0.59	0.59	0.81	0.81	0.93	0.92	0.67	0.67
Mg (mg/l)	0.007	0.007	0.007	0.014	0.014	0.007	0.007	0	0
Fe (mg/l)	0.094	0.094	0.094	0.072	0.072	0.116	0.115	0.08	0.079
NH_3 (mg/l)	16	24	16	160	131	22	15	95	77
Cl (mg/l)	2242	2255	2242	2242	2228	2627	2612	2209	2189
SO_4 (mg/l)	120	121	120	121	120	143	143	119	117
F (mg/l)	31	31	31	30	30	35	35	27	27
B (mg/l)	5	5	5	5	5	4	4	4	4
CO_2 (mg/l)	512	754	512	3987	1946	716	555	2297	1456
H_2S (mg/l)	4.86	5.1	4.86	21.64	14.65	2.65	2.99		
Steam phase									
CO_2 (mg/l)	7616	24,816	7606	620,640	224,980	16,383	7624	311,154	149,751
H_2S (mg/l)	13.29	32	13.28	899.82	399.66	11.31	7.54		
NH_3 (mg/l)	122	187	122	1176	988	172	117	714	589
Gas phase									
CO_2 (bar-g)	0.104	0.34	0.104	8.51	3.08	0.224	0.104	4.26	2.05
H_2S (bar-g)	0.000235	0.000566	0.000235	0.0159	0.00707	0.0002	0.000133		
NH_3 (bar-g)	0.00432	0.00661	0.00431	0.0417	0.035	0.00608	0.00413	0.0253	0.0208
Flow-rate		100%		75%		50%		25%	
WHP (bar-g)		7.15		11.7		15.5		18.05	
Q_{total} (t/h)		130		96		67		33	
Disch. enthalpy (kJ/kg)	1180		1180		1209		1207		1294
Calcul. enthalpy (kJ/kg)		1060	1180	1084	1211	1094	1211	1133	1295

Table 12: Alteration minerals observed in well cuttings and associated with fossil geothermal systems in Iceland as well as mineral types hosting trace elements in geothermal systems(Kaasalainen, Stefánsson, Giroud, & Arnórsson, 2015).

Alteration minerals				Well scales	Mineral types hosting trace elements						
Mineral	Salinity	Temperature		Mineral	Element	Native	Sulfide	Sulfate	(Hydr)oxides	Carbonate	Silicate
Quartz	dil, sal	>180 °C	Common	Calcite	Ag	x	x				
Chalcedony	dil, sal	<180 °C	Common	Al-silicate	As		x				
Calcite	dil, sal	Whole range	Common	Mg-silicate	Ba			x		x	x?
Albite	dil, sal	>150 °C	Common	Fe-silicate	Cd		x				
Adularia	dil, sal	Whole range	Rare, sporadic	Fe–Mg-silicate	Co		x				
Smectites	dil, sal	<200 °C	Common	Zn-silicate	Cr				x		
Zeolites	dil, sal	<120 °C/ <280 °C[b]	Common	Pyrite	Cu		x	x			
Mixed-layer clays	dil, sal	200–250 °C	Common	Marcasite	Mo		x		x		
Chlorite	dil, sal	>230 °C	Common	Other metal sulfides	Mn		x		x?	x	x
Epidote	dil, sal	>200 °C	Common	Pyrrhotite	Ni		x		x		
Prehnite	dil, sal	>200 °C	Common	Magnetite	Pb		x				
Clinozoisite	dil, sal		Common	Hematite	Sb		x				
Actinolite	dil, sal	>280–300 °C	Common	Anhydrite	Sr			x		x	x
Amphibole	dil, sal	>280–300 °C	Common	Anglesite	V		x		x?		
Grossular	dil, sal	>300 °C	Common		W		x				
Wollastonite	dil, sal	>200 °C	Common		Zn		x		x		
Anhydrite	sal	Whole range	Common								
Magnetite	sal		Common								
Goethite	dil		All depths								
Pyrite	dil, sal	Whole range	Common								
Pyrrhotite	dil		Common								
Sphalerite	sal, dil?	Sporadic									
Chalcopyrite	sal, dil?	Sporadic									
Galena	sal, dil?	Sporadic									

Appendix B: Simulation Parameters

Table 13: Well parameters used for simulation of the reservoir section.

Parameters	Value
Tf	450
Tw	440

rto – tubing outside radius	0.3749985
rci – casing inside radius	0.718747125
rti – tubing inside radius	0.333332
rco – casing outside radius	0.802080125
$rins$ – insulation radius	0.5499985
rwb - wellbore radius	1.0416625

hL – liquid convective heat transfer coefficient,	500
kt – conductivity of tubing material	25
hc – convective heat transfer coefficient	100
kc – conductivity of casing material	25
hr – radiative heat transfer coefficient	2
$kcem$ – conductivity of settled cement	

k_outer insulator	5
k_inner insulator	0.02
t_outer insulator thickness	0.175
t_inner insulator	0.175

Table 14: Well Parameters used for simulating the middle section of the well.

Parameters	Value
Tf	440
Tw	340

rto – tubing outside radius	0.3749985
rci – casing inside radius	0.718747125
rti – tubing inside radius	0.333332
rco – casing outside radius	0.802080125
$rins$ – insulation radius	0.5499985
rwb - wellbore radius	1.0416625
rwb-INTERMEDIATE	0.72916375
rwb-SURFACE_CASING	1.083329
rwb-CONDUCTOR_CASING	1.499994
rcoINTERMEDIATE	0.557289438
rcoSURFACE_CASING	0.83333
rcoCONDUCTOR_CASING	1.249995
rciINTERMEDIATE	0.47916475
rciSURFACE_CASING	0.760413625
rciCONDUCTOR_CASING	1.142912095

hL – liquid convective heat transfer coefficient,	500
kt – conductivity of tubing material	25
hc – convective heat transfer coefficient	100
kc – conductivity of casing material	25
hr – radiative heat transfer coefficient	2
$kcem$ – conductivity of settled cement	

k_outer insulator	5
k_inner insulator	0.02
t_outer insulator thickness	0.175
t_inner insulator	0.175

Table 15: Well parameters used for simulating the top section of the well.

Parameters	Value
Tf	410
Tw	170

rto – tubing outside radius	0.583331
rci – casing inside radius	0.718747125
rti – tubing inside radius	0.499998
rco – casing outside radius	0.802080125
$rins$ – insulation radius	0.758331
rwb - wellbore radius	1.0416625
rwb-INTERMEDIATE	0.72916375
rwb-SURFACE_CASING	1.083329
rwb-CONDUCTOR_CASING	1.499994
rcoINTERMEDIATE	0.557289438
rcoSURFACE_CASING	0.83333
rcoCONDUCTOR_CASING	1.249995
rciINTERMEDIATE	0.47916475
rciSURFACE_CASING	0.760413625
rciCONDUCTOR_CASING	1.142912095

hL – liquid convective heat transfer coefficient,	500
kt – conductivity of tubing material	25
hc – convective heat transfer coefficient	100
kc – conductivity of casing material	25
hr – radiative heat transfer coefficient	2
$kcem$ – conductivity of settled cement	

k_outer insulator	5
k_inner insulator	0.02
t_outer insulator thickness	0.175
t_inner insulator	0.175